Electronic Supplementary Material (ESI) for Organic Chemistry Frontiers.

Acenaphthylene-Fused Ullazines: From Electron-Rich to Dipolar π-Extended Monopyrroles

Supplementary Information

by Joanna Hager,[a] Seongsoo Kang,[b] Piotr J. Chmielewski,[a] Tadeusz Lis,[a] Dongho Kim,[*,b] and Marcin Stępień[*a]

Table of Contents

Experimental

General. Dichloromethane was distilled from calcium hydride when used as reaction solvent. Dimethylformamide and tetrahydrofurane were dried using a commercial solvent purification system. All other solvents and reagents were used as received. Microwave reactions were performed in a CEM Discover unit using external infrared temperature control system monitoring. Compounds **1**, **9**, **10a** and **10b** were synthesized as previously reported.[1–3] ^{1}H NMR spectra were recorded on high-field spectrometers (^{1}H frequency 500.13 or 600.13 MHz), equipped with broadband inverse or conventional gradient probeheads. Spectra were referenced to the residual solvent signal (chloroform-*d*, 7.24 ppm, dichloromethane-d_2, 5.32 ppm, toluene-d_8 7.09 ppm). ^{13}C NMR spectra were recorded with ^{1}H broadband decoupling and referenced to solvent signals ($^{13}CDCl_3$, 77.0 ppm). High resolution mass spectra were recorded using electrospray or MALDI ionization in the positive mode. Absorption spectrometry was performed using Agilent Cary 60 UV-Vis. Electrochemical measurements (DCM, 0.1 M $[Bu_4N][PF_6]$, 293 K) were performed on an Autolab(Metrohm) potentiostat/galvanostat system using a glassy-carbon working electrode, platinum wire as the auxiliary electrode, and silver/silver chloride as a reference electrode. The voltammograms were referenced against the half-wave potential of Fc^+/Fc. HPLC separations were carried out by means of Chirex® 3010 analytical column (25 cm length, 4.6 mm i.d.) packed with 5 µm silica gel coated with covalently bound (S)-valine and dinitroaniline using Merck-Hitachi LaChrom series connected to a flow-cell mounted on Jasco J-1500 spectropolarimeter. The separated fractions were analyzed by the same HPLC setup to establish enantiomeric excesses. The CD spectra were recorded in dichloromethane. Spectra were recorded by means of J-1500 CD spectrometer by Jasco with a Peltier temperature controller at 298 K. Melting points were set using Stuart Melting Point SMP30.

Computational methods. Density functional theory (DFT) calculations were performed using Gaussian 16.[4] DFT geometry optimizations were carried out in unconstrained C_1 symmetry, using molecular mechanics or semi-empirical models as starting geometries. DFT geometries were refined to meet standard convergence criteria, and the existence of a stationary point was verified by a normal modefrequency calculation. Geometry optimizations and frequency calculations were performed using the hybrid functional B3LYP combined with the 6-31G(d,p) basis set.[5–8]

X-ray crystallography. X-ray quality crystals were grown by slow diffusion of methanol into a chloroform solution of **6**. Diffraction measurements were performed on a Rigaku Oxford Diffraction XtaLAB Synergy R diffractometer equipped with HyPix-Arc 150 detector with Cu Kα radiation. The data were collected at 100 K, corrected for Lorenz and polarization effects. Data collection, cell refinement, data reduction and analysis, as well as empirical absorption correction were carried out with CrysAlisPro (Rigaku OD, 2020). All structures were solved by direct methods with the SHELXS-97 program and refined using SHELXL-2013[9] with anisotropic thermal parameters for non-H atoms. In the final refinement cycles, all H atoms were treated as riding atoms in geometrically optimized positions. CCDC 2101458 contains the supplementary crystallographic data for this paper. These data can be obtained free of charge from the Cambridge Crystallographic Data Centre via http://www.ccdc.cam.ac.uk/data_request/cif.

Steady-state measurements. Steady-state absorption spectra were measured on a UV/Vis/NIRspectrometer (Varian, Cary5000) and fluorescence spectra were measured on a fluorescence spectrophotometer (Hitachi, F-2500). Fluorescence spectra are spectrally corrected by using the correction factor of the fluorescence spectrophotometer. HPLC-grade solvents were

purchased from SigmaAldrich and used without further purification. All steady-state measurements were carried out by using a quartz cuvette with a pathlength of 1 cm at ambient temperatures.

Picosecond Time-resolved Fluorescence Measurements. A time-correlated single-photon-counting (TCSPC) system was used for measurements of spontaneous fluorescence decay. As an excitation light source, we used a mode-locked Ti:sapphire laser (Spectra Physics, MaiTai BB) which provides ultrashort pulse (center wavelength of 800 nm with 80 fs at FWHM) with high repetition rate (80 MHz). This high repetition rate was reduced to 800 kHz by using homemade pulse-picker. The pulse-picked output was frequency doubled by a 1-mm-thick BBO crystal (type-I, q = 29.2°, EKSMA). The fluorescence was collected by a microchannel plate photomultiplier (MCP-PMT, Hamamatsu, R3809U51) with a thermoelectric cooler (Hamamatsu, C4878) connected to a TCSPC board (Becker & Hickel SPC-130). The overall instrumental response function wasabout 25 ps (FWHM). A vertically polarized pump pulse by a Glan-laser polarizer was irradiated to samples, and a sheet polarizer set at an angle complementary to the magic angle (54.7°), was placed in the fluorescence collection path to obtain polarization-independent fluorescence decays.

Synthesis

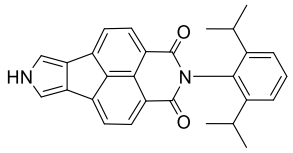

2-(2,6-diisopropylphenyl)pyrrolo[3',4':2,3]indeno[6,7,1-def]isoquinoline-1,3(2H,7H)-dione (1). Obtained according to a literature procedure.[1] **^{1}H NMR** (500 MHz, chloroform-*d*, 300 K): δ 8.41 (2H, d, ^3J = 7.4 Hz), 8.27 (1H, b), 7.63 (2H, d, ^3J = 7.4 Hz), 7.43 (1H, t, ^3J = 8.0 Hz), 7.29 (2H, d, ^3J = 8.0 Hz), 7.04 (2H, d, ^3J = 2.5 Hz), 2.78 (2H, sept, ^3J = 6.9 Hz), 1.14 (12H, d, ^3J = 6.9 Hz).

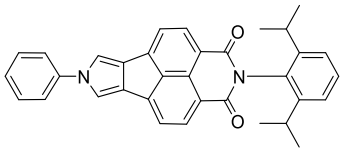

2-(2,6-diisopropylphenyl)-7-phenylpyrrolo[3',4':2,3]indeno[6,7,1-def]isoquinoline-1,3(2H,7H)-dione (2). Pyrrole **1** (500 mg, 1.2 mmol), copper(I) iodide (18.9 mg, 0.099 mmol) and potassium phosphate tribasic (441.7 mg, 2.08 mmol) were placed in a 10 mL pressure tube, followed by addition of iodobenzene (133 µL, 0.991 mmol), *trans*-1,2-cyclohexylamine (12 µL, 0.099 mmol) and dioxane (1.05 mL). The reaction mixture was purged with nitrogen for 5 min, sealed and stirred in 110 °C for 17 h. The reaction mixture was cooled down to room temperature, diluted with dichloromethane and filtered through celite pad. The fitrate was then evaporated under reduced pressure. The crude product was purified by column chromatography (silica, dichloromethane) to get compound **2** (474 mg, 96%) as pale brown solid. **^{1}H NMR** (500 MHz, chloroform-*d*, 300 K): δ 8.44 (2H, d, ^3J = 7.4 Hz), 7.67 (2H, d, ^3J = 7.4 Hz), 7.52 – 7.42 (5H, m), 7.35 (3H, m), 7.30 (2H, d, ^3J = 7.8 Hz), 2.79 (2H, sept, ^3J = 6.9 Hz), 1.15 (12H, d, ^3J = 6.9 Hz). **^{13}C NMR** (151 MHz, chloroform-*d*, 300 K): δ 164.20, 145.89, 140.23, 139.61, 136.68, 133.04, 131.39, 130.45, 129.90, 129.24, 126.83, 126.78, 123.85, 120.66, 120.12, 119.55, 115.99, 29.04, 24.02. **HRMS** (ESI–TOF): *m*/*z*: $[M + Na]^+$ Calcd for $C_{34}H_{28}N_2O_2Na^+$: 519.2043; Found 519.2085.

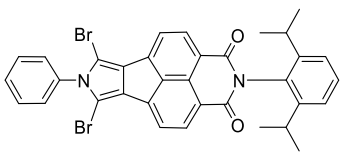

6,8-dibromo-2-(2,6-diisopropylphenyl)-7-phenylpyrrolo[3',4':2,3]indeno[6,7,1-def]isoquinoline-1,3(2H,7H)-dione (3). Compound **2** (470 mg, 0.95 mmol), *N*-Bromosuccinimide (354 mg, 1.95 mmol) and dichloromethane (5.92 mL) were placed in a dried 25 mL round-bottom flask. The flask was protected from light and the reaction mixture was purged with nitrogen for 5 min. The mixture was allowed to stir at room temperature for 4 h. The reaction was then quenched with water, extracted with dichloromethane and washed with saturated aqueous solution of sodium bicarbonate. The

combined organic layers were dried over anhydrous sodium sulfate, and the solvent was removed on a rotary evaporator under high vacuum to afford dibrominated compound **3** (613 mg, 99%) as an orange solid, without further purification. **^{1}H NMR** (500 MHz, chloroform-*d*, 300 K): δ 8.49 (2H, d, ^3J = 7.4 Hz), 7.81 (2H, d, ^3J = 7.4 Hz), 7.58 (3H, m), 7.45 (1H, t, ^3J = 7.8 Hz), 7.39 (2H, m), 7.30 (2H, d, ^3J = 7.8 Hz), 2.79 (2H, sept, ^3J = 6.9 Hz), 1.15 (12H, d, ^3J = 6.9 Hz). **^{13}C NMR** (125 MHz, chloroform-*d*, 300 K): δ 164.08, 145.88, 137.71, 136.46, 135.77, 133.00, 131.28, 129.92, 129.86, 129.39, 129.34, 129.12, 126.71, 123.92, 120.59, 119.14, 101.83, 29.08, 24.04. **HRMS** (ESI–TOF): *m*/*z*: $[M + Na]^+$ Calcd for $C_{34}H_{26}Br_2N_2O_2Na^+$: 675.0253; Found 675.0257.

General procedure for the synthesis of α-arylated precursors 4a-c. Compound **3** (1.0 equiv) and suitable phenylboronic acid (2.2 equiv) were placed in microwave vial equipped with magnetic stirring bar. Then, tetrakis(triphenylphosphine)palladium(0) (0.06 equiv) and sodium carbonate (5 equiv) were added along with solvent mixture (dioxane and water (10:1 v/v) and the reaction mixture was purged with nitrogen for 10 min. The vial was sealed and placed in microwave reactor, where reaction was held for 3 h (100 °C, PowerMax mode). The mixture was diluted with brine and extracted with dichloromethane. The combined organic layers, strongly red-coloured, were dried over anhydrous sodium sulfate, filtered and evaporated under reduced pressure. The crude product was purified by column chromatography (silica, dichloromethane).

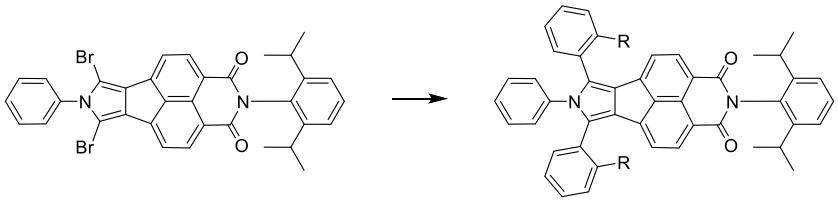

3

4a: R = H
4b: R = Cl
4c: R = CHO

Scheme S1. Synthesis of compounds **4a-c**.

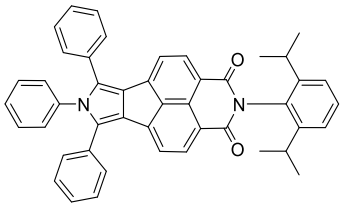

2-(2,6-diisopropylphenyl)-6,7,8-triphenylpyrrolo[3',4':2,3]indeno[6,7,1-def]isoquinoline-1,3(2H,7H)-dione (4a). Prepared *via* general procedure using compound **3** (66 mg, 0.1 mmol), phenylboronic acid (28.5 mg, 0.22 mmol), $Pd(PPh_3)_4$ (7 mg, 0.006 mmol) and Na_2CO_3 (53.5 mg, 0.504 mmol) in dioxane/water mixture (0.66 mL/66 µL). Product was obtained as a pale red powder (31.2 mg, 48%). **^{1}H NMR** (500 MHz, chloroform-*d*, 300 K): δ 8.35 (2H, d, ^3J = 7.4 Hz), 7.65 (2H, d, ^3J = 7.4 Hz), 7.43 (1H, t, ^3J = 7.9 Hz), 7.36 – 7.25 (15H, m), 7.07 (2H, m), 2.79 (2H, sept, ^3J = 6.8 Hz), 1.15 (12H, d, ^3J = 6.8 Hz). **^{13}C NMR** (125 MHz, chloroform-*d*, 300 K): δ 164.25, 145.91, 139.94, 137.74, 136.98, 132.96,

132.69, 131.52, 131.19, 129.15, 129.01, 128.95, 128.50, 128.18, 128.02, 127.28, 126.94, 123.83, 119.94, 118.52, 77.02, 29.03, 24.03. **HRMS** (ESI–TOF): *m*/*z*: $[M + H]^+$ Calcd for $C_{46}H_{36}N_2O_2H^+$: 649.2850; Found 649.2824. **Melting point:** 341 - 342 °C.

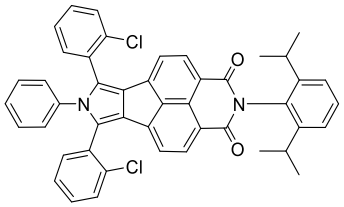

6,8-bis(2-chlorophenyl)-2-(2,6-diisopropylphenyl)-7-phenylpyrrolo[3',4':2,3]indeno[6,7,1-def]isoquinoline-1,3(2H,7H)-dione (4b). Prepared *via* general procedure using compound **3** (165 mg, 0.25 mmol), (2-chlorophenyl)boronic acid (88.5 mg, 0.56 mmol), $Pd(PPh_3)_4$ (17.5 mg, 0.015 mmol) and Na_2CO_3 (133.6 mg, 1.26 mmol) in dioxane/water mixture (1.65 mL/165 µL). Product was obtained as orange powder (155 mg, 86%). **^{1}H NMR** (600 MHz, chloroform-*d*, 300 K): δ 8.35 (2H, m), 7.53 (1H, m), 7.42 (3H, m), 7.34 – 7.25 (7H, m), 7.17 – 7.09 (5H, m), 6.97 (2H, m), 2.77 (2H, m), 1.13 (12H, m). **^{13}C NMR** (151 MHz, chloroform-*d*, 300 K): δ 164.31, 164.30, 145.98, 145.90, 139.60, 139.58, 137.37, 136.76, 134.72, 134.48, 132.87, 132.82, 132.54, 132.31, 131.51, 130.53, 130.46, 130.21, 130.05, 129.99, 129.96, 129.17, 128.78, 128.70, 128.53, 128.44, 128.39, 127.87, 127.81, 127.63, 127.53, 126.65, 126.59, 126.51, 123.84, 123.80, 123.77, 120.22, 119.96, 119.73, 77.01, 53.41, 29.71, 29.04, 24.00, 23.94. **HRMS** (MALDI–TOF): *m*/*z*: $[M + H]^+$ Calcd for $C_{46}H_{34}Cl_2N_2O_2H^+$: 717.2070; Found 717.2090. **Melting point:** 173 - 174 °C.

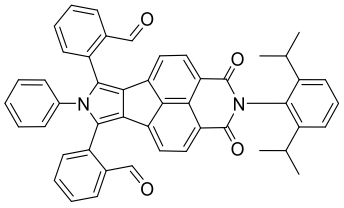

2,2'-(2-(2,6-diisopropylphenyl)-1,3-dioxo-7-phenyl-1,2,3,7-tetrahydropyrrolo[3',4':2,3]indeno[6,7,1-def]isoquinoline-6,8-diyl)dibenzaldehyde (4c). Prepared *via* general procedure using compound **3** (92 mg, 0.141 mmol), (2-formylphenyl)boronic acid (48.4 mg, 0.309 mmol), $Pd(PPh_3)_4$ (9.75 mg, 0.008 mmol) and Na_2CO_3 (74.5 mg, 0.703 mmol) in dioxane/water mixture (0.92 mL/92 µL). Product was obtained as orange powder (76 mg, 77%). **^{1}H NMR** (500 MHz, chloroform-*d*, 300 K): δ 10.14 (1H, d, ^4J = 0.7 Hz), 10.12 (1H, d, ^4J = 0.7 Hz), 8.33 (2H, m), 7.98 (2H, m), 7.62 (2H, m), 7.55 (2H, m), 7.45 (3H, m), 7.29 (4H, m), 7.18 – 7.10 (3H, m), 6.88 (2H, m), 2.75 (2H, m), 1.13 (12H, m). **^{13}C NMR** (151 MHz, chloroform-*d*, 300 K): δ 190.44, 190.34, 164.00, 145.85, 138.47, 136.83, 134.85, 134.74, 134.01, 133.90, 133.74, 133.64, 132.98, 131.50, 131.38, 131.30, 130.13, 130.11, 129.51, 129.26, 129.17, 129.12, 128.99, 128.77, 128.37, 128.30, 128.08, 126.83, 123.85, 123.78, 120.65, 120.62, 119.21,

119.18, 77.01, 29.70, 29.06, 24.02, 23.99, 23.95. **HRMS** (ESI–TOF): *m*/*z*: [M + Na]$^+$ Calcd for $C_{48}H_{36}N_2O_4Na^+$: 727.2567; Found 727.2538.

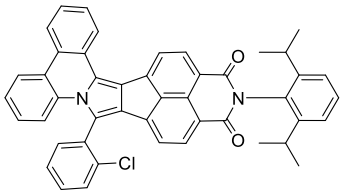

6-(2-chlorophenyl)-2-(2,6-diisopropylphenyl)-1H-pyrido[3'',4'',5'':5',6']acenaphtho[1',2':3,4]pyrrolo[1,2-f]phenanthridine-1,3(2H)-dione (5a). Compound **4b** (10 mg, 0.014 mmol), tris(dibenzylideneacetone)dipalladium(0) (2.55 mg, 0.0028 mmol) and potassium phosphate tribasic (29.6 mg, 0.14 mmol) were placed in pressure tube equipped with magnetic stirring bar. Then, dimethylformamide (0.67 mL) was added and the mixture was purged with nitrogen for 10 min. The tube was sealed and stirred in 155 °C for 4 h. After cooling to room temperature, the mixture was diluted with dichloromethane and washed with water. Organic layer was dried over anhydrous sodium sulfate, filtered and evaporated under reduced pressure. The crude product was roughly separated from the reaction mixture as red powder by column chromatography (silica, dichloromethane) (1.25 mg, 13%, not fully purified). **^{1}H NMR** (500 MHz, chloroform-*d*, 300 K): δ 8.59 (1H, m), 8.56 (1H, d, ^3J = 7.7 Hz), 8.38 (2H, m), 8.32 (1H, d, ^3J = 7.4 Hz), 8.21 (1H, d, ^3J = 7.7 Hz), 7.77 (2H, m), 7.69 (1H, m), 7.64 (1H, m), 7.58 (2H, m), 7.43 (1H, t, ^3J = 7.9 Hz), 7.36 (1H, m), 7.30 (4H, m), 7.19 (1H, m), 2.79 (2H, m), 1.14 (12H, m).

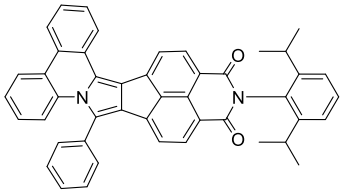

2-(2,6-diisopropylphenyl)-6-phenyl-1H-pyrido[3'',4'',5'':5',6']acenaphtho[1',2':3,4]pyrrolo[1,2-f]phenanthridine-1,3(2H)-dione (5b). Compound **4b** (10 mg, 0.014 mmol), dichlorobis(tricyclohexylphosphine)palladium(II) (2.10 mg, 0.0028 mmol) and potassium phosphate tribasic (29.6 mg, 0.14 mmol) were placed in pressure tube equipped with magnetic stirring bar. Then, dimethylformamide (0.67 mL) was added and the mixture was purged with nitrogen for 10 min. The tube was sealed and stirred in 155 °C for 4 h. After cooling to room temperature, the mixture was diluted with dichloromethane and washed with water. Organic layer was dried over anhydrous sodium sulfate, filtered and evaporated under reduced pressure. The crude product was separated from the reaction mixture by column chromatography (silica, dichloromethane) and was further purified using semi-preparative TLC (silica, dichloromethane) to give the product as a red powder (2.2 mg, 24%, not fully purified). **^{1}H NMR** (500 MHz, chloroform-*d*, 300 K): δ 8.56 (2H, m), 8.34 (3H, m), 8.18 (1H, d, , ^3J = 7.7 Hz), 7.75 (1H, m), 7.69 (2H, m), 7.60 (4H, m), 7.48 (1H, d, ^3J = 7.4 Hz), 7.43 (1H, m), 7.37 (1H, dd, ^3J = 8.6 Hz, ^4J = 0.9 Hz), 7.33 (1H, m), 7.29 (2H, d, ^3J = 7.8 Hz), 7.14 (1H, m), 2.80 (2H, sept, ^3J = 6.9 Hz), 1.15 (12H, m).

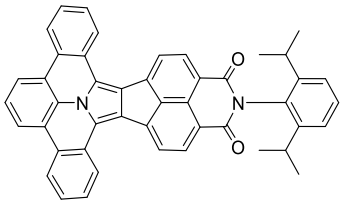

2-(2,6-Diisopropylphenyl)-1H-benzo[7,8]pyrido[3'',4'',5'':5',6']acenaphtho[1',2':1,2]indolizino[6,5,4,3-def]phenanthridine-1,3(2H)-dione (6). Compound **4b** (30 mg, 0.042 mmol), tris(dibenzylideneacetone)dipalladium(0) (7.66 mg, 0.0084 mmol) and potassium phosphate tribasic (88.7 mg, 0.42 mmol) were placed in microwave vial equipped with magnetic stirring bar. Then, dimethylformamide (2.01 mL) was added and the mixture was purged with nitrogen for 10 min. The vial was sealed and placed in microwave reactor. The reaction was held for 1 h (155 °C, PowerMax mode). After cooling to room temperature, the mixture was diluted with dichloromethane and washed with water. Organic layer was dried over anhydrous sodium sulfate, filtered and evaporated under reduced pressure. The crude product was then dissolved in dichloromethane and precipitated with *n*-hexane. After washing with cold *n*-hexane, the precipitate was dried and recrystallized from methanol. The insoluble material was filtered off and dried in vacuum to give the product as an dark violet powder (17.7 mg, 66%). **^{1}H NMR** (500 MHz, chloroform-*d*, 300 K): δ 8.51 (2H, d, ^3J = 7.5 Hz), 8.41 (2H, d, ^3J = 7.7 Hz), 8.32 (2H, d, ^3J = 8.1 Hz), 8.27 (2H, d, ^3J = 8.1 Hz), 8.10 (2H, d, ^3J = 7.7 Hz), 7.71 (2H, t, ^3J = 7.2 Hz), 7.60 (2H, t, ^3J = 7.3 Hz), 7.58 (1H, t, ^3J = 8.2 Hz), 7.47 (1H, t, ^3J = 8.0 Hz), 7.34 (2H, d, ^3J = 8.0 Hz), 2.88 (2H, m), 1.21 (12H, d, ^3J = 6.9 Hz). **^{13}C NMR** spectrum of **6** is not available due to strong aggregation. No peak was observed even the measurement was conducted overnight. **HRMS** (MALDI–TOF): *m*/*z*: $[M + H]^+$ Calcd for $C_{46}H_{32}N_2O_2H^+$: 645.2537; Found 645.2575. **Melting point:** melting not observed up to 390 °C.

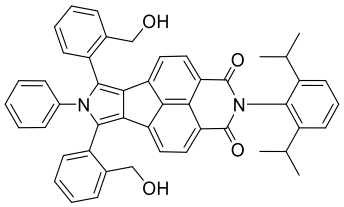

2-(2,6-Diisopropylphenyl)-6,8-bis(2-(hydroxymethyl)phenyl)-7-phenylpyrrolo[3',4':2,3]indeno[6,7,1-def]isoquinoline-1,3(2H,7H)-dione (7). Compound **4c** (22 mg, 0.031 mmol) and sodium borohydride (4.82 mg, 0.125 mmol) were placed in flame-dried 5 mL round-bottom flask, that was put in an ice-bath. After addition of tetrahydrofurane (1.2 mL) the reaction mixture was purged with nitrogen for 5 min and then stirred under nitrogen for 18 h, allowing it to slowly warm up to room temperature. The reaction mixture was then transferred to separatory funnel with 1M solution of hydrochloric acid and extracted with dichloromethane. Combined extracts were dried over anhydrous sodium sulfate and filtered. Solvents were evaporated under reduced pressure yielding orange solid (18 mg), which was used without further purification. **^{1}H NMR** (500 MHz,

chloroform-*d*, 300 K): δ 8.31 (2H, m), 7.53 (2H, m), 7.42 (3H, m), 7.37 – 7.26 (6H, m), 7.22 (2H, m), 7.09 (3H, m), 7.01 (1H, m), 6.96 (1H, m), 4.57 (4H, m), 2.75 (2H, m), 1.12 (12H, m).

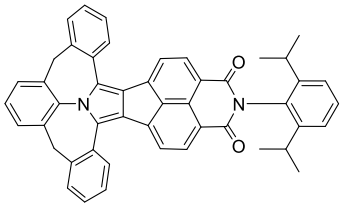

17-(2,6-Diisopropylphenyl)-5,9-dihydro-16H-13b1,17-diazatribenzo[2',3':5',6':8',9']heptaleno[1',10':4,5,6]pentaleno[1,2,3-cd]phenalene-16,18(17H)-dione (8). Compound **7** (18 mg, 0.025 mmol) was placed in flame-dried 5 mL round-bottom flask. Dichloromethane (1.45 mL) was added and the mixture was placed in an ice-bath and purged with nitrogen for 5 min. Concentrated sulfuric acid (8.46 µL, 0.152 mmol) was added dropwise to the mixture, causing rapid colour change from orange to dark violet. The reaction mixture was then allowed to warm to room remperature and stirred for 18 h. Reaction was quenched with addition of saturated solution of sodium bicarbonate and extracted with dichloromethane. The combined organic layers were dried over anhydrous sodium sulfate, and the solvent was removed on a rotary evaporator under high vacuum to afford ullazine **8** as pink solid, which was further purified using column chromatography (8 mg, 38% over two steps from **4c**). **^{1}H NMR** (600 MHz, chloroform-*d*, 300 K): δ 8.38 (2H, d, ^{3}J = 7.4 Hz), 7.90 (2H, d, ^{3}J = 7.1 Hz), 7.77 (2H, d, ^{3}J = 7.4 Hz), 7.42 (7H, m), 7.29 (2H, d, ^{3}J = 7.8 Hz), 7.22 (2H, d, ^{3}J = 7.2 Hz), 7.17 (1H, m), 4.14 (2H, d, ^{2}J = 13.4 Hz), 3.66 (2H, d, ^{2}J = 13.3 Hz), 2.80 (2H, sept, ^{3}J = 6.9 Hz), 1.15 (12H, d, ^{3}J = 6.9 Hz). **^{13}C NMR** (151 MHz, chloroform-*d*, 300 K): δ 164.18, 145.90, 141.21, 139.89, 137.51, 132.97, 132.19, 129.79, 129.54, 129.19, 128.59, 127.97, 127.16, 127.15, 127.01, 126.31, 123.82, 120.16, 118.62, 39.41, 29.05, 24.02, 23.99. **HRMS** (ESI–TOF): *m*/*z*: $[M + H]^+$ Calcd for $C_{48}H_{36}N_2O_2H^+$: 673.2850; Found 673.2820.

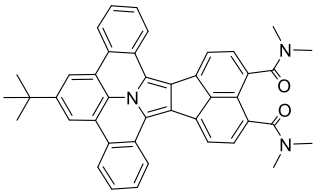

9-(tert-butyl)-N1,N1,N17,N17-tetramethylacenaphtho[1',2':1,2]benzo[7,8]indolizino[6,5,4,3-def]phenanthridine-1,17-dicarboxamide (11). Compounds **9** (10 mg, 0.028 mmol) and **10a** (13.71 mg, 0.031 mmol) were dissolved in dichloromethane (1.14 mL) in flame-dried 5 mL round-bottom flask. After purging with nitrogen for 5 min, triethylamine (anhydrous, nitrogen-bubbled, 46.41 µL, 0.333 mmol) was added in one portion. The reaction mixture instantly became darker and fumy. It was left in room temperature for 5 min and was then evaporated under reduced pressure. Such obtained cycloaddition product was instantly used further without any purification. 2,3-Dichloro-5,6-dicyano-

1,4-benzoquinone (12.88 mg, 0.056 mmol) was added to the flask along with toluene (1.14 mL). The reaction mixture was purged with nitrogen for 10 min and left in room temperature for 3 h. During the reaction formation of dark red precipitate was observed. After quenching the reaction with water, the red powder was collected by vacuum filtration. The crude product was then dissolved in dichloromethane, precipitated and washed with *n*-hexane. After vacuum drying compound **11** was obtained as red solid material (15.20 mg, 89%). **^{1}H NMR** (500 MHz, chloroform-*d*, 300 K): δ 8.33 (2H, d, ^{3}J = 7.6 Hz), 8.16 (4H, m), 8.00 (2H, d, ^{3}J = 7.3 Hz), 7.56 (2H, t, ^{3}J = 7.6 Hz), 7.48 (2H, d, ^{3}J = 7.3 Hz), 7.44 (2H, t, ^{3}J = 7.6 Hz), 3.14 (6H, s), 3.01 (6H, s). **^{13}C NMR** (125 MHz, chloroform-*d*, 300 K): δ 171.16, 146.07, 138.33, 134.61, 131.90, 128.79, 128.09, 127.44, 126.85, 126.69, 125.74, 125.02, 124.87, 123.73, 122.67, 122.07, 121.01, 120.07, 117.92, 77.02, 39.55, 39.52, 35.20, 34.96, 31.75. **HRMS** (ESI–TOF): *m*/*z*: $[M + Na]^+$ Calcd for $C_{42}H_{35}N_3O_2Na^+$: 636.2621; Found 636.2615. **Melting point:** 234 - 235 °C.

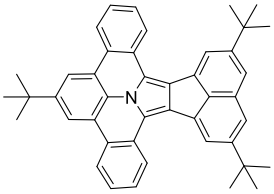

2,9,16-tri-tert-butylacenaphtho[1',2':1,2]benzo[7,8]indolizino[6,5,4,3-def]phenanthridine (12). Compounds **9** (10 mg, 0.014 mmol) and **10b** (12.79 mg, 0.031 mmol) were dissolved in dichloromethane (1.14 mL) in flame-dried 5 mL round-bottom flask. After purging with nitrogen for 5 min, triethylamine (anhydrous, nitrogen-bubbled, 46.41 µL, 0.333 mmol) was added in one portion. The reaction mixture instantly became darker and fumy. It was left in room temperature for 5 min and was then evaporated under reduced pressure. Such obtained cycloaddition product was instantly used further without any purification. 2,3-Dichloro-5,6-dicyano-1,4-benzoquinone (12.88 mg, 0.056 mmol) was added to the flask along with toluene (1.14 mL). The reaction mixture was purged with nitrogen for 10 min and left in room temperature for 3 h. After quenching the reaction with water, it was extracted with dichloromethane, dried over anhydrous sodium sulfate and evaporetaed under reduced pressure. Crude product was purified by column chromatography (silica, dichloromethane) to yield light yellow powder (16.00 mg, 99%). **^{1}H NMR** (500 MHz, chloroform-*d*, 300 K): δ 8.71 (2H, dd, ^{3}J = 8.4 Hz, ^{4}J = 1.0 Hz), 8.42 (2H, dd, ^{3}J = 8.4 Hz, ^{4}J = 1.0 Hz), 8.38 (2H, s), 8.34 (2H, d, ^{4}J = 1.2 Hz), 7.73 (4H, m), 7.56 (2H, m), 1.58 (18H, s), 1.56 (9H, s). **^{13}C NMR** (125 MHz, chloroform-*d*, 300 K): δ 150.87, 146.07, 134.86, 132.75, 130.12, 129.44, 128.22, 126.73, 126.55, 126.54, 125.23, 125.16, 122.92, 122.30, 120.47, 120.24, 119.04, 117.91, 35.60, 35.26, 31.82, 29.72. **HRMS** (ESI–TOF): *m*/*z*: $[M]^+$ Calcd for $C_{44}H_{41}N^+$: 583.3234; Found 583.3227. **Melting point:** melting not observed up to 390 °C.

Additional Schemes

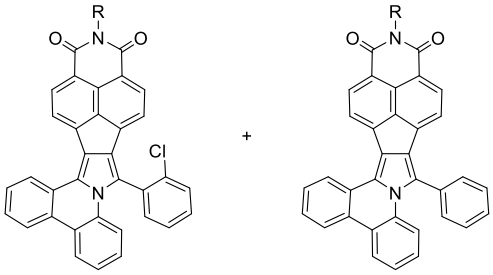

5a **5b**

Scheme S2. Structures of sideproducts of **4b** cyclodehydrohalogenation reaction.

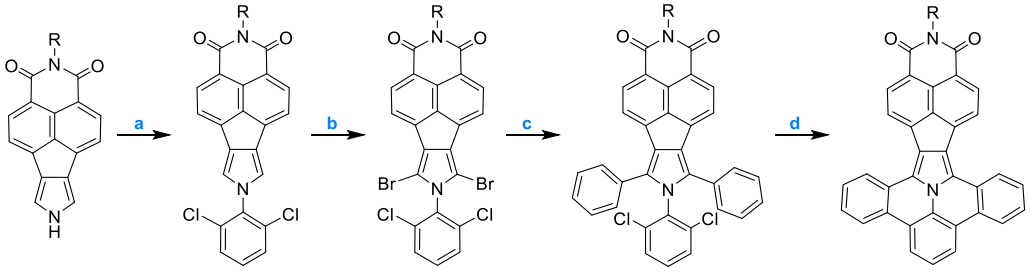

1 R = dipp **S1** **S2** **S3** **6**

Scheme S3. Inverse pathway of ullazine **6** synthesis: (**a**) 1,3-dichloro-2-fluorobenzene, NaH, DMF, 60 °C; 24 h; (**b**) NBS, DCM, RT; 24 h; (**c**) phenylboronic acid, $Pd(PPh_3)_4$, Na_2CO_3, dioxane/water, reflux, 24 h; (**d**) $Pd_2(dba)_3$, K_3PO_4, DMF, 155 °C, 4 h.

Additional Figures

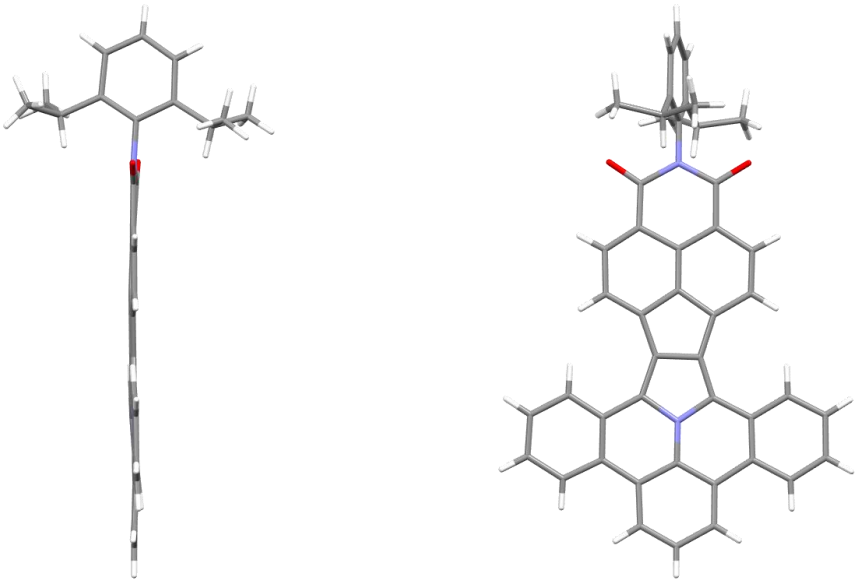

Figure S1. X-ray crystal structure of **6**. Solvent molecules and disorder positions are removed for clarity.

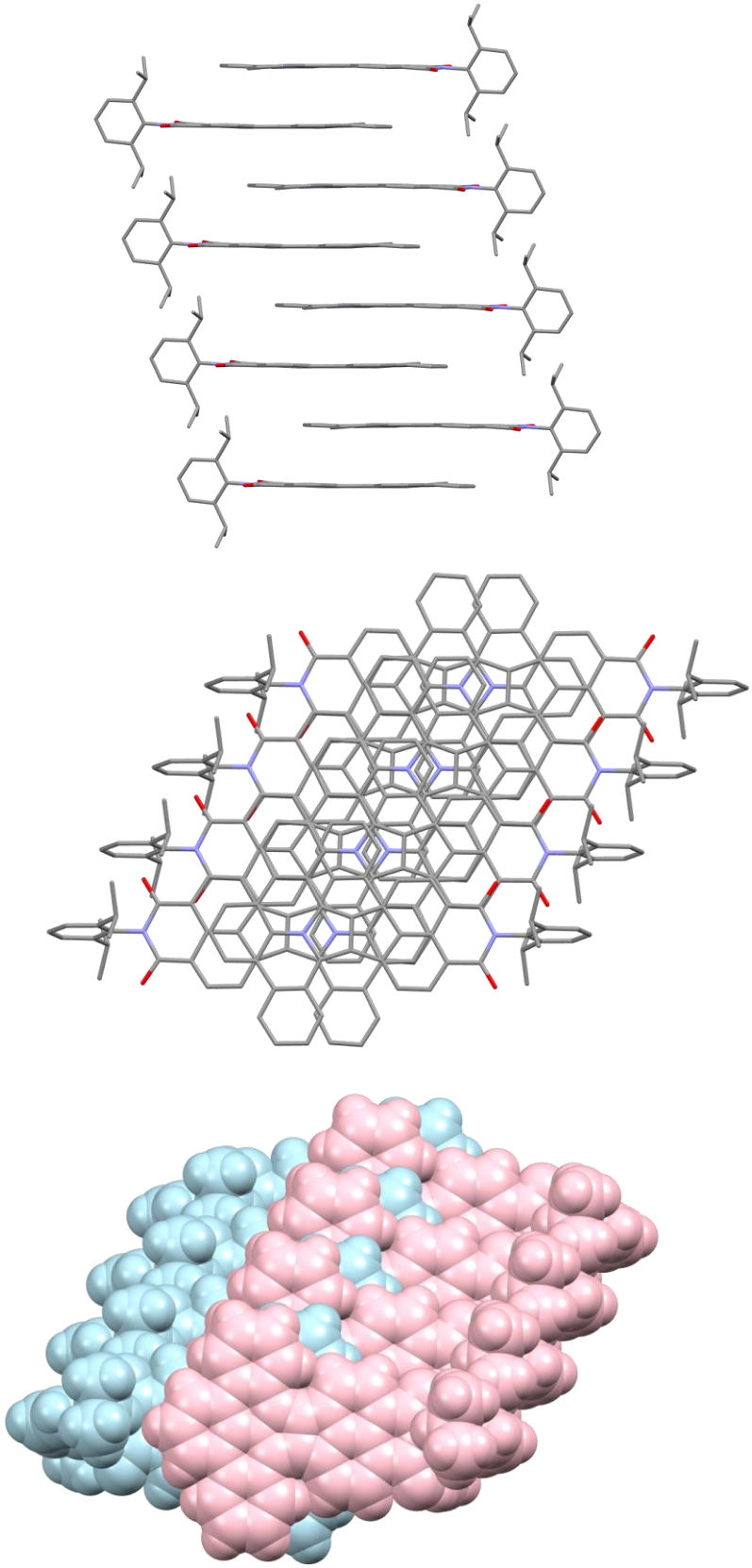

Figure S2. Packing diagrams of **6** obtained in X-ray crystallographic analyses. Hydrogen atoms, solvent molecules and disorder positions are removed for clarity.

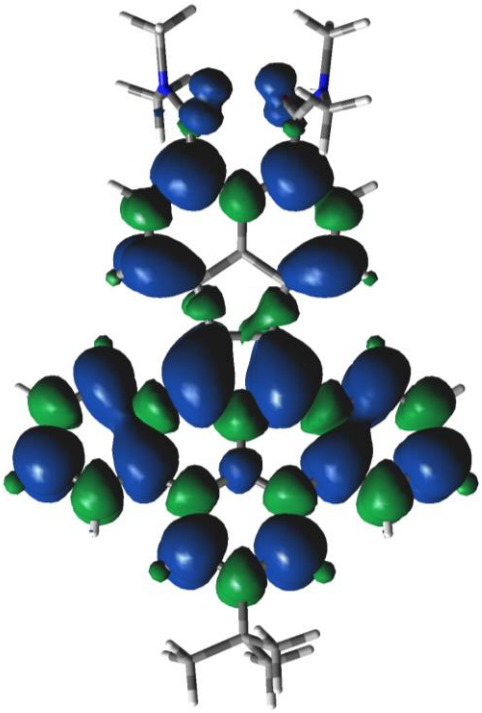

Figure S3. Spin-density calculations for **11$^{\bullet+}$.** All calculations were performed at the level of B3LYP/6-31G(d,p) theory.

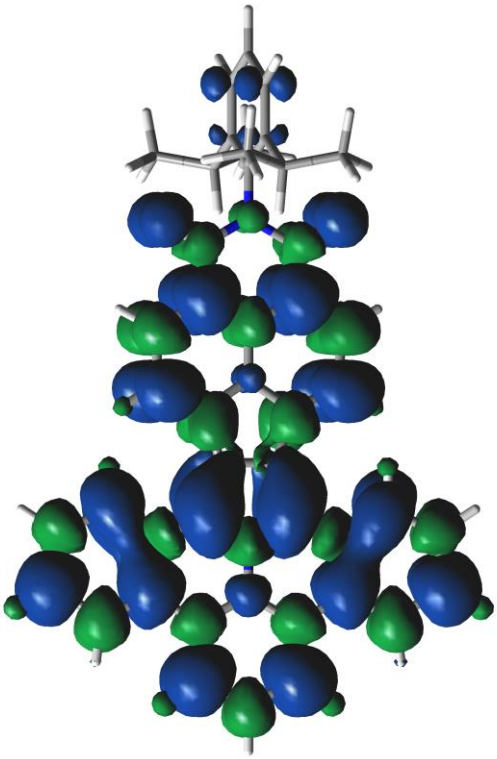

Figure S4. Spin-density calculations for **12**$^{\bullet+}$**.** All calculations were performed at the level of B3LYP/6-31G(d,p) theory.

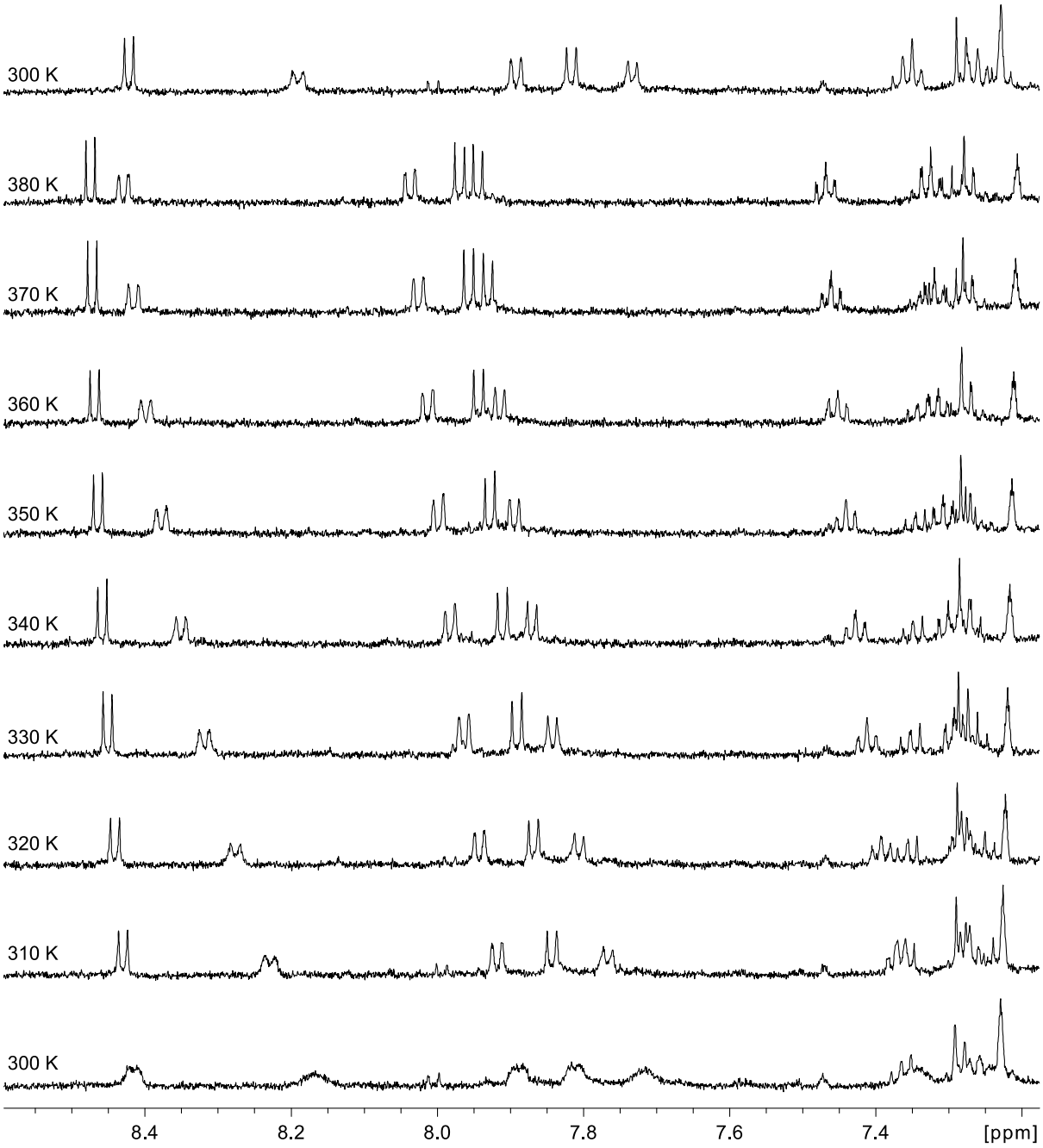

Figure S5. Variable temperature ^{1}H NMR spectra (600 MHz, toluene-d_8) of **6.**

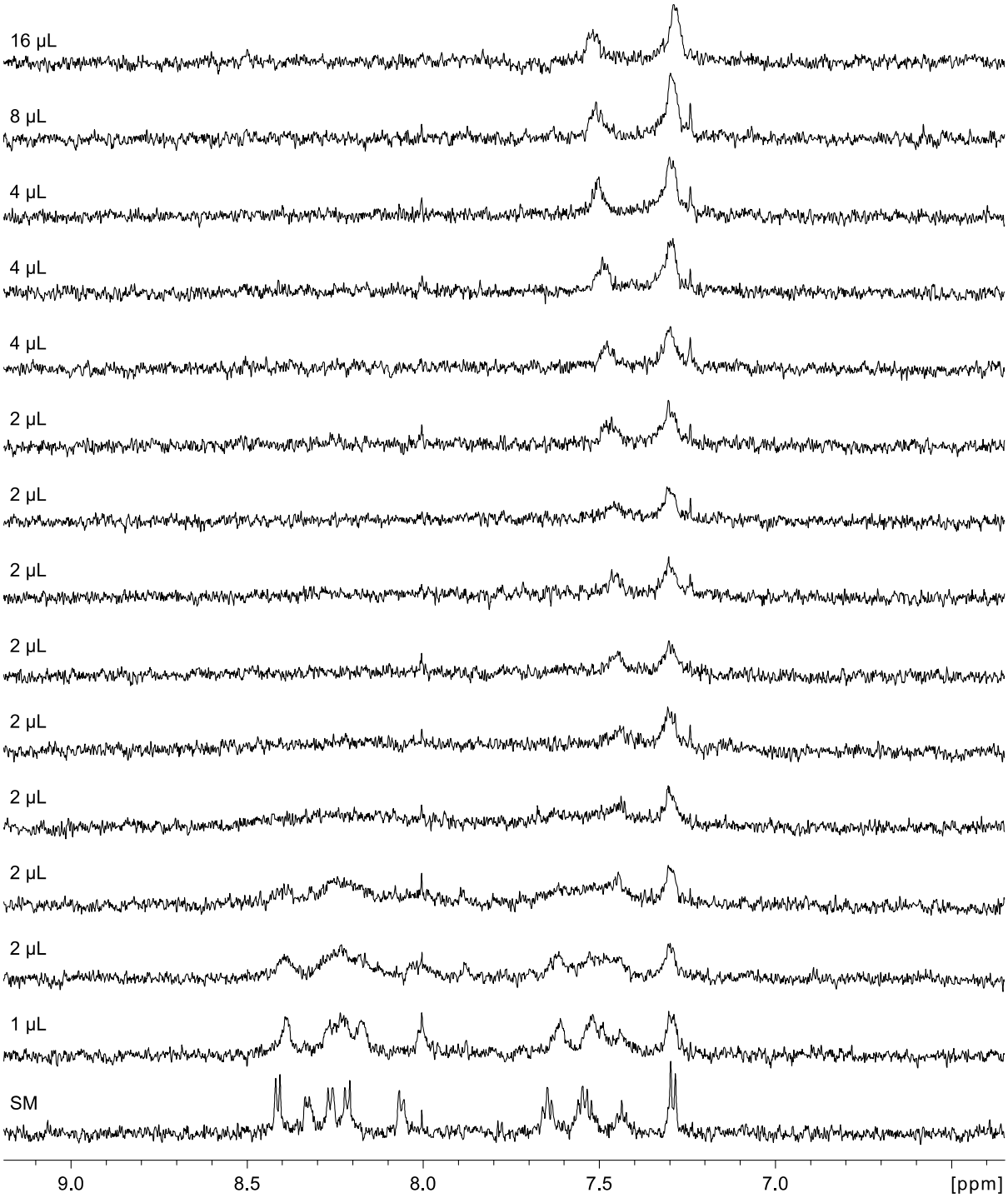

Figure S6. ^{1}H NMR titration spectra (600 MHz, dichloromethane-d_2, 300 K) obtained upon addition of $SbCl_5$ solution (10 µL of 1M $SbCl_5$ in DCM were diluted with 1.2 mL of DCM-d_2) to DCM-d_2 solution of **6**.

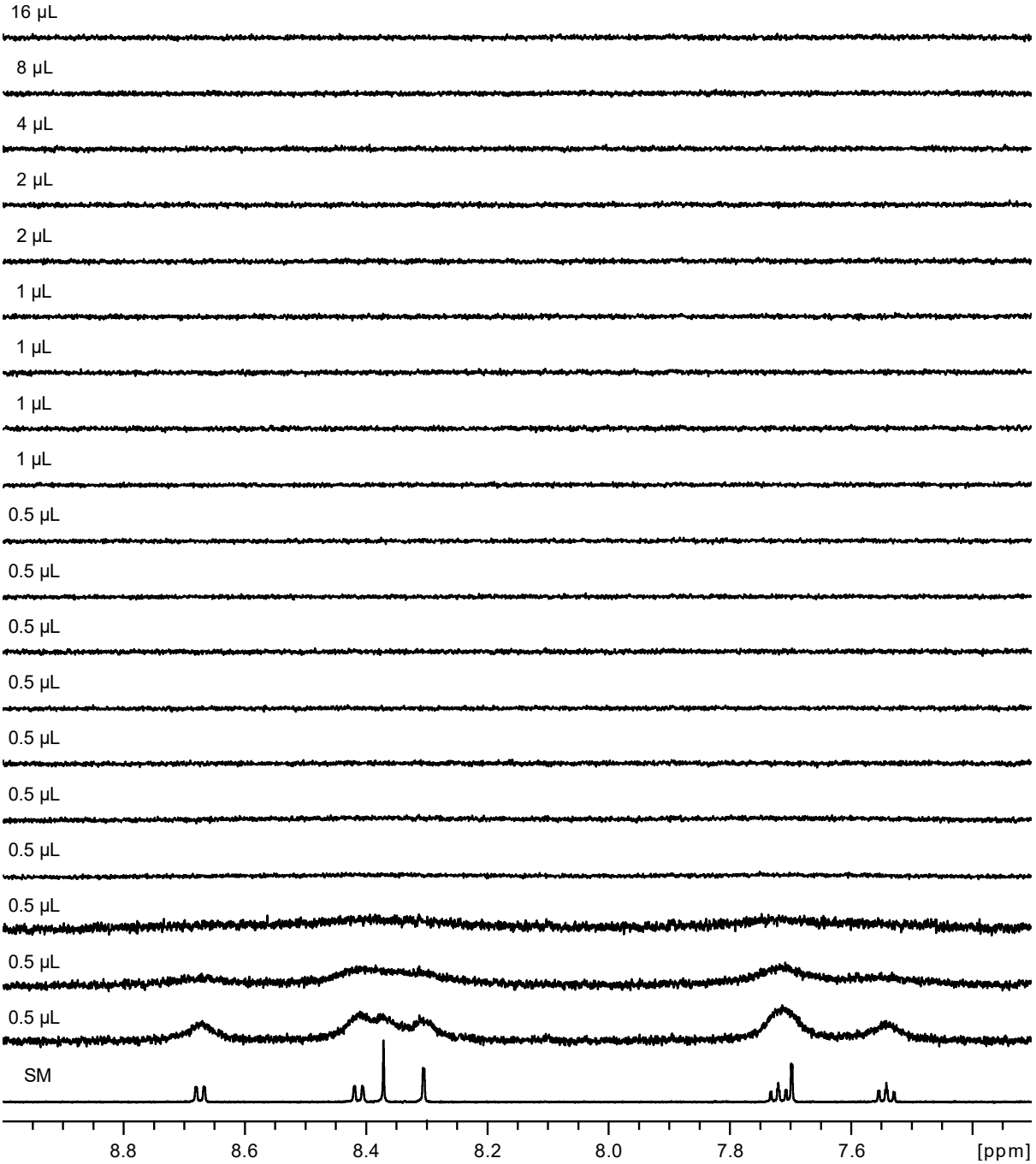

Figure S7. ^{1}H NMR titration spectra (600 MHz, dichloromethane-d_2, 300 K) obtained upon addition of $SbCl_5$ solution (10 µL of 1M $SbCl_5$ in DCM were diluted with 5.1 mL of DCM-d_2) to DCM-d_2 solution of **12**.

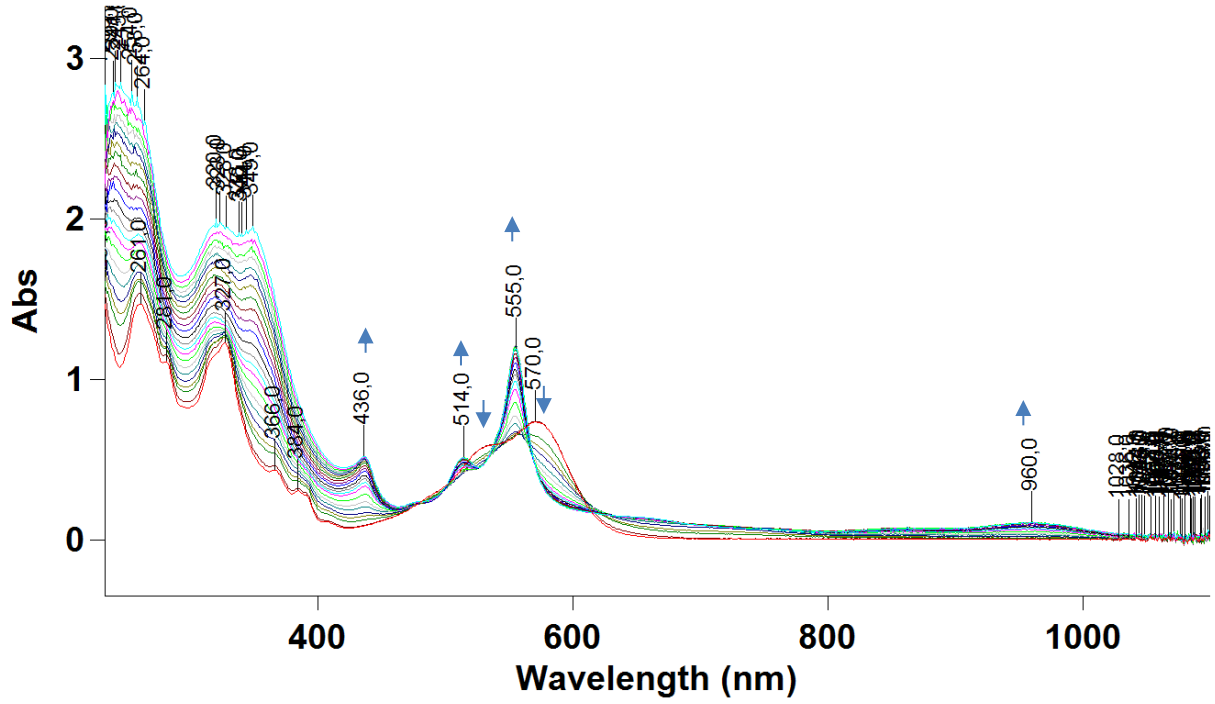

Figure S8. UV-Vis scale oxidation of **6** with $FeCl_3$ (to 0.2 mM dichloromethane solution of **6** 5 µL of 12.5 mM dichloromethane solution of $FeCl_3$ were added each step).

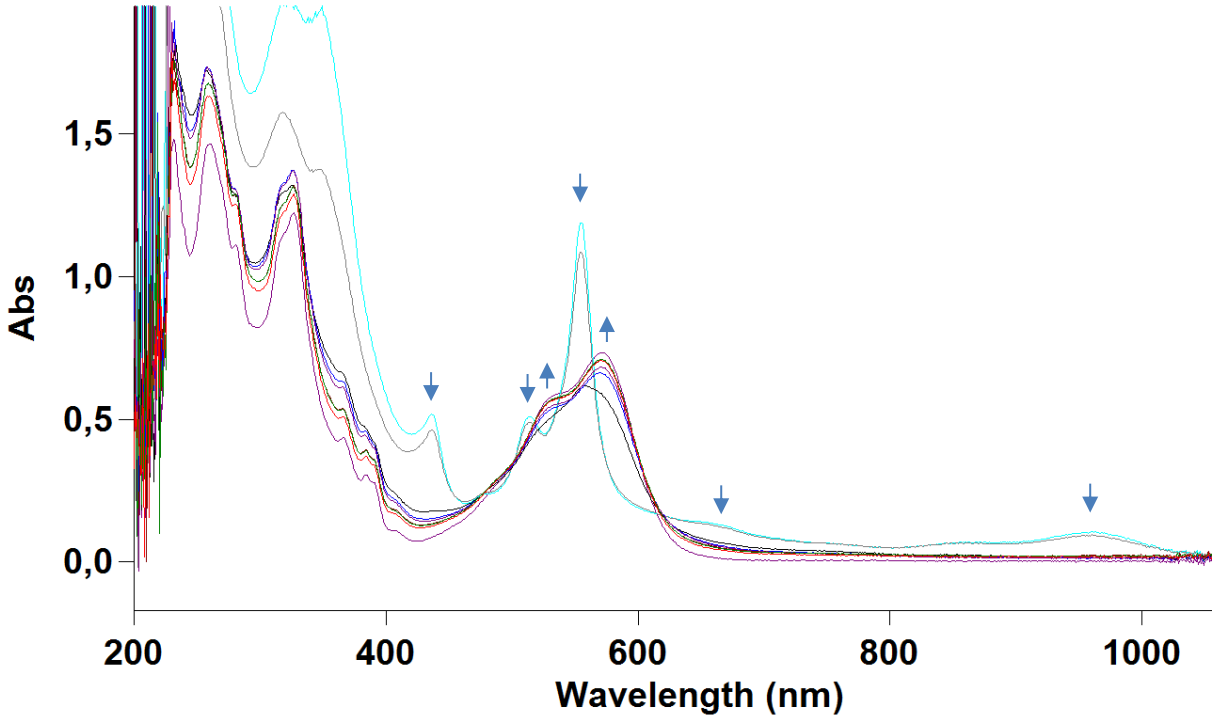

Figure S9. UV-Vis scale Zn-reduction to **6**.

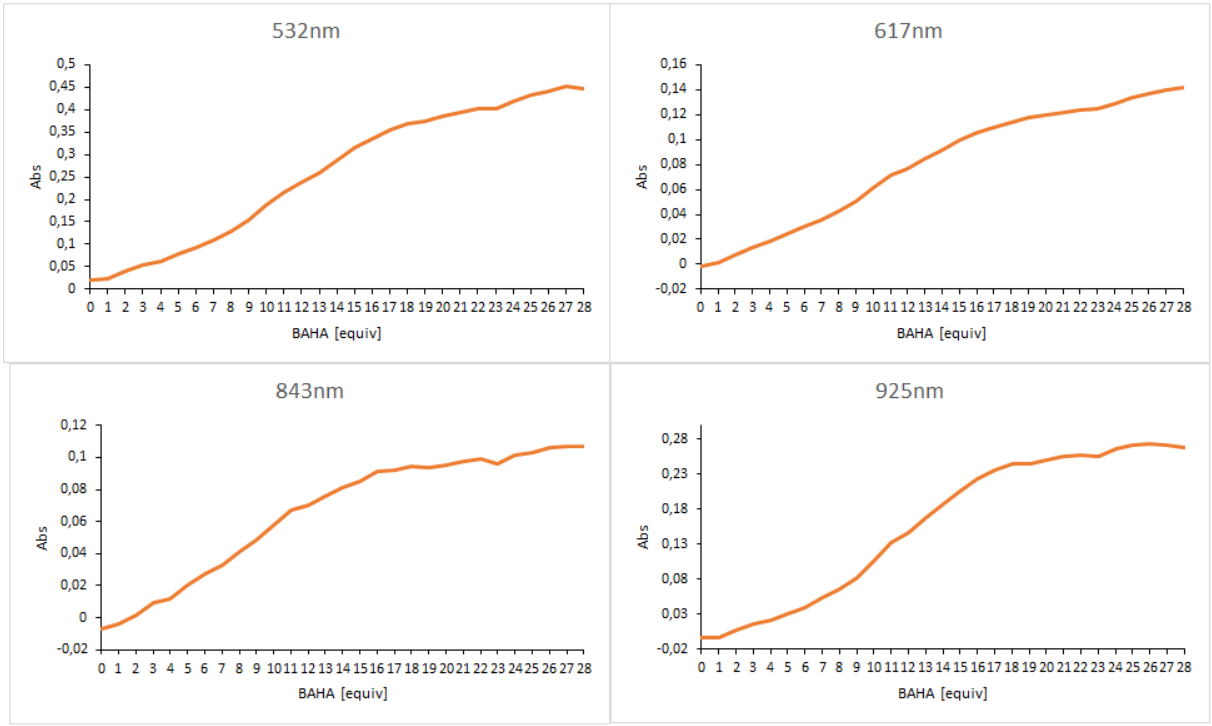

Figure S10. Titration curves observed for **12** at 532, 617, 843 and 925 nm wavelengths.

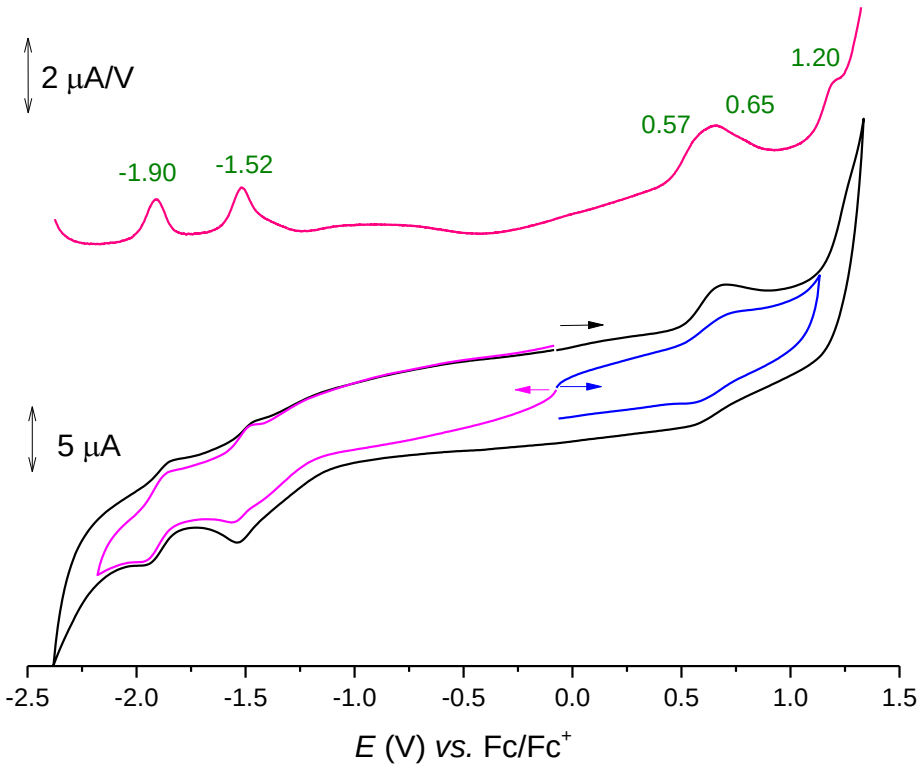

Figure S11. Differential pulse (top, red trace) and cyclic (bottom) voltammograms for **6** in DCM. The green numbers are peak potentials in volts referenced with ferrocene/ferrocenium couple potential. The arrows indicate directions of the potential sweeps. Conditions: supporting electrolyte, $[Bu_4N]PF_6$; working electrode, glassy carbon; reference electrode, Ag/AgCl; auxiliary electrode, platinum rod.

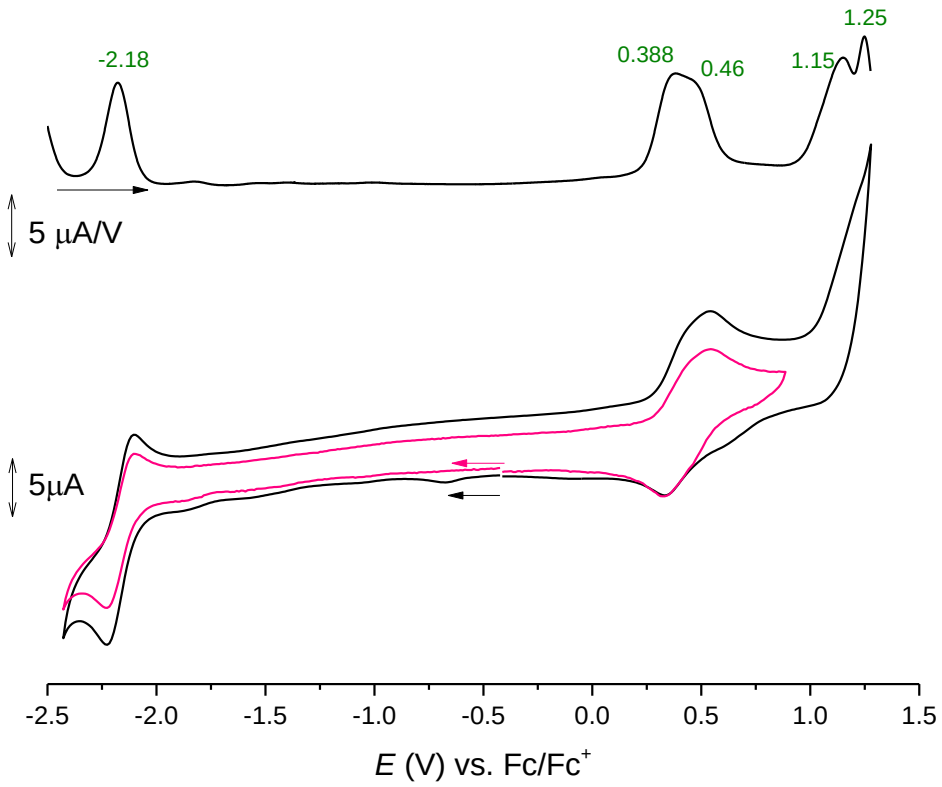

Figure S12. Differential pulse (top, red trace) and cyclic (bottom) voltammograms for **11** in DCM. The green numbers are peak potentials in volts referenced with ferrocene/ferrocenium couple potential. The arrows indicate directions of the potential sweeps. Conditions: supporting electrolyte, $[Bu_4N]PF_6$; working electrode, glassy carbon; reference electrode, Ag/AgCl; auxiliary electrode, platinum rod.

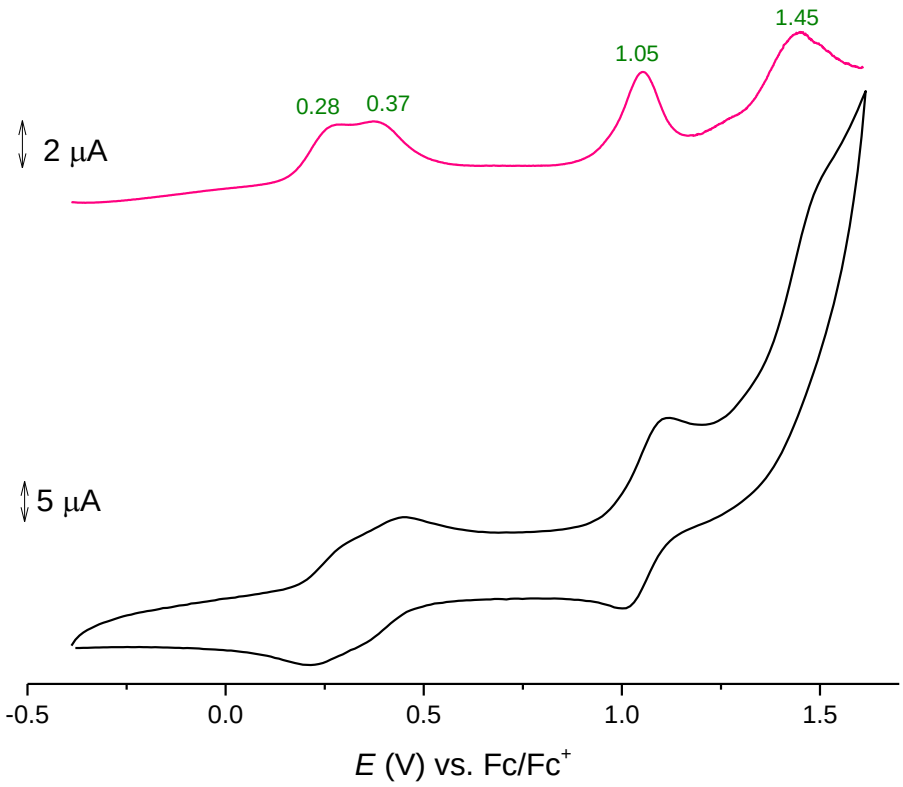

Figure S13. Differential pulse (top, red trace) and cyclic (bottom) voltammograms for **12** in DCM. The green numbers are peak potentials in volts referenced with ferrocene/ferrocenium couple potential. Conditions: supporting electrolyte, $[Bu_4N]PF_6$; working electrode, glassy carbon; reference electrode, Ag/AgCl; auxiliary electrode, platinum rod.

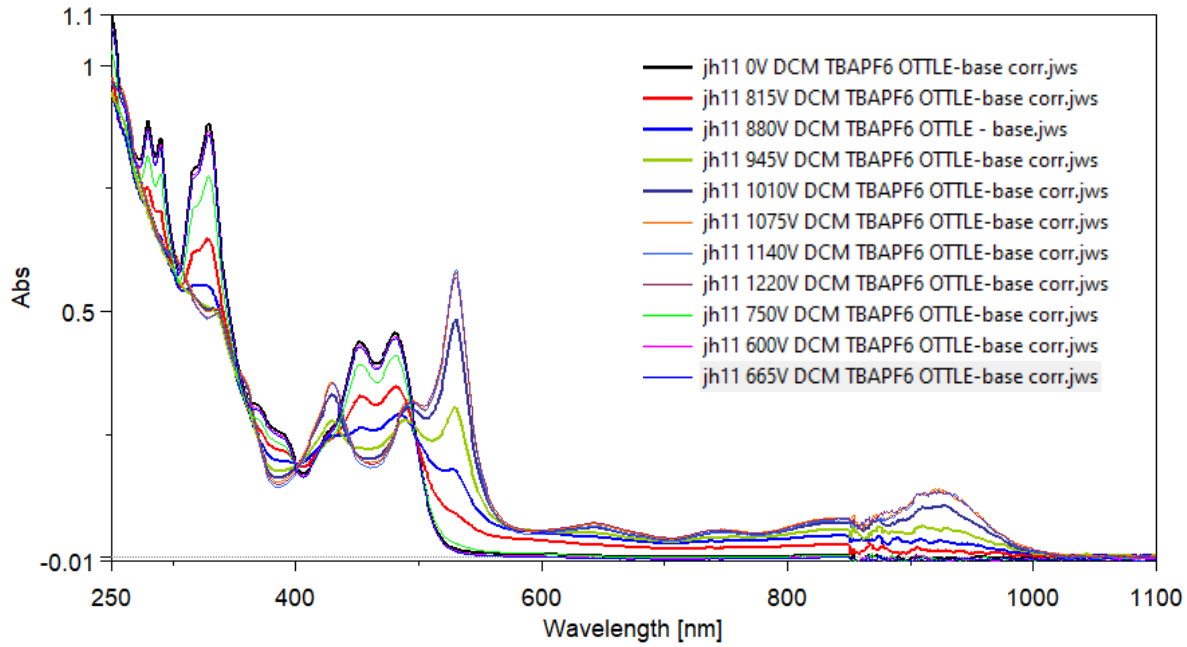

Figure S14. In-situ UV-Vis oxidation of **11** in $TBABF_6$/DCM obtained by potential scanning between 0.0 and 1.3 V vs. Ag/Ag^+.

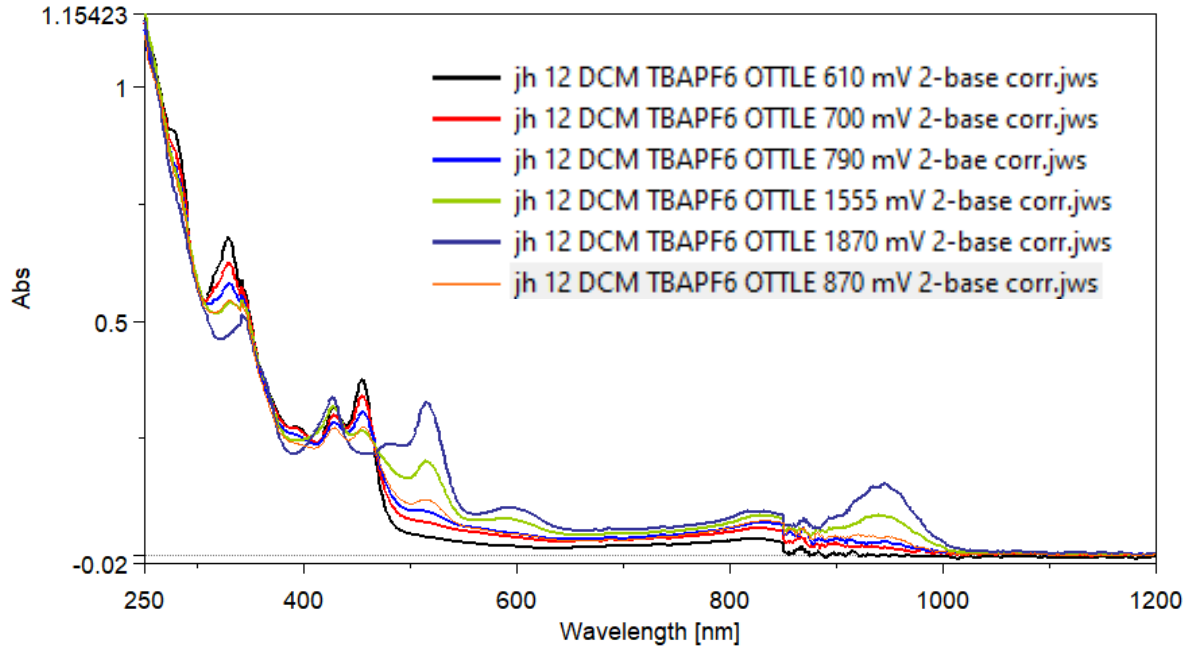

Figure S15. In-situ UV-Vis oxidation of **12** in $TBABF_6$/DCM obtained by potential scanning between 0.25 and 1.9 V vs. Ag/Ag^+.

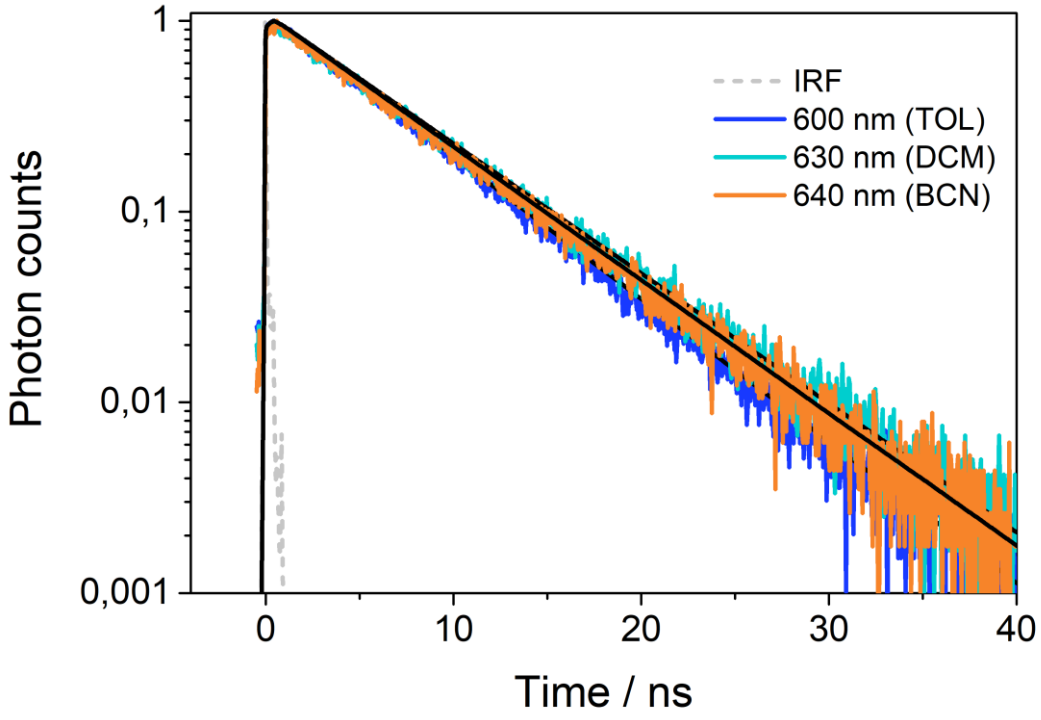

Figure S16. Time-resolved fluorescence decay profile of **6** in toluene, dichloromethane and benzonitrile.

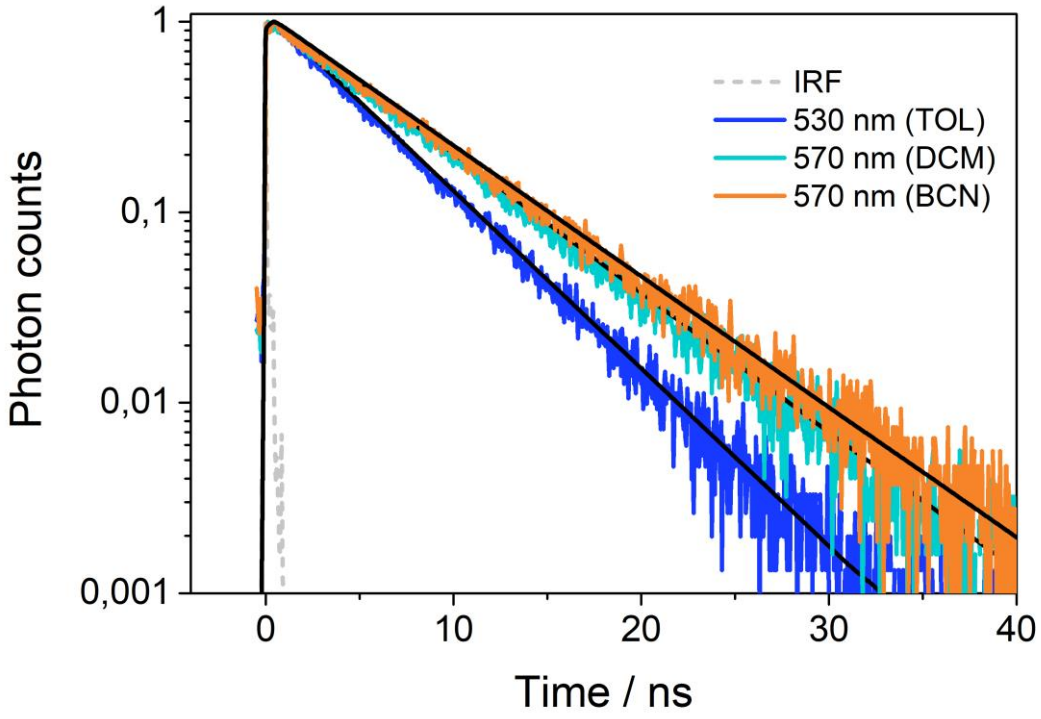

Figure S17. Time-resolved fluorescence decay profile of **4a** in toluene, dichloromethane and benzonitrile.

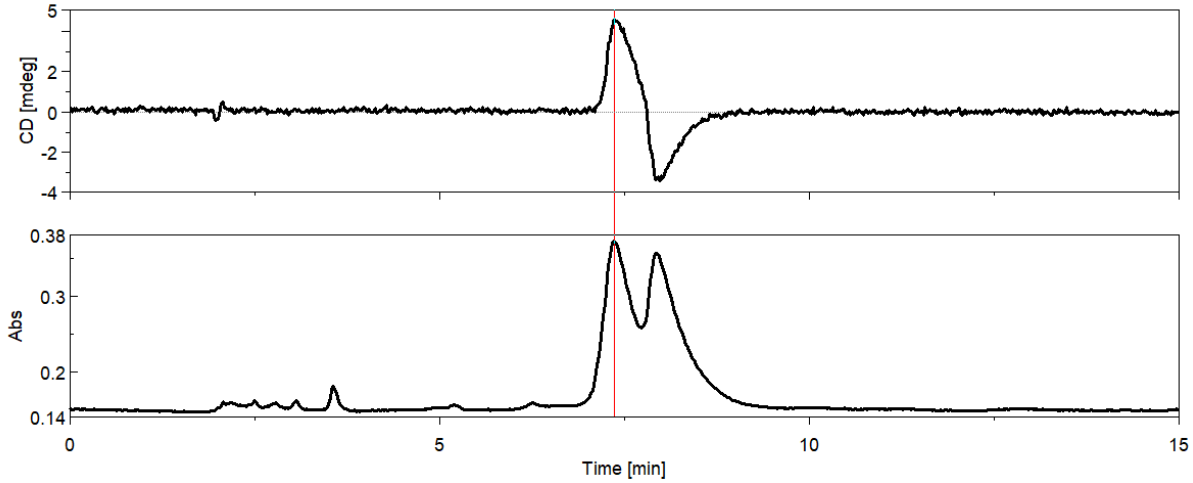

Figure S18. CD (top) and chiral-phase HPLC (bottom) profiles of racemic **8** (DCM/hexane=40/60; 303 nm).

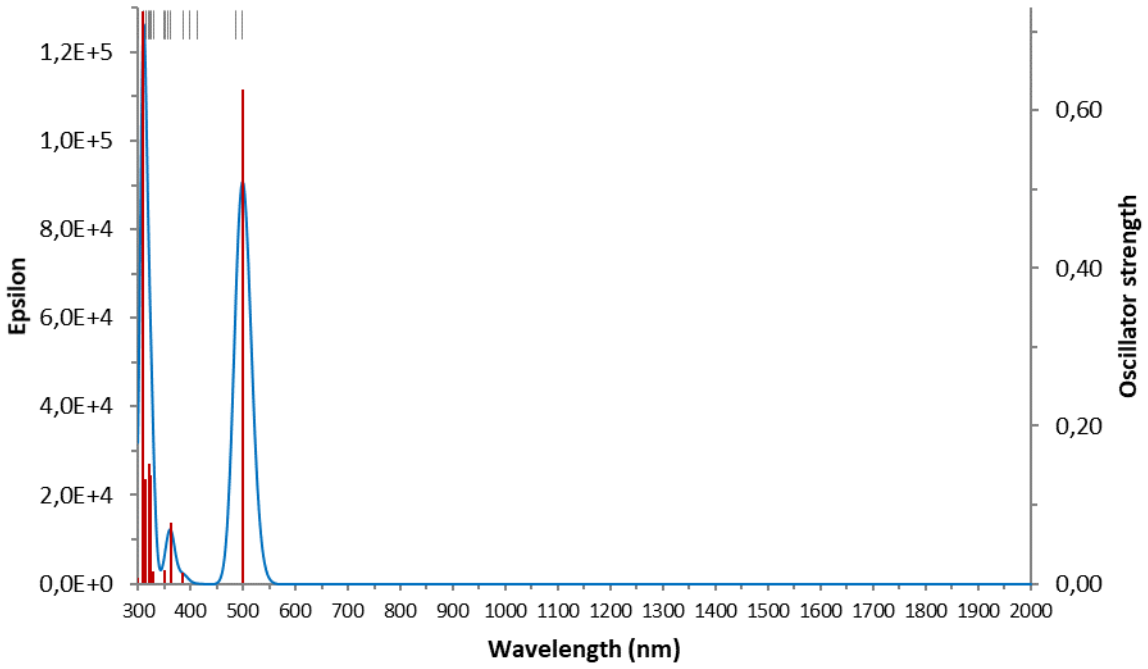

Figure S19. Simulated electronic absorption spectrum of **6** (TDA/B3LYP/6-31G(d,p))

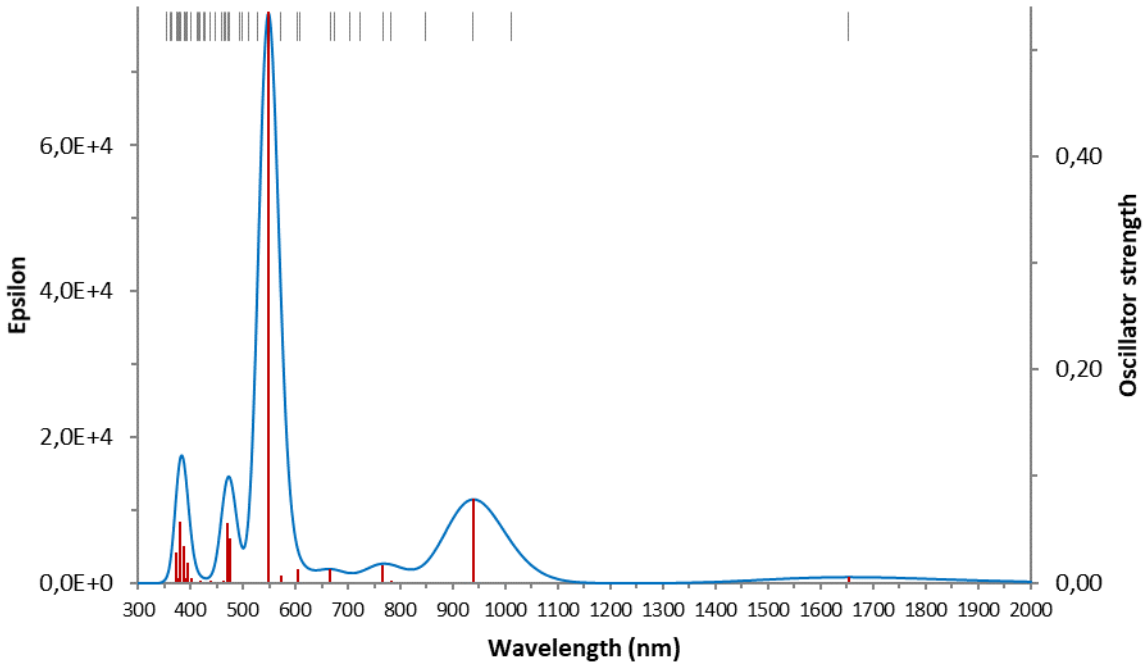

Figure S20. Simulated electronic absorption spectrum of **6**$^{\bullet+}$ (TDA/B3LYP/6-31G(d,p))

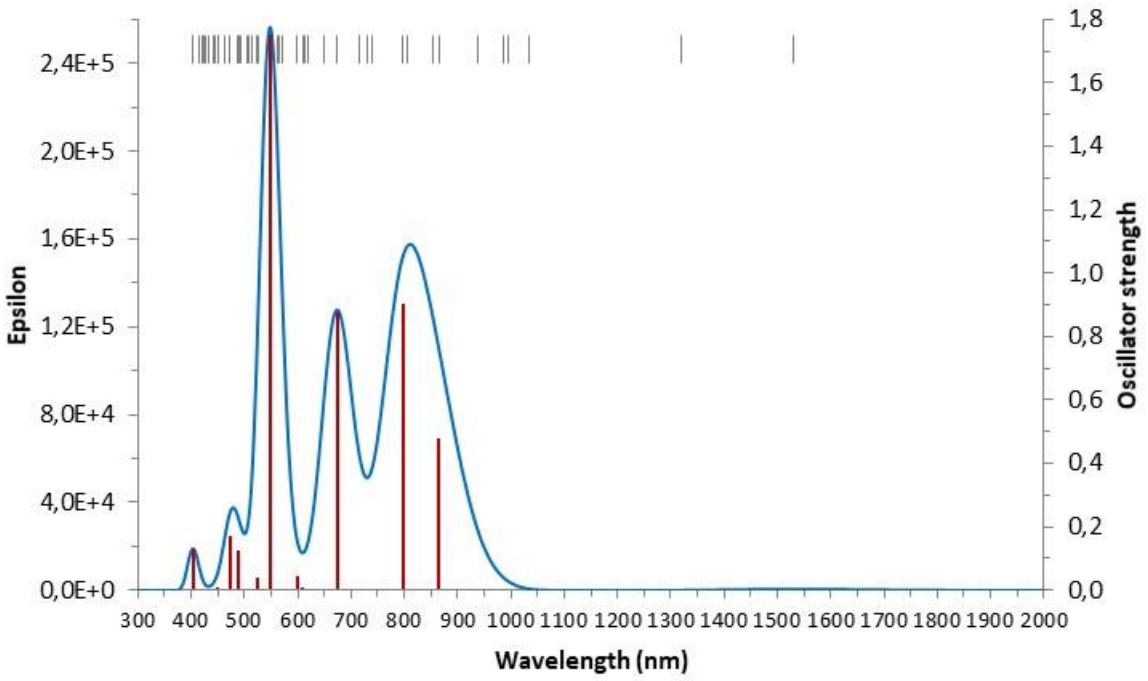

Figure S21. Simulated electronic absorption spectrum of $\mathbf{6}^{2+}$ (TDA/B3LYP/6-31G(d,p))

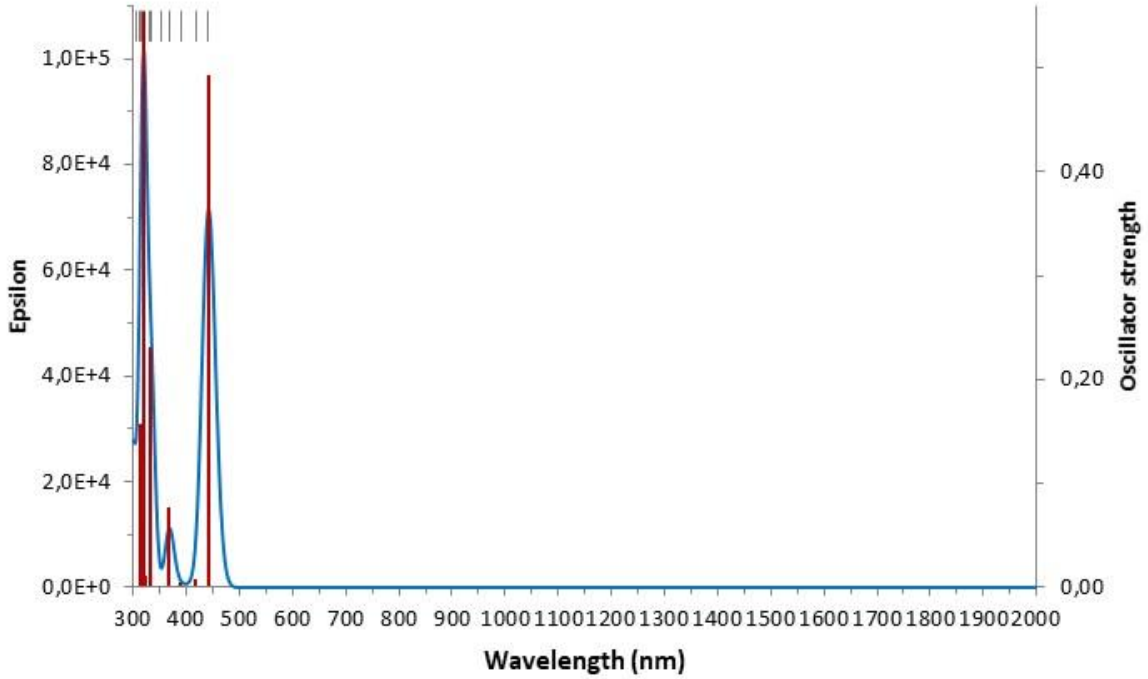

Figure S22. Simulated electronic absorption spectrum of **11** (TDA/B3LYP/6-31G(d,p))

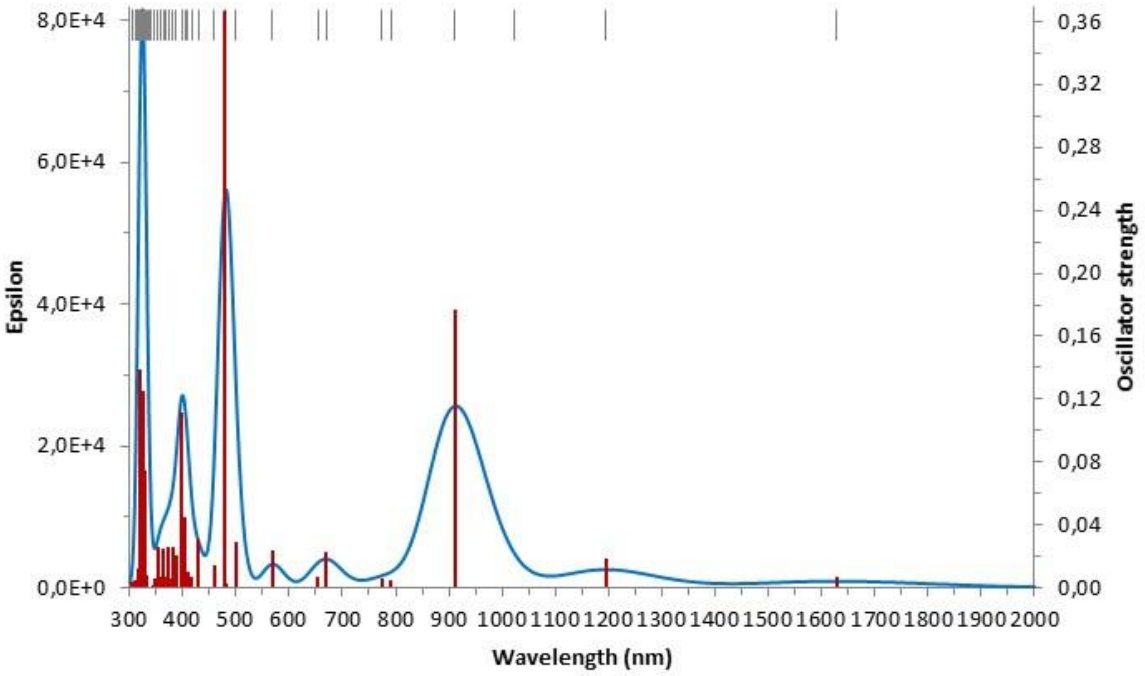

Figure S23. Simulated electronic absorption spectrum of **11**$^{\bullet+}$ (TDA/B3LYP/6-31G(d,p))

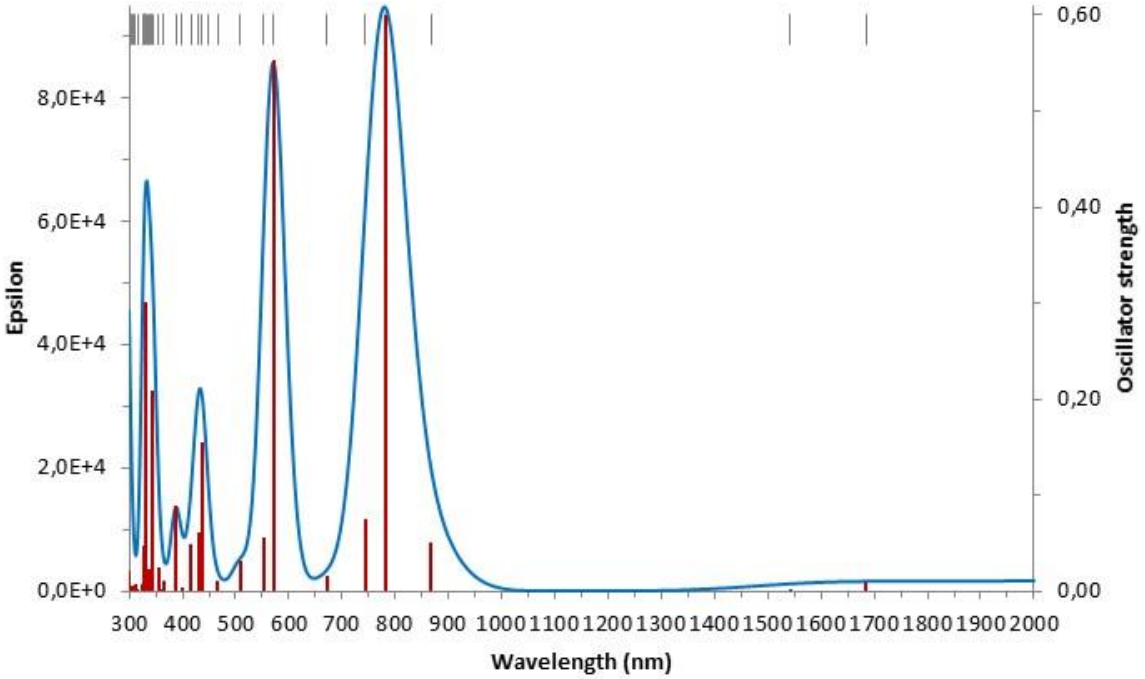

Figure S24. Simulated electronic absorption spectrum of **11**$^{2+}$ (TDA/B3LYP/6-31G(d,p))

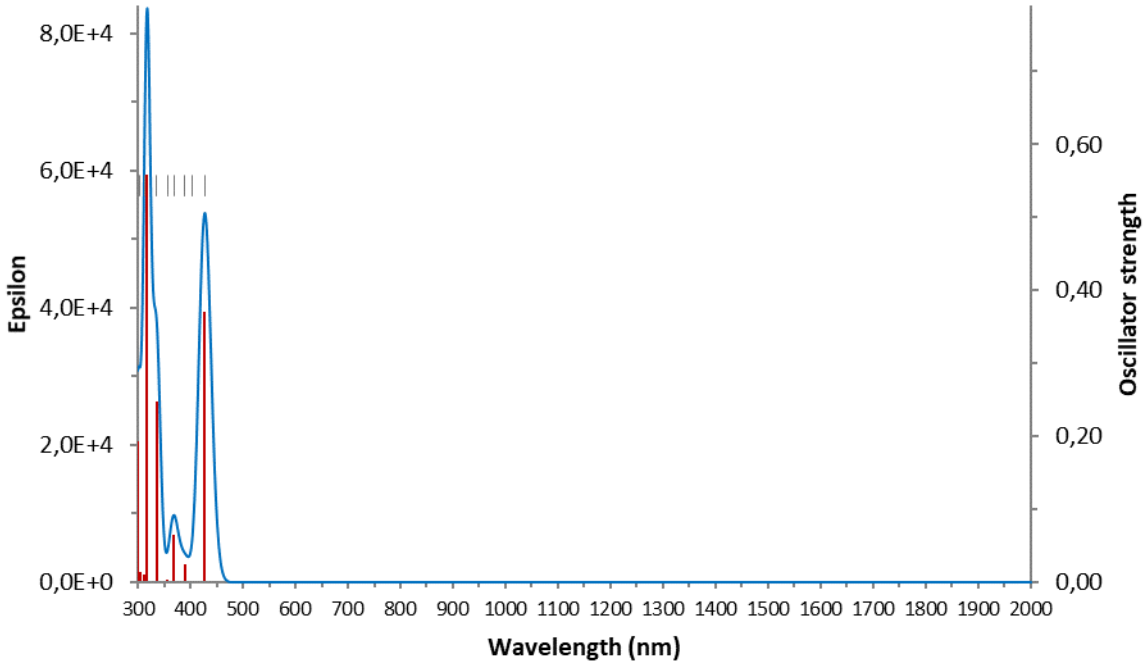

Figure S25. Simulated electronic absorption spectrum of **12** (TDA/B3LYP/6-31G(d,p))

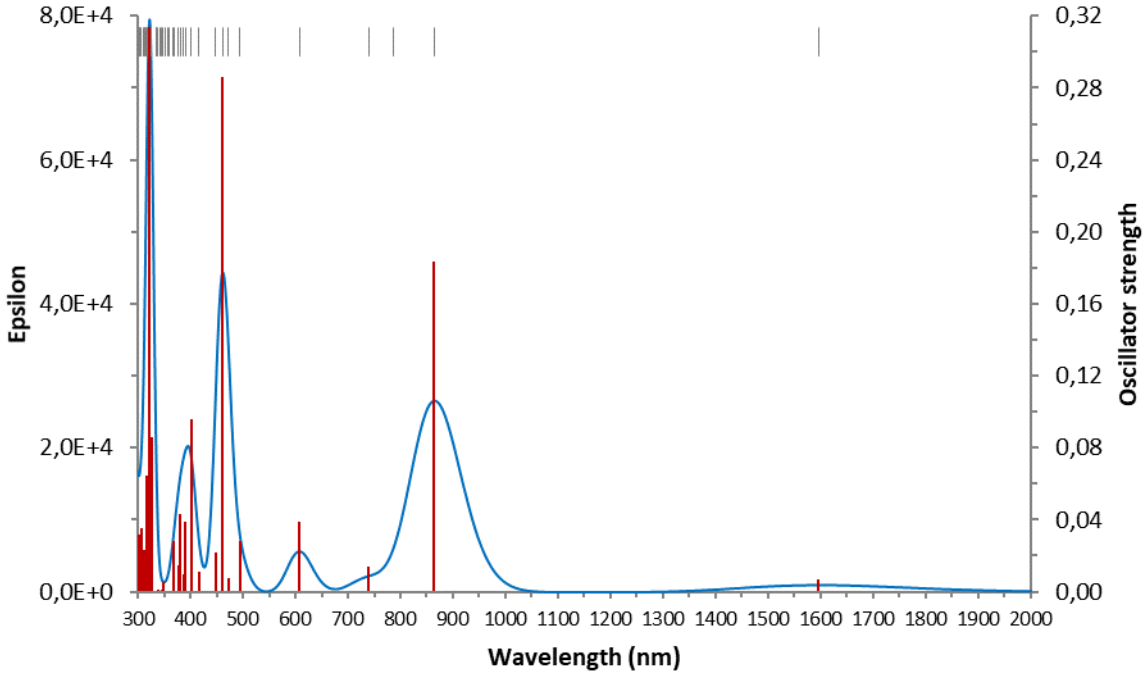

Figure S26. Simulated electronic absorption spectrum of **12**$^{\bullet+}$ (TDA/B3LYP/6-31G(d,p))

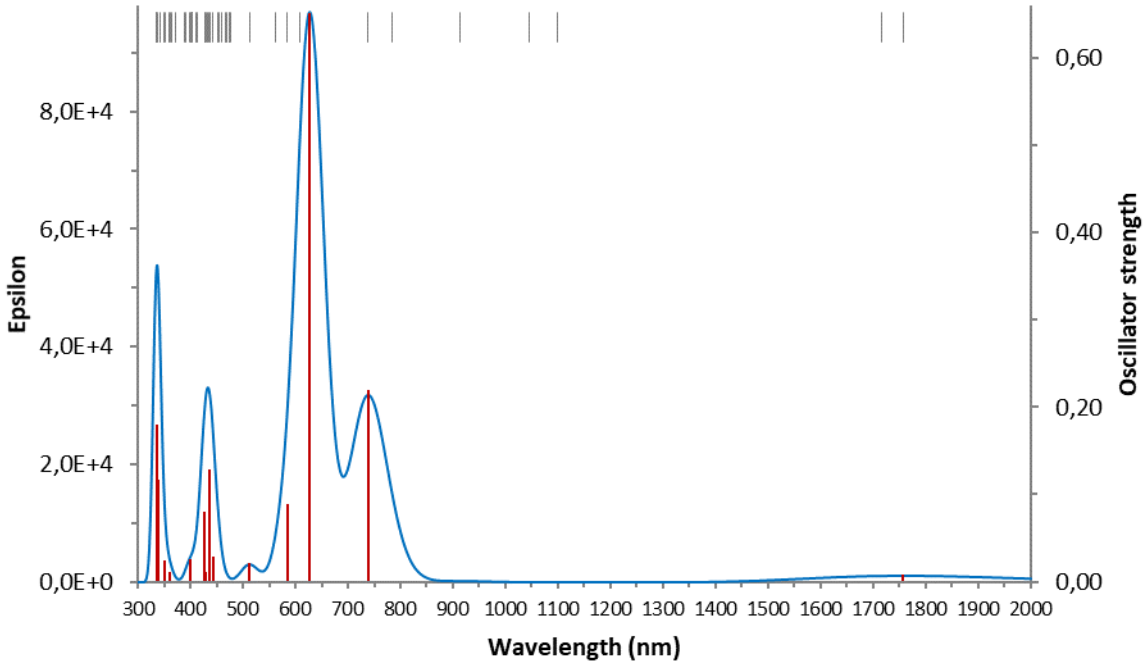

Figure S27. Simulated electronic absorption spectrum of **12**$^{2+}$ (TDA/B3LYP/6-31G(d,p))

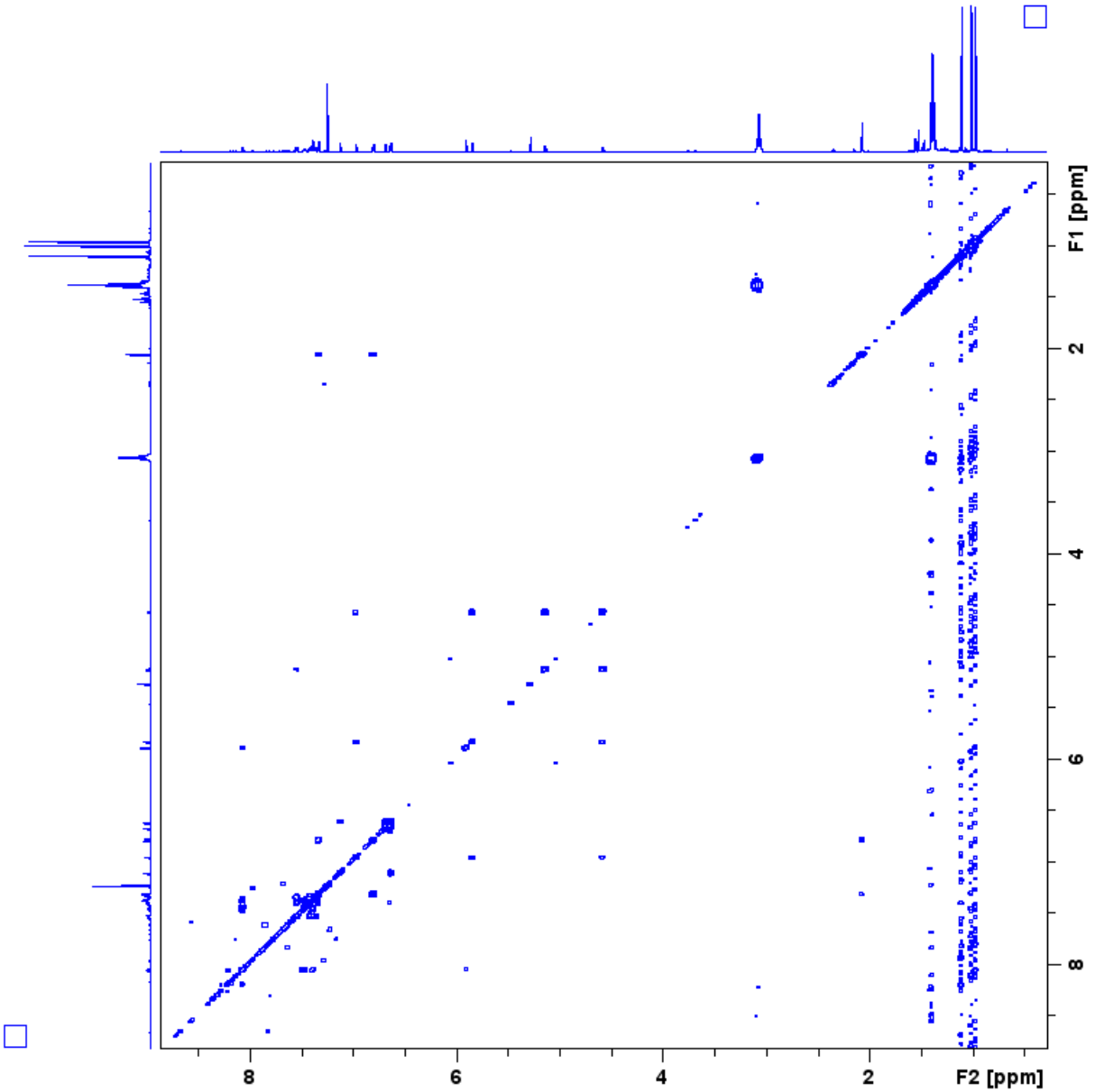

Figure S28. COSY spectrum of **12'** (500 MHz, chloroform-*d*, 300 K)

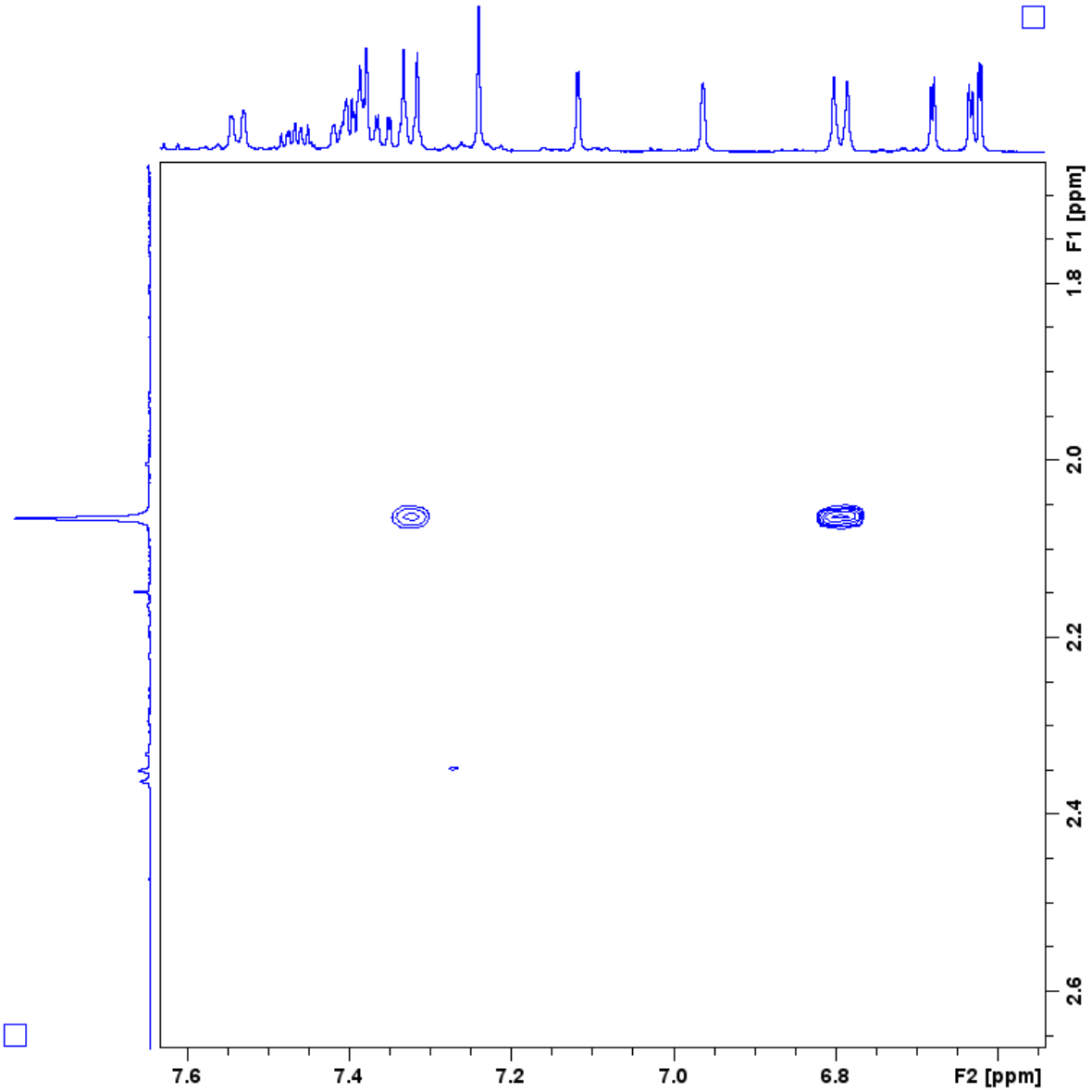

Figure S29. COSY spectrum of **12'** (500 MHz, chloroform-*d*, 300 K)

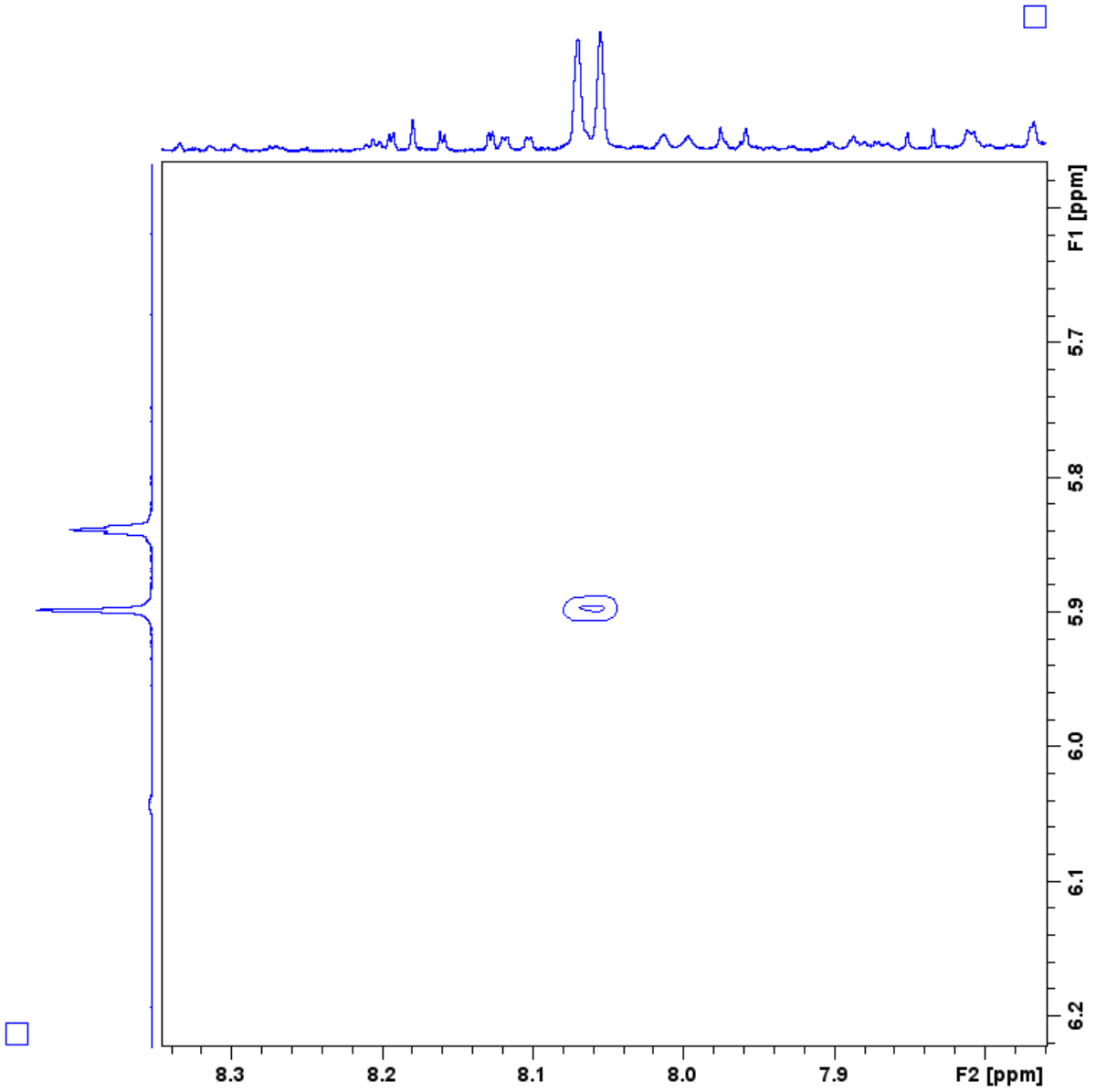

Figure S30. COSY spectrum of **12'** (500 MHz, chloroform-*d*, 300 K)

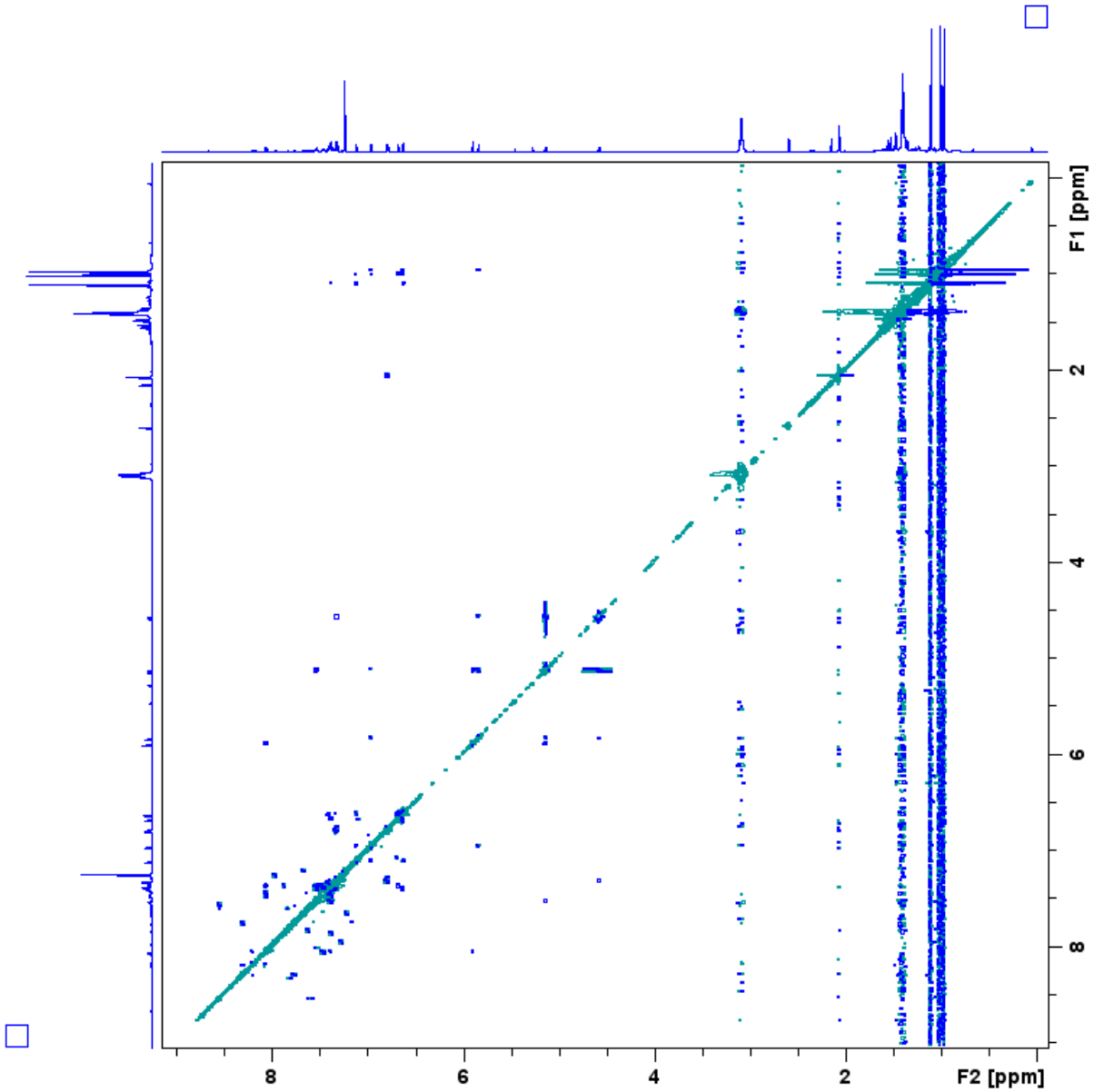

Figure S31. ROESY spectrum of **12'** (500 MHz, chloroform-*d*, 300 K)

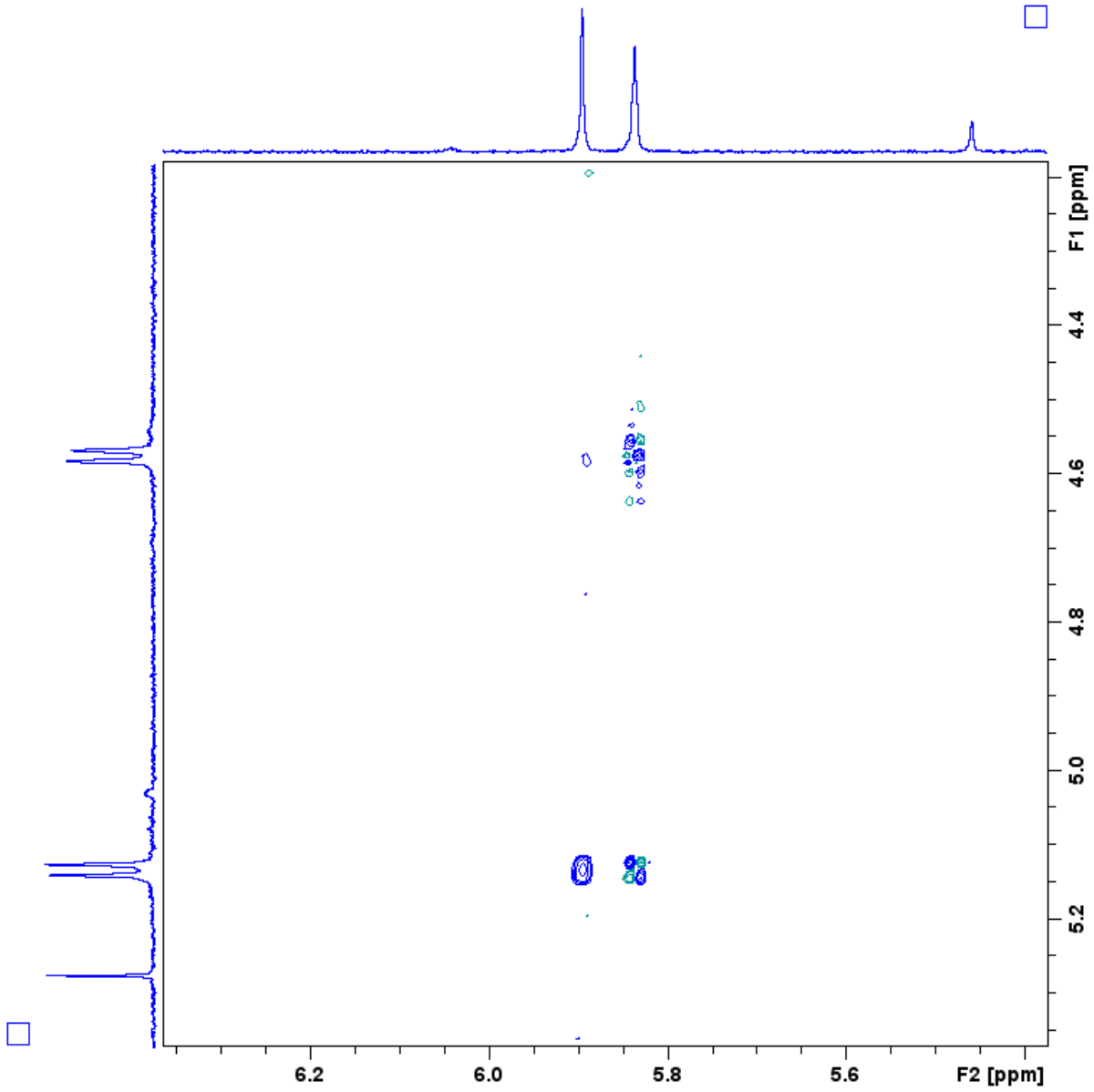

Figure S32. ROESY spectrum of **12'** (500 MHz, chloroform-*d*, 300 K)

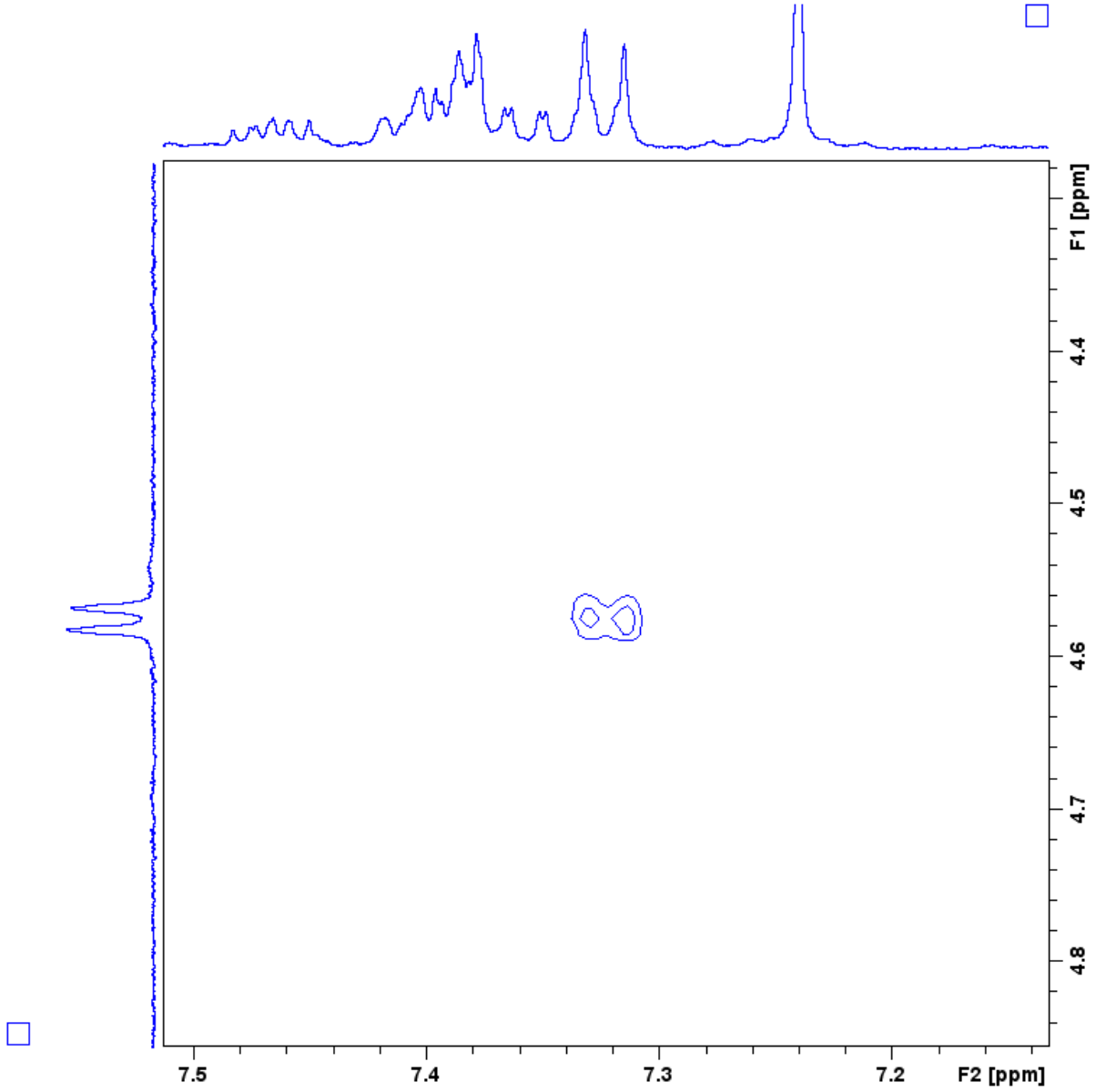

Figure S33. ROESY spectrum of **12'** (500 MHz, chloroform-*d*, 300 K)

Additional Tables

Table S1. Crystal data and structure refinement for **6**·0.6$CDCl_3$·0.4MeOH.

Identification code	hag4	
Empirical formula	$C_{46}H_{32}N_2O_2$·0.6$CDCl_3$·0.4MeOH	
Formula weight	729.78	
Temperature	100(2) K	
Wavelength	1.54184 Å	
Crystal system	Triclinic	
Space group	*P*-1	
Unit cell dimensions	*a* = 8.004(3) Å	α= 69.01(5)°.
	b = 15.289(5) Å	β= 83.97(4)°.
	c = 16.218(6) Å	γ = 86.68(4)°.
Volume	1842.3(13) $Å^3$	
Z	2	
Density (calculated)	1.316 Mg/m^3	
Absorption coefficient	1.797 mm^{-1}	
F(000)	760	
Crystal size	0.120 x 0.010 x 0.010 mm^3	
Theta range for data collection	2.930 to 66.993°.	
Index ranges	-7<=h<=9, -18<=k<=17, -19<=l<=18	
Reflections collected	21540	
Independent reflections	6492 [R(int) = 0.1141]	
Completeness to theta = 67.000°	98.7 %	
Absorption correction	Semi-empirical from equivalents	
Max. and min. transmission	1.00000 and 0.61200	
Refinement method	Full-matrix least-squares on F^2	
Data / restraints / parameters	6492 / 2 / 501	
Goodness-of-fit on F^2	1.165	
Final R indices [I>2sigma(I)]	R1 = 0.1716, wR2 = 0.3934	
R indices (all data)	R1 = 0.3542, wR2 = 0.4984	
Extinction coefficient	n/a	
Largest diff. peak and hole	0.644 and -0.392 e.$Å^{-3}$	

Table S2. Electronic transitions calculated for **6** using the TDA/B3LYP/6-31G(d,p) level of theory.

No.	Energy (cm^{-1})	λ (nm)	f[a]	Major excitations[b]
1	20034	499.2	0.626	HOMO»LUMO (94%)
2	20606	485.3	0.002	H–1»LUMO (98%)
3	24209	413.1	0.001	H–2»LUMO (99%)
4	25118	398.1	0.000	H–3»LUMO (91%)
5	25916	385.9	0.015	H–4»LUMO (17%) HOMO»L+1 (77%)
6	27594	362.4	0.077	H–1»L+1 (20%) HOMO»L+2 (70%)
7	27950	357.8	0.000	H–6»LUMO (89%)
8	28404	352.1	0.018	H–4»LUMO (76%) HOMO»L+1 (14%)
9	28634	349.2	0.000	HOMO»L+3 (91%)
10	30355	329.4	0.016	H–7»LUMO (50%) H–1»L+1 (28%) HOMO»L+4 (12%)
11	30802	324.7	0.138	H–8»LUMO (21%) H–7»LUMO (11%) H–1»L+1 (39%)
12	31030	322.3	0.153	H–5»LUMO (82%)
13	31293	319.6	0.000	H–10»LUMO (94%)
14	31740	315.1	0.132	H–8»LUMO (69%) H–7»LUMO (12%)
15	32264	309.9	0.726	H–1»L+2 (79%) HOMO»L+5 (10%)
16	33282	300.5	0.008	H–9»LUMO (46%) H–7»LUMO (13%) HOMO»L+4 (30%)
17	34107	293.2	0.061	H–1»L+3 (82%) HOMO»L+5 (11%)
18	34523	289.7	0.002	H–2»L+1 (100%)
19	34751	287.8	0.002	H–4»L+2 (15%) H–2»L+2 (33%) HOMO»L+4 (10%) HOMO»L+6 (32%)
20	34900	286.5	0.002	H–2»L+2 (65%) HOMO»L+6 (20%)
21	35601	280.9	0.006	H–11»LUMO (32%) H–9»LUMO (24%) HOMO»L+4 (22%)
22	35860	278.9	0.020	H–11»LUMO (62%)
23	36164	276.5	0.021	H–4»L+2 (64%) HOMO»L+6 (25%)
24	36227	276.0	0.000	H–3»L+1 (99%)
25	36370	275.0	0.396	H–1»L+3 (11%) HOMO»L+5 (57%)
26	36388	274.8	0.026	H–3»L+2 (90%)
27	37459	267.0	0.110	H–4»L+1 (74%)
28	37681	265.4	0.051	H–1»L+4 (79%)
29	38361	260.7	0.001	H–12»LUMO (26%) H–5»L+2 (31%) H–4»L+3 (13%) H–2»L+3 (17%)
30	38501	259.7	0.000	H–12»LUMO (10%) H–2»L+3 (79%)
31	38577	259.2	0.032	H–5»L+1 (82%)
32	38748	258.1	0.005	H–12»LUMO (22%) H–7»L+1 (12%) H–4»L+3 (10%) H–1»L+5 (39%)
33	39134	255.5	0.020	H–12»LUMO (10%) H–5»L+2 (23%) H–1»L+5 (12%) HOMO»L+7 (37%)
34	39415	253.7	0.051	H–12»LUMO (17%) H–7»L+1 (12%) H–1»L+5 (30%) HOMO»L+7 (21%)
35	39582	252.6	0.108	H–5»L+2 (26%) H–4»L+3 (16%) HOMO»L+7 (25%)
36	40070	249.6	0.000	H–6»L+2 (20%) H–3»L+3 (69%)
37	40301	248.1	0.000	H–6»L+2 (66%) H–3»L+3 (26%)
38	40395	247.6	0.674	H–1»L+6 (67%)
39	40535	246.7	0.050	H–7»L+2 (65%)
40	40587	246.4	0.001	H–6»L+1 (96%)
41	40896	244.5	0.121	H–8»L+1 (32%) H–7»L+1 (43%) H–4»L+3 (10%)
42	40944	244.2	0.003	H–2»L+4 (95%)
43	41170	242.9	0.002	H–14»LUMO (30%) H–7»L+2 (11%) HOMO»L+9 (28%) HOMO»L+10 (24%)
44	41452	241.2	0.212	H–8»L+1 (34%) H–5»L+3 (24%) H–4»L+3 (18%)
45	41463	241.2	0.001	H–8»L+2 (66%)
46	41596	240.4	0.028	H–13»LUMO (90%)
47	41967	238.3	0.000	H–2»L+5 (96%)
48	42051	237.8	0.000	HOMO»L+8 (97%)
49	42124	237.4	0.000	H–3»L+4 (86%)
50	42363	236.1	0.119	H–5»L+3 (47%)

[a] Oscillator strength. [b] Contributions smaller than 10% are not included. H = HOMO, L = LUMO. Orbitals are numbered consecutively regardless of possible degeneracies.

Table S3. Electronic transitions calculated for **6**$^{\bullet+}$ using the TDA/B3LYP/6-31G(d,p) level of theory.

No.	Energy (cm^{-1})	λ (nm)	f[a]	Major excitations[b]
1	2050	4877.4	0.027	HOMO(B)»LUMO(B) (99%)
2	3721	2687.1	0.000	H–1(B)»LUMO(B) (99%)
3	6048	1653.3	0.006	H–2(B)»LUMO(B) (98%)
4	9884	1011.8	0.000	H–3(B)»LUMO(B) (94%)
5	10655	938.6	0.079	H–4(B)»LUMO(B) (91%)
6	11807	846.9	0.001	H–5(B)»LUMO(B) (96%)
7	12776	782.7	0.002	H–2(A)»LUMO(A) (10%) HOMO(A)»LUMO(A) (40%) H–6(B)»LUMO(B) (46%)
8	13046	766.5	0.016	HOMO(A)»LUMO(A) (59%) H–6(B)»LUMO(B) (31%)
9	13850	722.0	0.000	H–7(B)»LUMO(B) (93%)
10	14226	702.9	0.001	HOMO(B)»L+1(B) (98%)
11	14841	673.8	0.000	H–1(A)»LUMO(A) (99%)
12	15014	666.0	0.012	H–8(B)»LUMO(B) (92%)
13	16454	607.8	0.000	H–1(B)»L+1(B) (98%)
14	16560	603.9	0.013	H–3(A)»LUMO(A) (15%) H–9(B)»LUMO(B) (77%)
15	17478	572.1	0.007	H–3(A)»LUMO(A) (51%) H–9(B)»LUMO(B) (16%) H–2(B)»L+1(B) (22%)
16	18245	548.1	0.535	H–2(A)»LUMO(A) (61%) H–6(B)»LUMO(B) (17%)
17	18983	526.8	0.000	H–10(B)»LUMO(B) (95%)
18	19573	510.9	0.000	H–4(A)»LUMO(A) (81%) H–3(B)»L+1(B) (11%)
19	20039	499.0	0.001	H–3(A)»LUMO(A) (28%) H–2(B)»L+1(B) (65%)
20	20274	493.2	0.000	H–11(B)»LUMO(B) (98%)
21	21058	474.9	0.042	H–8(A)»LUMO(A) (18%) H–6(A)»LUMO(A) (24%) H–2(A)»LUMO(A) (12%) H–6(B)»L+1(B) (15%) H–4(B)»L+1(B) (23%)
22	21205	471.6	0.056	H–14(B)»LUMO(B) (79%)
23	21474	465.7	0.001	H–5(A)»LUMO(A) (38%) H–13(B)»LUMO(B) (23%) H–5(B)»L+1(B) (20%)
24	21560	463.8	0.002	H–12(B)»LUMO(B) (53%) H–3(B)»L+1(B) (36%)
25	21704	460.7	0.001	H–12(B)»LUMO(B) (47%) H–3(B)»L+1(B) (43%)
26	22313	448.2	0.000	H–5(A)»LUMO(A) (11%) H–16(B)»LUMO(B) (30%) H–13(B)»LUMO(B) (39%) H–5(B)»L+1(B) (13%)
27	22823	438.2	0.002	H–16(B)»LUMO(B) (61%) H–13(B)»LUMO(B) (29%)
28	23353	428.2	0.000	H–7(A)»LUMO(A) (75%) H–7(B)»L+1(B) (12%)
29	23467	426.1	0.000	H–15(B)»LUMO(B) (99%)
30	23922	418.0	0.002	H–2(A)»L+1(A) (28%) HOMO(A)»L+1(A) (34%)
31	24130	414.4	0.001	H–2(A)»L+1(A) (12%) HOMO(A)»L+1(A) (64%)
32	24137	414.3	0.001	HOMO(A)»L+2(A) (96%)
33	24904	401.5	0.004	HOMO(B)»L+2(B) (84%)
34	25355	394.4	0.018	H–5(A)»LUMO(A) (10%) H–2(A)»L+2(A) (12%) H–5(B)»L+1(B) (21%) HOMO(B)»L+3(B) (30%)
35	25410	393.5	0.003	H–8(A)»LUMO(A) (27%) H–6(A)»LUMO(A) (46%) H–6(B)»L+1(B) (14%)
36	25436	393.2	0.000	H–5(A)»LUMO(A) (25%) H–5(B)»L+1(B) (35%) HOMO(B)»L+3(B) (25%)
37	25458	392.8	0.000	H–17(B)»LUMO(B) (98%)
38	25524	391.8	0.000	H–7(A)»LUMO(A) (14%) H–7(B)»L+1(B) (70%)
39	25718	388.8	0.004	H–11(A)»LUMO(A) (12%) H–9(A)»LUMO(A) (22%) H–9(B)»L+1(B) (24%) HOMO(B)»L+3(B) (24%)
40	25741	388.5	0.034	H–6(A)»LUMO(A) (12%) H–19(B)»LUMO(B) (18%) H–4(B)»L+1(B) (42%)
41	26221	381.4	0.057	H–3(A)»L+1(A) (20%) H–2(A)»L+2(A) (31%) HOMO(B)»L+3(B) (17%)
42	26373	379.2	0.001	H–1(A)»L+2(A) (98%)
43	26409	378.7	0.004	H–1(A)»L+1(A) (96%)
44	26576	376.3	0.000	H–18(B)»LUMO(B) (98%)
45	26742	373.9	0.002	H–3(A)»L+2(A) (12%) H–19(B)»LUMO(B) (56%)
46	26813	373.0	0.028	H–3(A)»L+1(A) (18%) H–2(A)»L+2(A) (19%) H–2(B)»L+2(B) (27%)
47	27512	363.5	0.000	H–1(B)»L+2(B) (100%)
48	27541	363.1	0.001	H–2(A)»L+1(A) (38%) H–4(B)»L+1(B) (10%)
49	28133	355.4	0.001	HOMO(A)»L+3(A) (77%) HOMO(B)»L+4(B) (10%)
50	28209	354.5	0.001	H–1(B)»L+3(B) (90%)

[a] Oscillator strength. [b] Contributions smaller than 10% are not included. H = HOMO, L = LUMO. Orbitals are numbered consecutively regardless of possible degeneracies.

Table S4. Electronic transitions calculated for $\mathbf{6}^{2+}$ using the TDA/B3LYP/6-31G(d,p) level of theory.

No.	Energy (cm^{-1})	λ (nm)	f[a]	Major excitations[b]
1	-2987	-3347.3	0.000	HOMO(A)»LUMO(A) (50%) HOMO(B)»LUMO(B) (50%)
2	2879	3472.9	0.000	H–1(A)»LUMO(A) (50%) H–1(B)»LUMO(B) (50%)
3	4174	2395.8	0.001	H–1(A)»LUMO(A) (50%) H–1(B)»LUMO(B) (50%)
4	4726	2115.8	0.000	H–2(A)»LUMO(A) (50%) H–2(B)»LUMO(B) (50%)
5	6533	1530.7	0.005	H–2(A)»LUMO(A) (49%) H–2(B)»LUMO(B) (49%)
6	7577	1319.8	0.000	H–3(A)»LUMO(A) (49%) H–3(B)»LUMO(B) (49%)
7	9658	1035.4	0.000	H–4(A)»LUMO(A) (49%) H–4(B)»LUMO(B) (49%)
8	10055	994.5	0.000	H–6(A)»LUMO(A) (49%) H–6(B)»LUMO(B) (49%)
9	10148	985.4	0.000	H–4(A)»LUMO(A) (49%) H–4(B)»LUMO(B) (49%)
10	10674	936.9	0.000	H–5(A)»LUMO(A) (49%) H–5(B)»LUMO(B) (49%)
11	11565	864.7	0.477	H–3(A)»LUMO(A) (27%) HOMO(A)»LUMO(A) (20%) H–3(B)»LUMO(B) (27%) HOMO(B)»LUMO(B) (20%)
12	11701	854.6	0.001	H–5(A)»LUMO(A) (50%) H–5(B)»LUMO(B) (50%)
13	12406	806.0	0.000	H–7(A)»LUMO(A) (46%) H–7(B)»LUMO(B) (46%)
14	12541	797.4	0.904	H–6(A)»LUMO(A) (22%) H–3(A)»LUMO(A) (14%) HOMO(A)»LUMO(A) (12%) H–6(B)»LUMO(B) (22%) H–3(B)»LUMO(B) (14%) HOMO(B)»LUMO(B) (12%)
15	13508	740.3	0.000	H–8(A)»LUMO(A) (49%) H–8(B)»LUMO(B) (49%)
16	13685	730.7	0.000	H–9(A)»LUMO(A) (44%) H–9(B)»LUMO(B) (44%)
17	13956	716.5	0.002	H–8(A)»LUMO(A) (49%) H–8(B)»LUMO(B) (49%)
18	13966	716.0	0.003	H–7(A)»LUMO(A) (48%) H–7(B)»LUMO(B) (48%)
19	14843	673.7	0.878	H–6(A)»LUMO(A) (16%) HOMO(A)»L+1(A) (23%) H–6(B)»LUMO(B) (16%) HOMO(B)»L+1(B) (23%)
20	15429	648.1	0.000	HOMO(A)»L+1(A) (49%) HOMO(B)»L+1(B) (49%)
21	16109	620.8	0.000	H–10(A)»LUMO(A) (41%) H–10(B)»LUMO(B) (41%)
22	16273	614.5	0.000	H–13(A)»LUMO(A) (41%) H–13(B)»LUMO(B) (41%)
23	16388	610.2	0.007	H–10(A)»LUMO(A) (28%) H–9(A)»LUMO(A) (20%) H–10(B)»LUMO(B) (28%) H–9(B)»LUMO(B) (20%)
24	16687	599.3	0.044	H–10(A)»LUMO(A) (21%) H–9(A)»LUMO(A) (23%) H–10(B)»LUMO(B) (21%) H–9(B)»LUMO(B) (23%)
25	17482	572.0	0.000	H–11(A)»LUMO(A) (49%) H–11(B)»LUMO(B) (49%)
26	17683	565.5	0.000	H–11(A)»LUMO(A) (50%) H–11(B)»LUMO(B) (50%)

No.	Energy (cm^{-1})	λ (nm)	f[a]	Major excitations[b]
27	17785	562.3	0.000	H–12(A)»LUMO(A) (49%) H–12(B)»LUMO(B) (49%)
28	18239	548.3	2047186.000	HOMO(A)»L+1(A) (25%) HOMO(B)»L+1(B) (25%)
29	19035	525.3	0.037	H–12(A)»LUMO(A) (49%) H–12(B)»LUMO(B) (49%)
30	19077	524.2	0.000	H–16(A)»LUMO(A) (11%) H–14(A)»LUMO(A) (34%) H–16(B)»LUMO(B) (11%) H–14(B)»LUMO(B) (34%)
31	19470	513.6	0.000	H–16(A)»LUMO(A) (22%) H–14(A)»LUMO(A) (15%) H–2(A)»L+1(A) (11%) H–16(B)»LUMO(B) (22%) H–14(B)»LUMO(B) (15%) H–2(B)»L+1(B) (11%)
32	19644	509.0	0.000	H–14(A)»LUMO(A) (49%) H–14(B)»LUMO(B) (49%)
33	19796	505.2	0.000	H–15(A)»LUMO(A) (50%) H–15(B)»LUMO(B) (50%)
34	20227	494.4	0.000	H–1(A)»L+1(A) (47%) H–1(B)»L+1(B) (47%)
35	20399	490.2	0.000	H–1(A)»L+1(A) (49%) H–1(B)»L+1(B) (49%)
36	20441	489.2	0.000	H–16(A)»LUMO(A) (16%) H–2(A)»L+1(A) (30%) H–16(B)»LUMO(B) (16%) H–2(B)»L+1(B) (30%)
37	20474	488.4	0.124	H–15(A)»LUMO(A) (48%) H–15(B)»LUMO(B) (48%)
38	21138	473.1	0.171	H–13(A)»LUMO(A) (36%) H–13(B)»LUMO(B) (36%)
39	21610	462.7	0.000	H–6(A)»L+1(A) (16%) H–3(A)»L+1(A) (27%) H–6(B)»L+1(B) (16%) H–3(B)»L+1(B) (27%)
40	22173	451.0	0.000	H–17(A)»LUMO(A) (50%) H–17(B)»LUMO(B) (50%)
41	22244	449.6	0.008	H–16(A)»LUMO(A) (46%) H–16(B)»LUMO(B) (46%)
42	22546	443.5	0.000	H–17(A)»LUMO(A) (50%) H–17(B)»LUMO(B) (50%)
43	22698	440.6	0.006	H–2(A)»L+1(A) (46%) H–2(B)»L+1(B) (46%)
44	23052	433.8	0.000	HOMO(A)»L+2(A) (47%) HOMO(B)»L+2(B) (47%)
45	23400	427.4	0.000	H–20(A)»LUMO(A) (11%) H–19(A)»LUMO(A) (33%) H–20(B)»LUMO(B) (11%) H–19(B)»LUMO(B) (33%)
46	23539	424.8	0.000	H–4(A)»L+1(A) (41%) H–4(B)»L+1(B) (41%)
47	23830	419.6	0.000	H–18(A)»LUMO(A) (46%) H–18(B)»LUMO(B) (46%)
48	24157	414.0	0.000	H–20(A)»LUMO(A) (25%) H–20(B)»LUMO(B) (25%)
49	24765	403.8	0.132	HOMO(A)»L+2(A) (41%) HOMO(B)»L+2(B) (41%)
50	24766	403.8	0.000	H–5(A)»L+1(A) (40%) H–5(B)»L+1(B) (40%)

[a] Oscillator strength. [b] Contributions smaller than 10% are not included. H = HOMO, L = LUMO. Orbitals are numbered consecutively regardless of possible degeneracies.

Table S5. Electronic transitions calculated for **11** using the TDA/B3LYP/6-31G(d,p) level of theory.

No.	Energy (cm^{-1})	λ (nm)	f[a]	Major excitations[b]
1	22691	440.7	0.493	HOMO»LUMO (90%)
2	23974	417.1	0.008	H–1»LUMO (95%)
3	25660	389.7	0.004	HOMO»L+1 (91%)
4	27237	367.2	0.077	H–1»L+1 (25%) HOMO»L+2 (58%) HOMO»L+3 (12%)
5	28242	354.1	0.001	HOMO»L+3 (83%)
6	30021	333.1	0.232	H–1»L+1 (61%) HOMO»L+2 (23%)
7	30156	331.6	0.030	H–3»LUMO (34%) H–2»LUMO (59%)
8	31105	321.5	0.012	H–4»LUMO (92%)
9	31355	318.9	0.554	H–3»LUMO (29%) H–1»L+2 (47%)
10	31711	315.3	0.000	H–7»LUMO (24%) HOMO»L+4 (64%)
11	31936	313.1	0.157	H–3»LUMO (27%) H–2»LUMO (20%) H–1»L+2 (34%)
12	32770	305.2	0.001	H–8»LUMO (10%) H–5»LUMO (75%)
13	33496	298.5	0.173	H–1»L+3 (84%) HOMO»L+5 (10%)
14	34019	294.0	0.001	H–6»LUMO (83%)
15	34563	289.3	0.027	H–8»LUMO (65%)
16	35180	284.3	0.047	H–7»LUMO (17%) H–2»L+2 (50%)
17	35439	282.2	0.036	H–7»LUMO (32%) H–2»L+2 (17%) HOMO»L+4 (10%) HOMO»L+6 (14%)
18	36108	276.9	0.084	H–2»L+1 (59%) HOMO»L+6 (15%)
19	36194	276.3	0.038	H–9»LUMO (11%) H–2»L+1 (18%) H–2»L+2 (11%) HOMO»L+6 (43%)
20	36537	273.7	0.200	H–1»L+4 (67%) HOMO»L+5 (22%)
21	37207	268.8	0.048	H–3»L+1 (69%)
22	37396	267.4	0.004	H–4»L+1 (22%) H–3»L+2 (32%)
23	37645	265.6	0.001	H–5»L+1 (13%) H–3»L+1 (15%) H–1»L+4 (12%) HOMO»L+5 (21%)
24	37700	265.3	0.009	H–4»L+1 (29%) H–3»L+2 (39%)
25	37777	264.7	0.001	H–9»LUMO (29%) H–4»L+1 (30%) HOMO»L+6 (10%)
26	38291	261.2	0.002	H–5»L+1 (60%) H–4»L+2 (11%)
27	38382	260.5	0.002	H–4»L+2 (77%)
28	38452	260.1	0.001	H–5»L+2 (34%) H–2»L+3 (16%)
29	39160	255.4	0.106	H–7»L+1 (14%) H–6»L+1 (19%) H–5»L+2 (29%)
30	39419	253.7	0.006	H–10»LUMO (45%) HOMO»L+7 (45%)
31	39540	252.9	0.010	H–10»LUMO (18%) H–1»L+5 (40%) HOMO»L+7 (19%)
32	39879	250.8	0.109	H–10»LUMO (10%) H–7»L+1 (11%) H–2»L+3 (11%) H–1»L+5 (34%) HOMO»L+7 (10%)
33	40043	249.7	0.010	H–7»L+1 (45%) H–6»L+1 (27%)
34	40208	248.7	0.048	H–6»L+1 (14%) H–5»L+3 (20%) H–2»L+3 (41%)
35	40303	248.1	0.172	H–6»L+2 (64%) H–1»L+6 (15%)
36	40572	246.5	0.052	H–7»L+2 (76%)
37	41082	243.4	0.022	H–8»L+1 (79%)
38	41321	242.0	0.073	H–11»LUMO (42%) H–8»L+2 (24%) H–3»L+3 (12%)
39	41381	241.7	0.303	H–11»LUMO (17%) H–8»L+2 (12%) H–6»L+2 (12%) H–1»L+6 (29%)
40	41446	241.3	0.224	H–8»L+2 (37%) H–1»L+6 (20%)
41	41531	240.8	0.031	H–11»LUMO (15%) H–5»L+3 (17%) H–3»L+3 (54%)
42	41866	238.9	0.032	H–4»L+3 (78%)
43	42011	238.0	0.066	H–8»L+2 (11%) H–3»L+4 (40%) H–2»L+4 (27%)
44	42206	236.9	0.031	H–4»L+3 (11%) HOMO»L+8 (62%)
45	42535	235.1	0.185	H–6»L+1 (10%) H–5»L+3 (32%)
46	42717	234.1	0.004	H–4»L+4 (88%)
47	42902	233.1	0.016	H–10»L+2 (26%) H–7»L+3 (14%) H–6»L+3 (11%)
48	42947	232.8	0.027	H–9»L+1 (69%)
49	43521	229.8	0.030	H–9»L+2 (72%)
50	43860	228.0	0.012	H–1»L+8 (11%)

[a] Oscillator strength. [b] Contributions smaller than 10% are not included. H = HOMO, L = LUMO. Orbitals are numbered consecutively regardless of possible degeneracies.

Table S6. Electronic transitions calculated for **11**$^{\bullet+}$ using the TDA/B3LYP/6-31G(d,p) level of theory.

No.	Energy (cm^{-1})	λ (nm)	f[a]	Major excitations[b]
1	6138	1629.2	0.007	H–1(B)»LUMO(B) (71%) HOMO(B)»LUMO(B) (17%)
2	8370	1194.7	0.018	H–1(B)»LUMO(B) (19%) HOMO(B)»LUMO(B) (80%)
3	9783	1022.2	0.001	H–2(B)»LUMO(B) (90%)
4	10969	911.6	0.177	H–3(B)»LUMO(B) (94%)
5	12642	791.0	0.005	H–5(B)»LUMO(B) (57%) H–4(B)»LUMO(B) (36%)
6	12910	774.6	0.006	H–5(B)»LUMO(B) (37%) H–4(B)»LUMO(B) (59%)
7	14913	670.5	0.023	H–6(B)»LUMO(B) (90%)
8	15277	654.6	0.007	H–7(B)»LUMO(B) (97%)
9	17601	568.2	0.024	H–8(B)»LUMO(B) (90%)
10	20020	499.5	0.030	H–9(B)»LUMO(B) (85%)
11	20805	480.7	0.002	H–2(A)»LUMO(A) (41%) H–10(B)»LUMO(B) (22%) H–1(B)»L+1(B) (16%)
12	20852	479.6	0.367	HOMO(A)»LUMO(A) (73%)
13	21766	459.4	0.015	H–2(A)»LUMO(A) (16%) H–10(B)»LUMO(B) (71%)
14	23311	429.0	0.032	H–1(A)»LUMO(A) (65%)
15	23942	417.7	0.007	H–4(A)»LUMO(A) (14%) H–1(A)»LUMO(A) (30%) HOMO(A)»L+2(A) (14%) H–3(B)»L+1(B) (12%)
16	24415	409.6	0.010	H–2(A)»LUMO(A) (14%) HOMO(A)»L+1(A) (21%) H–1(B)»L+1(B) (43%)
17	24752	404.0	0.045	H–3(A)»LUMO(A) (49%) H–2(A)»LUMO(A) (18%) HOMO(A)»L+1(A) (12%)
18	25064	399.0	0.010	HOMO(A)»L+2(A) (12%) HOMO(B)»L+1(B) (55%)
19	25127	398.0	0.112	H–3(A)»LUMO(A) (32%) HOMO(A)»L+1(A) (34%)
20	25790	387.7	0.021	H–4(A)»LUMO(A) (20%) HOMO(A)»L+2(A) (15%) H–3(B)»L+1(B) (15%) HOMO(B)»L+1(B) (12%)
21	26178	382.0	0.026	H–2(A)»L+1(A) (44%) H–11(B)»LUMO(B) (12%) H–1(B)»L+2(B) (13%)
22	26606	375.9	0.006	H–2(B)»L+1(B) (74%)
23	26726	374.2	0.026	H–11(B)»LUMO(B) (64%)
24	27120	368.7	0.007	H–5(A)»LUMO(A) (11%) H–2(A)»L+2(A) (24%) H–1(B)»L+3(B) (14%)
25	27489	363.8	0.025	H–7(A)»LUMO(A) (14%) H–6(A)»LUMO(A) (18%) H–4(A)»LUMO(A) (36%) H–3(B)»L+1(B) (10%)
26	27776	360.0	0.007	H–5(A)»LUMO(A) (49%)
27	27845	359.1	0.002	HOMO(A)»L+2(A) (19%) H–13(B)»LUMO(B) (30%)
28	28357	352.6	0.026	H–13(B)»LUMO(B) (24%) H–5(B)»L+1(B) (10%) H–3(B)»L+1(B) (17%)
29	28804	347.2	0.006	HOMO(A)»L+3(A) (19%) H–13(B)»LUMO(B) (15%) H–6(B)»L+1(B) (11%) H–3(B)»L+1(B) (10%)
30	28884	346.2	0.001	HOMO(A)»L+3(A) (51%)
31	29335	340.9	0.000	H–1(A)»L+1(A) (48%)
32	29399	340.1	0.000	H–1(A)»L+1(A) (41%) H–4(B)»L+1(B) (11%)
33	29573	338.1	0.000	H–12(B)»LUMO(B) (90%)
34	29917	334.3	0.001	H–8(A)»LUMO(A) (19%) H–14(B)»LUMO(B) (12%) H–5(B)»L+1(B) (13%) H–4(B)»L+1(B) (23%)
35	30200	331.1	0.009	H–14(B)»LUMO(B) (45%)
36	30508	327.8	0.075	H–2(A)»L+3(A) (14%) H–1(B)»L+2(B) (11%) H–1(B)»L+4(B) (11%)
37	30610	326.7	0.067	H–2(A)»L+2(A) (28%) H–1(B)»L+3(B) (27%)
38	30679	326.0	0.126	H–3(A)»L+1(A) (34%) H–2(A)»L+1(A) (25%)
39	30968	322.9	0.015	H–6(A)»L+1(A) (14%) H–4(A)»L+1(A) (13%)
40	31073	321.8	0.118	H–1(A)»L+2(A) (20%)
41	31153	321.0	0.001	H–15(B)»LUMO(B) (96%)
42	31224	320.3	0.138	H–6(A)»LUMO(A) (11%) H–3(A)»L+1(A) (41%)
43	31319	319.3	0.003	HOMO(B)»L+2(B) (43%)
44	31384	318.6	0.072	H–1(A)»L+2(A) (66%)
45	31687	315.6	0.012	H–4(A)»L+1(A) (39%) HOMO(B)»L+2(B) (12%)
46	31748	315.0	0.004	H–6(A)»LUMO(A) (16%) H–5(B)»L+1(B) (28%) H–4(B)»L+1(B) (12%)
47	31937	313.1	0.000	H–17(B)»LUMO(B) (10%) H–16(B)»LUMO(B) (80%)
48	32121	311.3	0.005	H–1(B)»L+3(B) (14%) HOMO(B)»L+3(B) (67%)
49	32605	306.7	0.001	H–3(A)»L+2(A) (26%) H–3(B)»L+2(B) (11%)
50	32762	305.2	0.004	H–3(A)»L+2(A) (18%) H–17(B)»LUMO(B) (10%) H–3(B)»L+2(B) (28%)

[a] Oscillator strength. [b] Contributions smaller than 10% are not included. H = HOMO, L = LUMO. Orbitals are numbered consecutively regardless of possible degeneracies.

Table S7. Electronic transitions calculated for **11**$^{2+}$ using the TDA/B3LYP/6-31G(d,p) level of theory.

No.	Energy (cm^{-1})	λ (nm)	f[a]	Major excitations[b]
1	4524	2210.5	0.012	H–3»LUMO (11%) HOMO»LUMO (88%)
2	5934	1685.3	0.008	H–4»LUMO (11%) H–2»LUMO (53%) H–1»LUMO (32%)
3	6484	1542.3	0.002	H–2»LUMO (43%) H–1»LUMO (50%)
4	11524	867.8	0.052	H–4»LUMO (76%) H–1»LUMO (13%)
5	12802	781.2	0.600	H–6»LUMO (14%) H–3»LUMO (62%)
6	13453	743.3	0.076	H–5»LUMO (88%)
7	14887	671.7	0.015	H–7»LUMO (87%)
8	17496	571.6	0.552	H–6»LUMO (74%) H–3»LUMO (13%)
9	18081	553.1	0.057	H–9»LUMO (23%) H–8»LUMO (65%)
10	19651	508.9	0.032	H–10»LUMO (10%) H–9»LUMO (70%) H–8»LUMO (13%)
11	21459	466.0	0.010	HOMO»L+1 (95%)
12	22312	448.2	0.000	H–11»LUMO (99%)
13	22936	436.0	0.155	H–10»LUMO (72%) H–1»L+1 (11%)
14	23251	430.1	0.060	H–1»L+1 (80%)
15	24033	416.1	0.049	H–2»L+1 (86%)
16	25019	399.7	0.002	H–13»LUMO (40%) H–12»LUMO (57%)
17	25040	399.4	0.004	H–13»LUMO (59%) H–12»LUMO (39%)
18	25805	387.5	0.089	H–3»L+1 (84%)
19	27384	365.2	0.011	HOMO»L+2 (95%)
20	27512	363.5	0.002	H–4»L+1 (82%)
21	28192	354.7	0.025	H–15»LUMO (14%) H–14»LUMO (72%)
22	29049	344.2	0.209	H–16»LUMO (17%) H–1»L+2 (66%)
23	29200	342.5	0.056	H–16»LUMO (59%) H–1»L+2 (21%)
24	29642	337.4	0.023	H–3»L+2 (22%) H–2»L+2 (28%) HOMO»L+3 (27%)
25	29769	335.9	0.000	H–3»L+2 (51%) HOMO»L+3 (31%)
26	29976	333.6	0.024	H–15»LUMO (34%) H–14»LUMO (11%) HOMO»L+3 (27%)
27	30281	330.2	0.301	H–15»LUMO (10%) H–5»L+1 (11%) H–2»L+2 (57%)
28	30510	327.8	0.015	H–17»LUMO (80%)
29	30540	327.4	0.048	H–17»LUMO (14%) H–2»L+3 (10%) H–1»L+3 (54%)
30	30718	325.5	0.007	H–15»LUMO (11%) H–5»L+1 (57%)
31	31595	316.5	0.001	H–18»LUMO (82%)
32	32082	311.7	0.008	H–2»L+3 (76%) H–1»L+3 (20%)
33	32569	307.0	0.006	H–6»L+1 (19%) H–4»L+2 (29%) H–3»L+3 (44%)
34	32850	304.4	0.003	HOMO»L+4 (87%)
35	32982	303.2	0.000	H–19»LUMO (98%)
36	33255	300.7	0.020	H–20»LUMO (68%)
37	33350	299.8	0.037	H–20»LUMO (12%) H–7»L+1 (58%)
38	33651	297.2	0.087	H–4»L+2 (24%) H–1»L+4 (43%)
39	33754	296.3	0.097	H–22»LUMO (10%) H–20»LUMO (10%) H–6»L+1 (28%) H–3»L+3 (32%)
40	34122	293.1	0.035	H–21»LUMO (52%) H–5»L+2 (22%)
41	34197	292.4	0.023	H–23»LUMO (23%) H–22»LUMO (36%) H–21»LUMO (12%)
42	34261	291.9	0.070	H–22»LUMO (10%) H–21»LUMO (12%) H–5»L+2 (40%)
43	34550	289.4	0.114	H–23»LUMO (50%) H–22»LUMO (18%)
44	34575	289.2	0.174	H–6»L+1 (16%) H–4»L+2 (25%) H–1»L+4 (28%)
45	34879	286.7	0.017	H–27»LUMO (55%) H–24»LUMO (28%)
46	35163	284.4	0.004	H–29»LUMO (19%) H–27»LUMO (33%) H–24»LUMO (33%)
47	35355	282.8	0.080	H–4»L+3 (33%) H–2»L+4 (40%)
48	35447	282.1	0.060	H–4»L+3 (34%) H–2»L+4 (38%)
49	35567	281.2	0.006	H–28»LUMO (74%) H–26»LUMO (10%)
50	35710	280.0	0.002	HOMO»L+5 (93%)

[a] Oscillator strength. [b] Contributions smaller than 10% are not included. H = HOMO, L = LUMO. Orbitals are numbered consecutively regardless of possible degeneracies.

Table S8. Electronic transitions calculated for **12** using the TDA/B3LYP/6-31G(d,p) level of theory.

No.	Energy (cm^{-1})	λ (nm)	f[a]	Major excitations[b]
1	23401	427.3	0.371	HOMO»LUMO (86%)
2	24846	402.5	0.000	H–1»LUMO (91%)
3	25682	389.4	0.024	HOMO»L+1 (90%)
4	27153	368.3	0.065	H–1»L+1 (24%) HOMO»L+2 (49%) HOMO»L+3 (22%)
5	28082	356.1	0.003	H–1»L+1 (15%) HOMO»L+3 (73%)
6	29807	335.5	0.247	H–1»L+1 (55%) HOMO»L+2 (28%)
7	31472	317.7	0.558	H–1»L+2 (82%)
8	31991	312.6	0.011	H–3»LUMO (39%) HOMO»L+4 (50%)
9	32951	303.5	0.013	H–2»LUMO (74%) H–1»L+3 (13%)
10	33324	300.1	0.192	H–1»L+3 (74%) HOMO»L+5 (12%)
11	34185	292.5	0.002	H–4»LUMO (73%) H–2»L+1 (11%)
12	35173	284.3	0.017	H–2»L+2 (80%)
13	35553	281.3	0.039	H–3»LUMO (22%) HOMO»L+4 (25%) HOMO»L+6 (22%)
14	36064	277.3	0.152	H–2»L+1 (65%)
15	36555	273.6	0.056	H–5»LUMO (33%) HOMO»L+6 (41%)
16	37008	270.2	0.138	H–3»L+2 (14%) H–1»L+4 (37%) HOMO»L+5 (31%)
17	37381	267.5	0.004	H–5»LUMO (25%) H–3»L+1 (57%)
18	37620	265.8	0.008	H–4»L+2 (24%) H–3»L+1 (11%) HOMO»L+6 (18%)
19	37827	264.4	0.000	H–4»L+1 (25%) H–3»L+2 (12%) H–1»L+4 (19%) HOMO»L+5 (19%)
20	38170	262.0	0.005	H–4»L+1 (44%) H–3»L+2 (29%)
21	38557	259.4	0.021	H–5»LUMO (10%) H–4»L+2 (32%) H–3»L+1 (11%) H–2»L+3 (13%)
22	38817	257.6	0.112	H–3»L+2 (36%) H–1»L+4 (33%)
23	39431	253.6	0.222	H–5»L+1 (15%) H–4»L+2 (19%) H–2»L+3 (40%)
24	39811	251.2	0.062	H–1»L+5 (75%)
25	40298	248.2	0.037	H–5»L+1 (41%) H–4»L+3 (30%) H–2»L+3 (17%)
26	40826	244.9	0.100	H–6»LUMO (70%) H–4»L+3 (14%)
27	41015	243.8	0.194	H–5»L+2 (59%) H–1»L+6 (16%)
28	41633	240.2	0.002	H–3»L+3 (86%)
29	41903	238.6	0.049	H–7»LUMO (45%) H–5»L+1 (11%) HOMO»L+7 (11%)
30	41981	238.2	0.529	H–5»L+2 (17%) H–1»L+6 (62%)
31	43097	232.0	0.092	H–7»LUMO (33%) H–4»L+3 (13%)
32	43239	231.3	0.048	H–6»L+2 (22%) H–5»L+3 (22%)
33	44069	226.9	0.015	H–7»L+1 (28%) HOMO»L+7 (27%)
34	44487	224.8	0.050	H–7»L+1 (10%) H–6»L+1 (11%) H–2»L+4 (20%) HOMO»L+7 (32%)
35	44596	224.2	0.008	H–5»L+3 (26%) HOMO»L+8 (52%)
36	44937	222.5	0.324	H–6»L+1 (47%) H–2»L+4 (16%)
37	45613	219.2	0.011	H–8»LUMO (17%) H–2»L+5 (56%)
38	46272	216.1	0.025	H–7»L+2 (60%)
39	46328	215.8	0.042	H–7»L+1 (14%) H–4»L+4 (55%) H–2»L+4 (10%)
40	46399	215.5	0.053	H–8»LUMO (46%) H–6»L+2 (14%) H–2»L+5 (10%)
41	46683	214.2	0.786	H–3»L+5 (33%) H–2»L+6 (21%)
42	47004	212.7	0.270	H–7»L+1 (24%) H–2»L+6 (36%)
43	47408	210.9	0.052	H–5»L+3 (11%) H–4»L+5 (17%) H–3»L+4 (19%)
44	47600	210.1	0.024	H–3»L+4 (23%) H–1»L+7 (35%)
45	47973	208.5	0.000	H–10»LUMO (76%)
46	48040	208.2	0.081	H–6»L+3 (11%) H–5»L+4 (13%) H–4»L+5 (38%) H–3»L+6 (10%)
47	48447	206.4	0.017	H–4»L+6 (33%) H–1»L+8 (35%)
48	48789	205.0	0.000	H–13»LUMO (45%) H–12»LUMO (22%) H–11»LUMO (10%)
49	48811	204.9	0.005	H–8»L+1 (22%) H–6»L+3 (17%)
50	49155	203.4	0.121	H–9»LUMO (46%) H–7»L+3 (17%) H–6»L+3 (14%)

[a] Oscillator strength. [b] Contributions smaller than 10% are not included. H = HOMO, L = LUMO. Orbitals are numbered consecutively regardless of possible degeneracies.

Table S9. Electronic transitions calculated for **12**$^{\bullet+}$ using the TDA/B3LYP/6-31G(d,p) level of theory.

No.	Energy (cm^{-1})	λ (nm)	f[a]	Major excitations[b]
1	6264	1596.5	0.007	HOMO(B)»LUMO(B) (98%)
2	11569	864.4	0.183	H–1(B)»LUMO(B) (89%)
3	12698	787.5	0.000	H–2(B)»LUMO(B) (96%)
4	13515	739.9	0.014	H–3(B)»LUMO(B) (90%)
5	16467	607.3	0.039	H–4(B)»LUMO(B) (91%)
6	20207	494.9	0.028	H–5(B)»LUMO(B) (86%)
7	21195	471.8	0.007	H–1(A)»LUMO(A) (13%) H–6(B)»LUMO(B) (68%)
8	21655	461.8	0.286	HOMO(A)»LUMO(A) (70%)
9	22303	448.4	0.022	H–1(A)»LUMO(A) (50%) H–6(B)»LUMO(B) (23%) HOMO(B)»L+1(B) (15%)
10	24039	416.0	0.011	H–2(A)»LUMO(A) (16%) HOMO(A)»L+2(A) (26%) H–1(B)»L+1(B) (21%)
11	24923	401.2	0.096	HOMO(A)»L+1(A) (58%) HOMO(B)»L+1(B) (20%)
12	25636	390.1	0.039	H–1(A)»LUMO(A) (26%) HOMO(B)»L+1(B) (47%)
13	25871	386.5	0.010	H–1(A)»L+1(A) (20%) HOMO(A)»L+2(A) (10%) H–7(B)»LUMO(B) (41%)
14	26245	381.0	0.043	H–7(B)»LUMO(B) (39%) H–1(B)»L+1(B) (16%)
15	26482	377.6	0.015	H–1(A)»L+1(A) (37%) HOMO(A)»L+2(A) (18%) HOMO(B)»L+2(B) (13%)
16	27098	369.0	0.028	H–3(A)»LUMO(A) (21%) H–1(A)»L+2(A) (17%) H–2(B)»L+1(B) (22%) HOMO(B)»L+3(B) (17%)
17	27264	366.8	0.001	H–3(A)»LUMO(A) (21%) H–1(A)»L+2(A) (18%) H–2(B)»L+1(B) (16%)
18	27834	359.3	0.000	H–8(B)»LUMO(B) (75%)
19	27982	357.4	0.001	HOMO(A)»L+2(A) (18%) H–11(B)»LUMO(B) (13%) H–8(B)»LUMO(B) (19%)
20	28334	352.9	0.000	H–9(B)»LUMO(B) (95%)
21	28700	348.4	0.005	H–11(B)»LUMO(B) (44%) H–10(B)»LUMO(B) (10%)
22	28996	344.9	0.001	H–1(A)»L+2(A) (10%) HOMO(A)»L+3(A) (71%)
23	29208	342.4	0.000	H–14(B)»LUMO(B) (13%) H–13(B)»LUMO(B) (52%) H–12(B)»LUMO(B) (13%)
24	29623	337.6	0.001	H–14(B)»LUMO(B) (58%) H–13(B)»LUMO(B) (12%)
25	29840	335.1	0.000	H–13(B)»LUMO(B) (10%) H–12(B)»LUMO(B) (65%) H–10(B)»LUMO(B) (17%)
26	29922	334.2	0.000	H–12(B)»LUMO(B) (16%) H–11(B)»LUMO(B) (15%) H–10(B)»LUMO(B) (65%)
27	30668	326.1	0.086	H–1(A)»L+2(A) (11%) H–1(A)»L+3(A) (11%) HOMO(B)»L+2(B) (17%) HOMO(B)»L+4(B) (13%)
28	30747	325.2	0.050	H–1(A)»L+2(A) (13%) H–1(A)»L+3(A) (13%) HOMO(B)»L+3(B) (16%) HOMO(B)»L+4(B) (10%)
29	30943	323.2	0.057	H–2(A)»L+1(A) (22%) H–1(B)»L+2(B) (11%) HOMO(B)»L+3(B) (12%)
30	31031	322.3	0.314	H–2(A)»LUMO(A) (20%) H–1(A)»L+1(A) (12%) HOMO(B)»L+2(B) (19%) HOMO(B)»L+3(B) (13%)
31	31435	318.1	0.000	H–16(B)»LUMO(B) (15%) H–15(B)»LUMO(B) (77%)
32	31563	316.8	0.064	H–4(A)»LUMO(A) (14%)
33	31606	316.4	0.001	H–17(B)»LUMO(B) (85%)
34	31868	313.8	0.008	H–16(B)»LUMO(B) (56%)
35	31981	312.7	0.007	H–4(A)»L+1(A) (15%) H–2(A)»L+1(A) (12%)
36	32082	311.7	0.023	H–2(A)»LUMO(A) (14%) H–3(B)»L+1(B) (10%) H–1(B)»L+1(B) (25%)
37	32613	306.6	0.035	H–3(A)»LUMO(A) (15%) H–2(B)»L+1(B) (14%) H–1(B)»L+2(B) (34%)
38	33036	302.7	0.032	H–3(A)»LUMO(A) (11%) H–2(A)»L+1(A) (13%) H–19(B)»LUMO(B) (20%)
39	33089	302.2	0.002	H–18(B)»LUMO(B) (56%)
40	33228	301.0	0.011	H–2(A)»L+1(A) (15%) H–19(B)»LUMO(B) (16%) H–1(B)»L+2(B) (17%)
41	33453	298.9	0.001	H–5(A)»LUMO(A) (10%) H–19(B)»LUMO(B) (25%)
42	33548	298.1	0.000	H–4(A)»LUMO(A) (22%) H–3(B)»L+1(B) (38%) H–1(B)»L+3(B) (10%)
43	33942	294.6	0.011	H–4(A)»LUMO(A) (21%) H–18(B)»LUMO(B) (13%) H–1(B)»L+3(B) (16%)
44	34296	291.6	0.060	H–3(A)»L+1(A) (42%) H–1(A)»L+3(A) (15%) HOMO(B)»L+4(B) (19%)
45	34528	289.6	0.038	H–5(A)»LUMO(A) (17%) H–19(B)»LUMO(B) (10%) H–4(B)»L+1(B) (18%)
46	34602	289.0	0.112	H–3(B)»L+3(B) (11%)
47	35160	284.4	0.021	H–1(A)»L+4(A) (14%) H–2(B)»L+5(B) (12%) HOMO(B)»L+5(B) (15%)
48	35370	282.7	0.012	H–5(A)»LUMO(A) (13%) HOMO(A)»L+4(A) (39%)
49	35767	279.6	0.087	H–2(A)»L+2(A) (41%) H–1(B)»L+3(B) (13%)
50	35946	278.2	0.046	H–3(A)»L+2(A) (15%)

[a] Oscillator strength. [b] Contributions smaller than 10% are not included. H = HOMO, L = LUMO. Orbitals are numbered consecutively regardless of possible degeneracies.

Table S10. Electronic transitions calculated for **12**$^{2+}$ using the TDA/B3LYP/6-31G(d,p) level of theory.

No.	Energy (cm^{-1})	λ (nm)	f[a]	Major excitations[b]
1	3457	2892.8	0.000	HOMO(A)»LUMO(A) (49%) HOMO(B)»LUMO(B) (49%)
2	5689	1757.9	0.008	HOMO(A)»LUMO(A) (48%) HOMO(B)»LUMO(B) (48%)
3	5824	1717.0	0.000	H–1(A)»LUMO(A) (49%) H–1(B)»LUMO(B) (49%)
4	9093	1099.7	0.000	H–2(A)»LUMO(A) (49%) H–2(B)»LUMO(B) (49%)
5	9558	1046.3	0.000	H–3(A)»LUMO(A) (49%) H–3(B)»LUMO(B) (49%)
6	10946	913.6	0.001	H–2(A)»LUMO(A) (49%) H–2(B)»LUMO(B) (49%)
7	12752	784.2	0.000	H–4(A)»LUMO(A) (48%) H–4(B)»LUMO(B) (48%)
8	13543	738.4	0.219	H–3(A)»LUMO(A) (31%) H–1(A)»LUMO(A) (16%) H–3(B)»LUMO(B) (31%) H–1(B)»LUMO(B) (16%)
9	15926	627.9	0.652	H–3(A)»LUMO(A) (17%) H–1(A)»LUMO(A) (28%) H–3(B)»LUMO(B) (17%) H–1(B)»LUMO(B) (28%)
10	16408	609.5	0.000	H–5(A)»LUMO(A) (43%) H–5(B)»LUMO(B) (43%)
11	17093	585.1	0.089	H–4(A)»LUMO(A) (40%) H–4(B)»LUMO(B) (40%)
12	17780	562.4	0.000	H–6(A)»LUMO(A) (41%) H–6(B)»LUMO(B) (41%)
13	19519	512.3	0.021	H–5(A)»LUMO(A) (41%) H–5(B)»LUMO(B) (41%)
14	20964	477.0	0.000	H–7(A)»LUMO(A) (39%) H–7(B)»LUMO(B) (39%)
15	21100	473.9	0.000	H–10(A)»LUMO(A) (32%) H–7(A)»LUMO(A) (10%) H–10(B)»LUMO(B) (32%) H–7(B)»LUMO(B) (10%)
16	21137	473.1	0.001	H–7(A)»LUMO(A) (49%) H–7(B)»LUMO(B) (49%)
17	21356	468.3	0.000	H–8(A)»LUMO(A) (49%) H–8(B)»LUMO(B) (49%)
18	21466	465.9	0.000	H–8(A)»LUMO(A) (50%) H–8(B)»LUMO(B) (50%)
19	21738	460.0	0.000	HOMO(A)»L+1(A) (43%) HOMO(B)»L+1(B) (43%)
20	22037	453.8	0.000	H–9(A)»LUMO(A) (50%) H–9(B)»LUMO(B) (50%)
21	22104	452.4	0.000	H–9(A)»LUMO(A) (50%) H–9(B)»LUMO(B) (50%)
22	22553	443.4	0.029	H–10(A)»LUMO(A) (46%) H–10(B)»LUMO(B) (46%)
23	22916	436.4	0.000	H–11(A)»LUMO(A) (44%) H–11(B)»LUMO(B) (44%)
24	22976	435.2	0.128	H–6(A)»LUMO(A) (32%) H–6(B)»LUMO(B) (32%)
25	23138	432.2	0.000	H–1(A)»L+1(A) (34%) H–1(B)»L+1(B) (34%)
26	23188	431.2	0.000	H–12(A)»LUMO(A) (47%) H–12(B)»LUMO(B) (47%)
27	23372	427.9	0.011	H–12(A)»LUMO(A) (43%) H–12(B)»LUMO(B) (43%)
28	23377	427.8	0.080	H–11(A)»LUMO(A) (35%) H–11(B)»LUMO(B) (35%)
29	24251	412.3	0.000	H–13(A)»LUMO(A) (41%) H–13(B)»LUMO(B) (41%)
30	24309	411.4	0.000	H–16(A)»LUMO(A) (27%) H–16(B)»LUMO(B) (27%)
31	24727	404.4	0.000	H–14(A)»LUMO(A) (47%) H–14(B)»LUMO(B) (47%)
32	24770	403.7	0.000	H–17(A)»LUMO(A) (32%) H–17(B)»LUMO(B) (32%)
33	24798	403.3	0.000	H–13(A)»LUMO(A) (47%) H–13(B)»LUMO(B) (47%)
34	24852	402.4	0.000	H–14(A)»LUMO(A) (47%) H–14(B)»LUMO(B) (47%)
35	24868	402.1	0.000	H–15(A)»LUMO(A) (49%) H–15(B)»LUMO(B) (49%)
36	24943	400.9	0.025	HOMO(A)»L+1(A) (41%) HOMO(B)»L+1(B) (41%)
37	25069	398.9	0.000	H–15(A)»LUMO(A) (49%) H–15(B)»LUMO(B) (49%)
38	25594	390.7	0.000	HOMO(A)»L+2(A) (42%) HOMO(B)»L+2(B) (42%)
39	25742	388.5	0.000	H–2(A)»L+1(A) (42%) H–2(B)»L+1(B) (42%)
40	26948	371.1	0.000	HOMO(A)»L+3(A) (20%) HOMO(B)»L+3(B) (20%)
41	27503	363.6	0.000	H–22(A)»LUMO(A) (12%) H–22(B)»LUMO(B) (12%)
42	27683	361.2	0.011	H–16(A)»LUMO(A) (31%) H–16(B)»LUMO(B) (31%)
43	27753	360.3	0.000	H–22(A)»LUMO(A) (12%) H–21(A)»LUMO(A) (12%) H–22(B)»LUMO(B) (12%) H–21(B)»LUMO(B) (12%)
44	28448	351.5	0.025	H–17(A)»LUMO(A) (36%) H–17(B)»LUMO(B) (36%)
45	28668	348.8	0.000	H–21(A)»LUMO(A) (10%) HOMO(A)»L+3(A) (14%) H–21(B)»LUMO(B) (10%) HOMO(B)»L+3(B) (14%)
46	29211	342.3	0.000	H–1(A)»L+2(A) (40%) H–1(B)»L+2(B) (40%)
47	29605	337.8	0.117	H–18(A)»LUMO(A) (29%) H–18(B)»LUMO(B) (29%)
48	29741	336.2	0.000	H–18(A)»LUMO(A) (43%) H–18(B)»LUMO(B) (43%)
49	29749	336.1	0.181	H–19(A)»LUMO(A) (22%) H–18(A)»LUMO(A) (10%) HOMO(A)»L+2(A) (11%) H–19(B)»LUMO(B) (22%) H–18(B)»LUMO(B) (10%) HOMO(B)»L+2(B) (11%)
50	29839	335.1	0.075	H–19(A)»LUMO(A) (22%) H–18(A)»LUMO(A) (10%) H–19(B)»LUMO(B) (22%) H–18(B)»LUMO(B) (10%)

[a] Oscillator strength. [b] Contributions smaller than 10% are not included. H = HOMO, L = LUMO. Orbitals are numbered consecutively regardless of possible degeneracies.

Table S11. Energy comparison of ullazines and its oxidized forms.

code	formula	SCF E[a]	ZPV[b]	lowest freq.[c]	H[d]	G[e]
		a.u.	a.u.	cm-1	a.u.	a.u.
6	C46H32N2O2	-2032.302919	0.654724	10.72	-2031.609655	-2031.608710
$6^{\bullet+}$	C46H32N2O2	-2032.069741	0.654519	12.14	-2031.376541	-2031.375597
6^{2+}	C46H32N2O2	-2031.726440	0.653749	12.06	-2031.033748	-2031.032804
11	C42H35N3O2	-1936.406904	0.668312	15.01	-1935.697910	-1935.697910
$11^{\bullet+}$	C42H35N3O2	-1936.189029	0.668064	15.24	-1935.48096	-1935.480016
11^{2+}	C42H35N3O2	-1935.854832	0.667586	15.25	-1935.146848	-1935.145904
12	C44H41N	-1756.290674	0.726735	16.68	-1755.525524	-1755.524580
$12^{\bullet+}$	C44H41N	-1756.077322	0.726703	17.09	-1755.312049	-1755.311105
12^{2+}	C44H41N	-1755.742776	0.726380	17.55	-1754.976610	-1754.976610

NMR Spectra

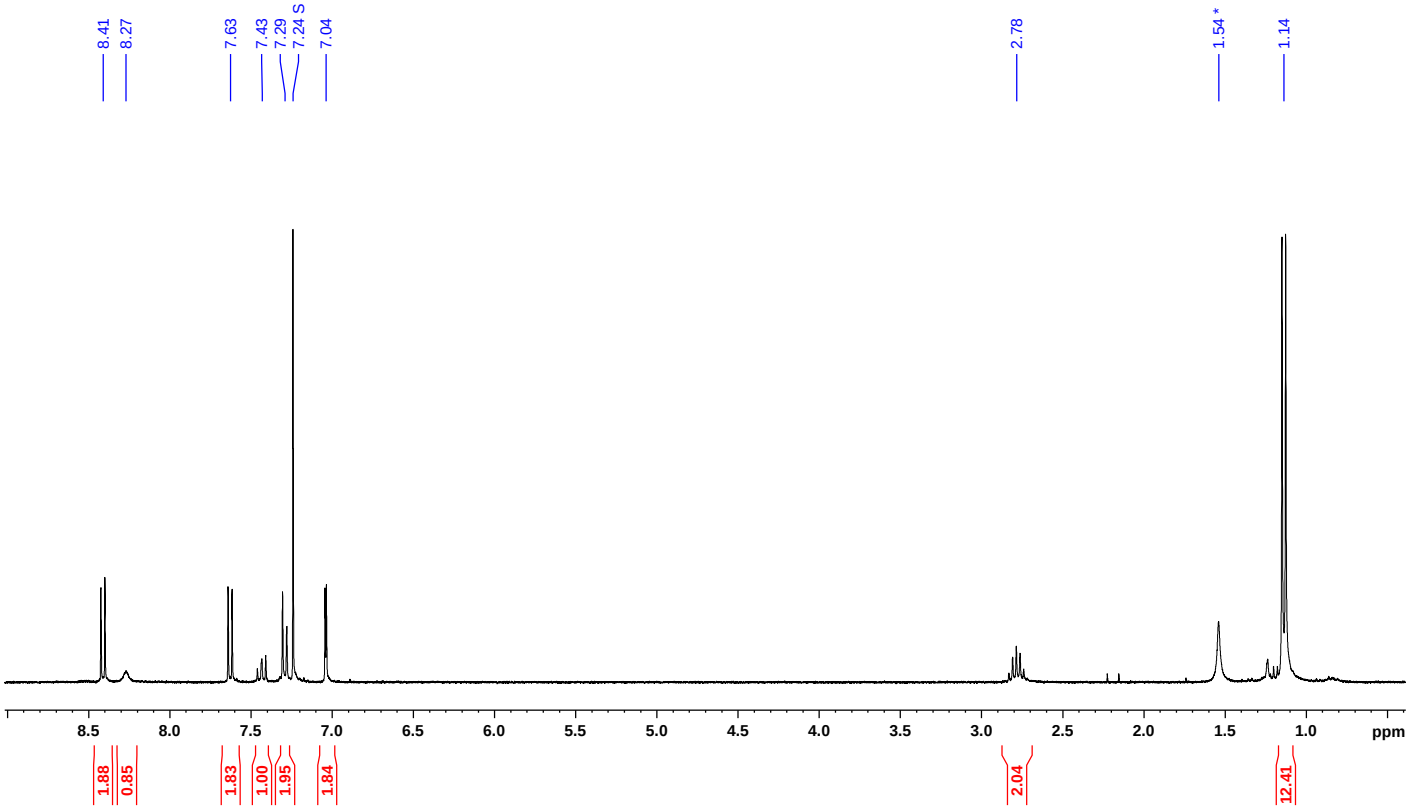

Figure S33. ^{1}H NMR spectrum of **1** (500 MHz, chloroform-*d*, 300 K).

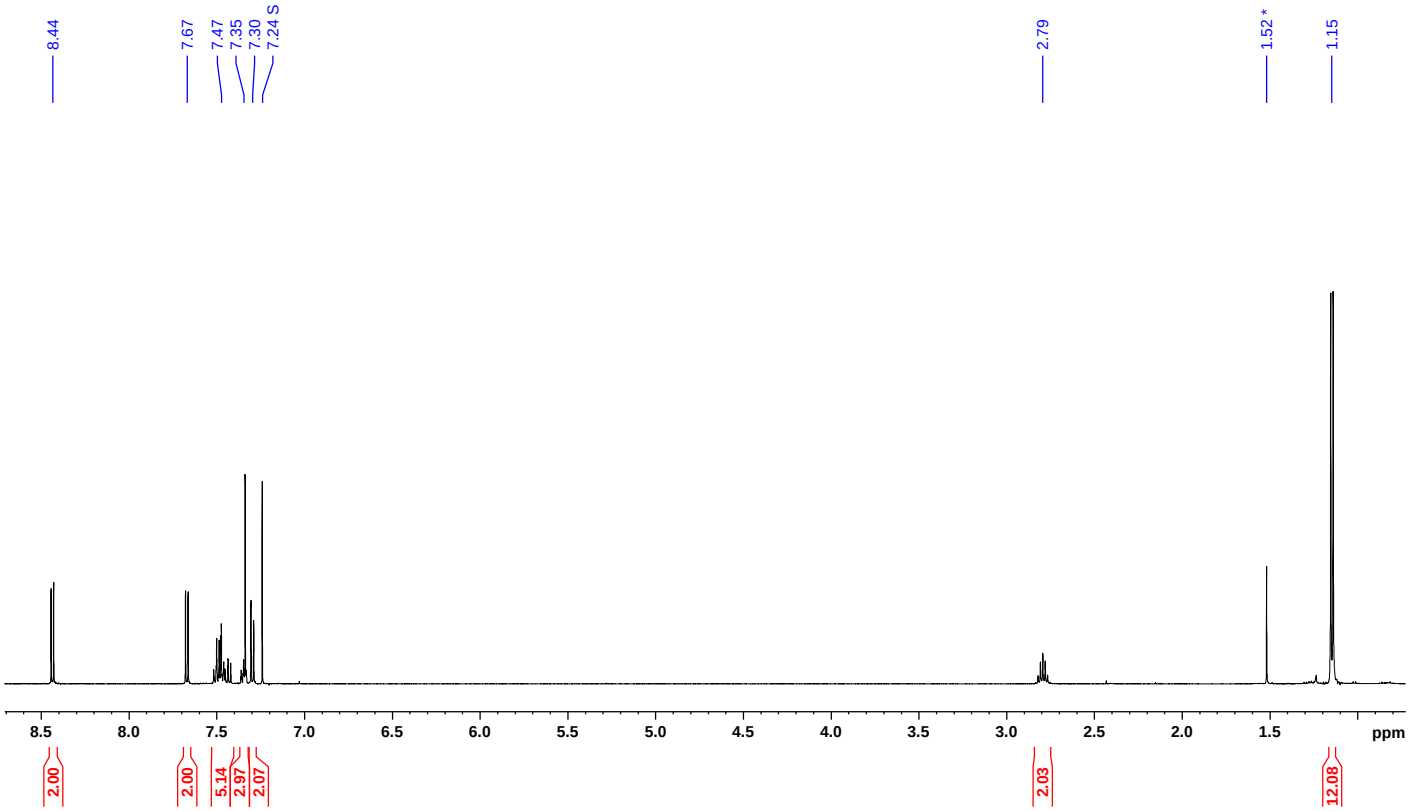

Figure S34. ^{1}H NMR spectrum of **2** (500 MHz, chloroform-*d*, 300 K).

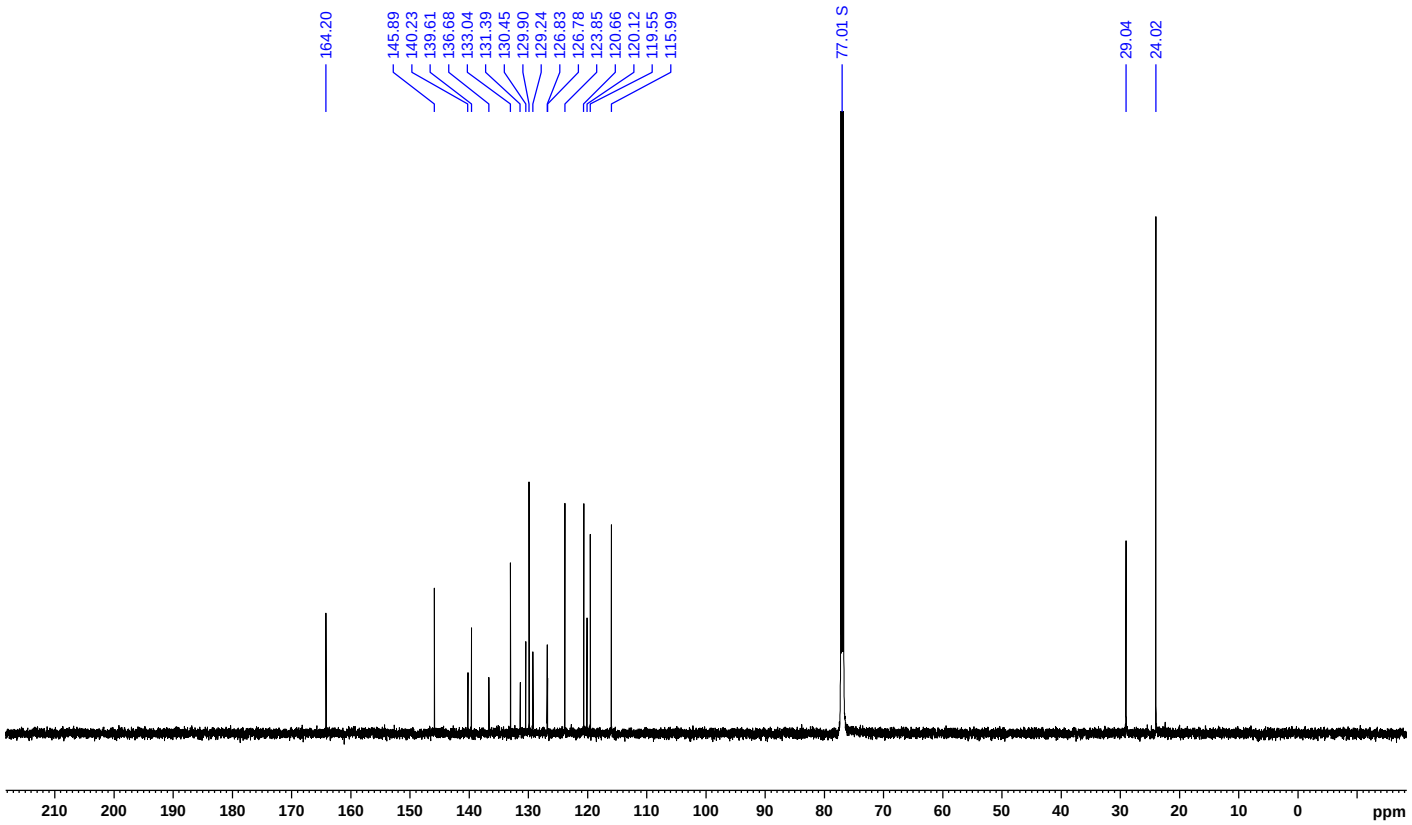

Figure S32. ^{13}C NMR spectrum of **2** (151 MHz, chloroform-*d*, 300 K).

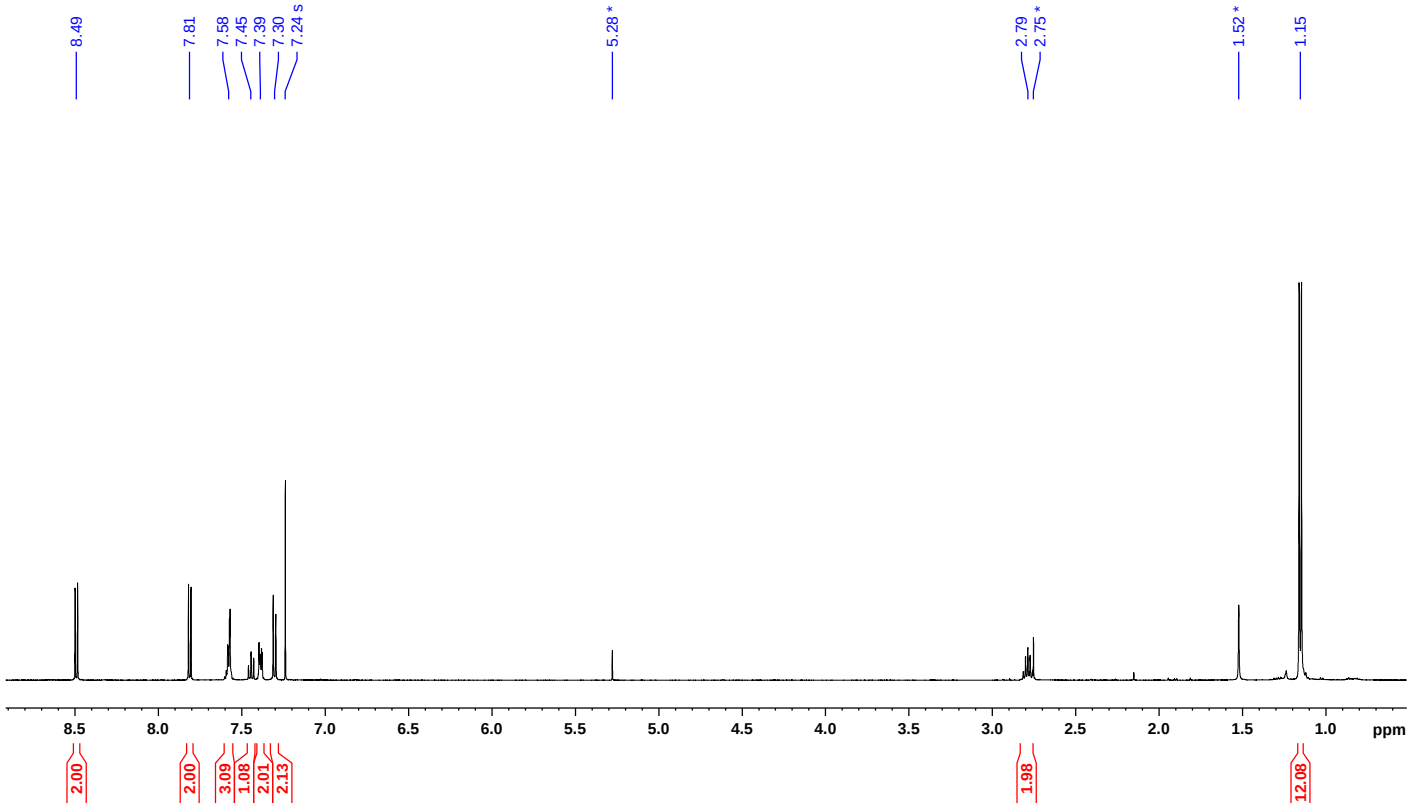

Figure S36. ^{1}H NMR spectrum of **3** (500 MHz, chloroform-*d*, 300 K).

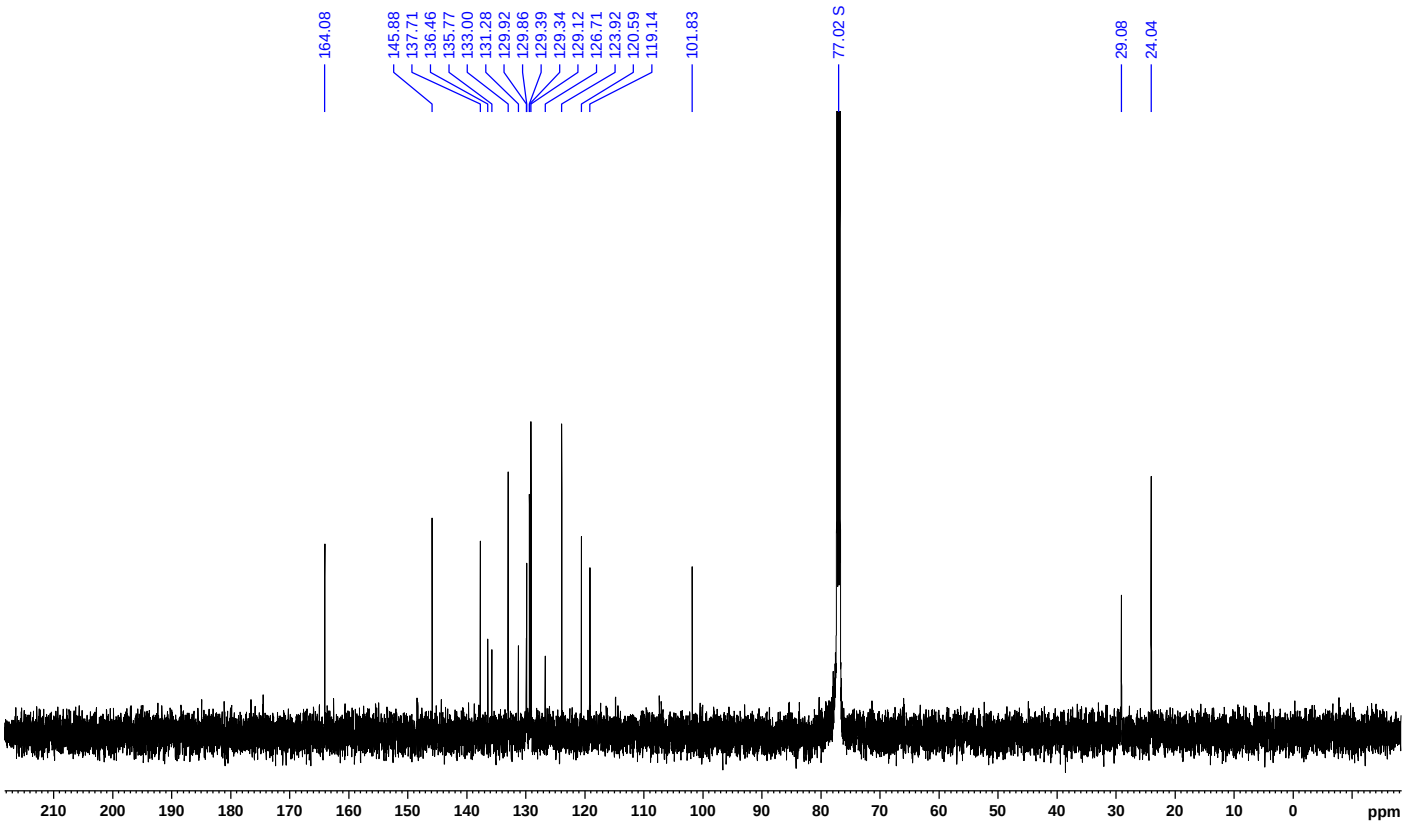

Figure S37. ^{13}C NMR spectrum of **3** (151 MHz, chloroform-*d*, 300 K).

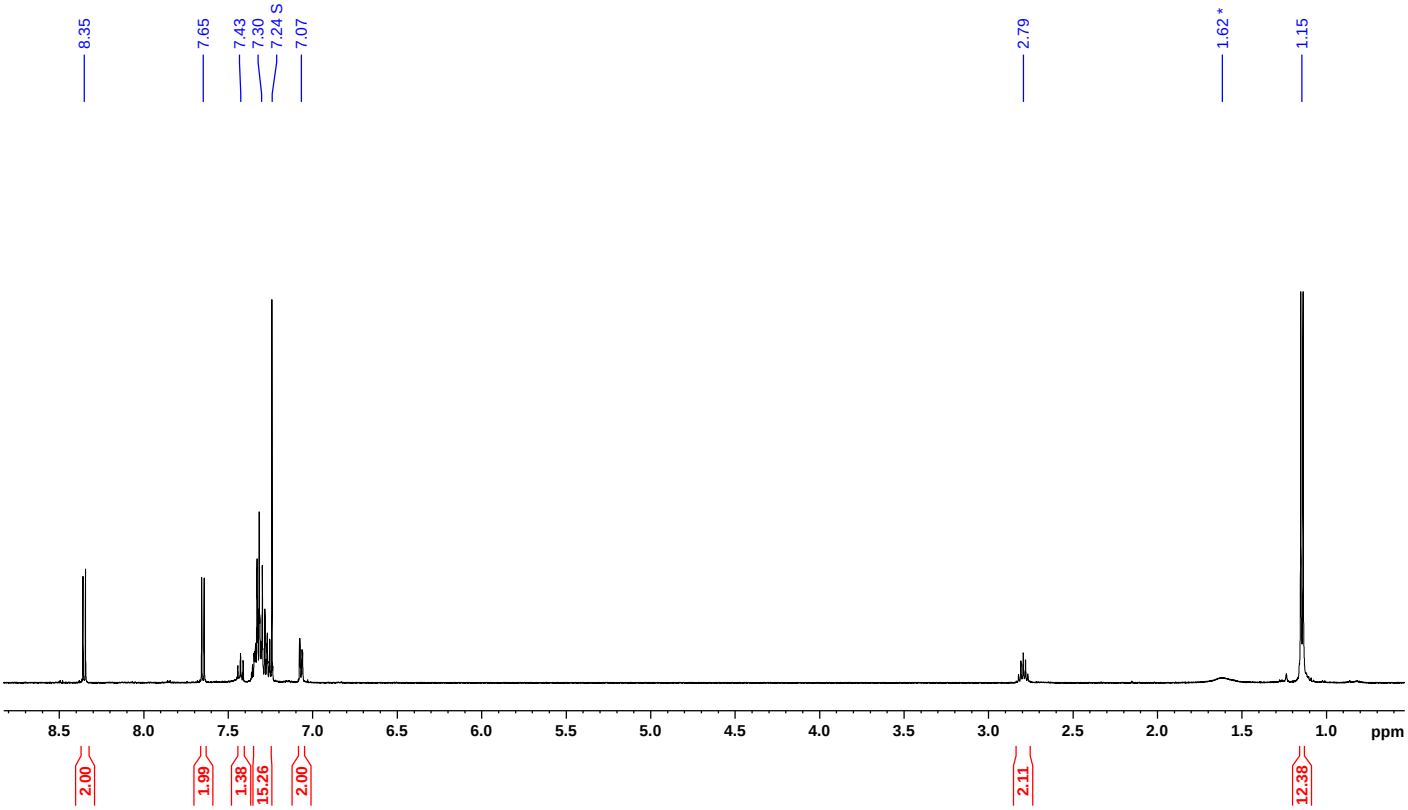

Figure S38. ^{1}H NMR spectrum of **4a** (500 MHz, chloroform-*d*, 300 K).

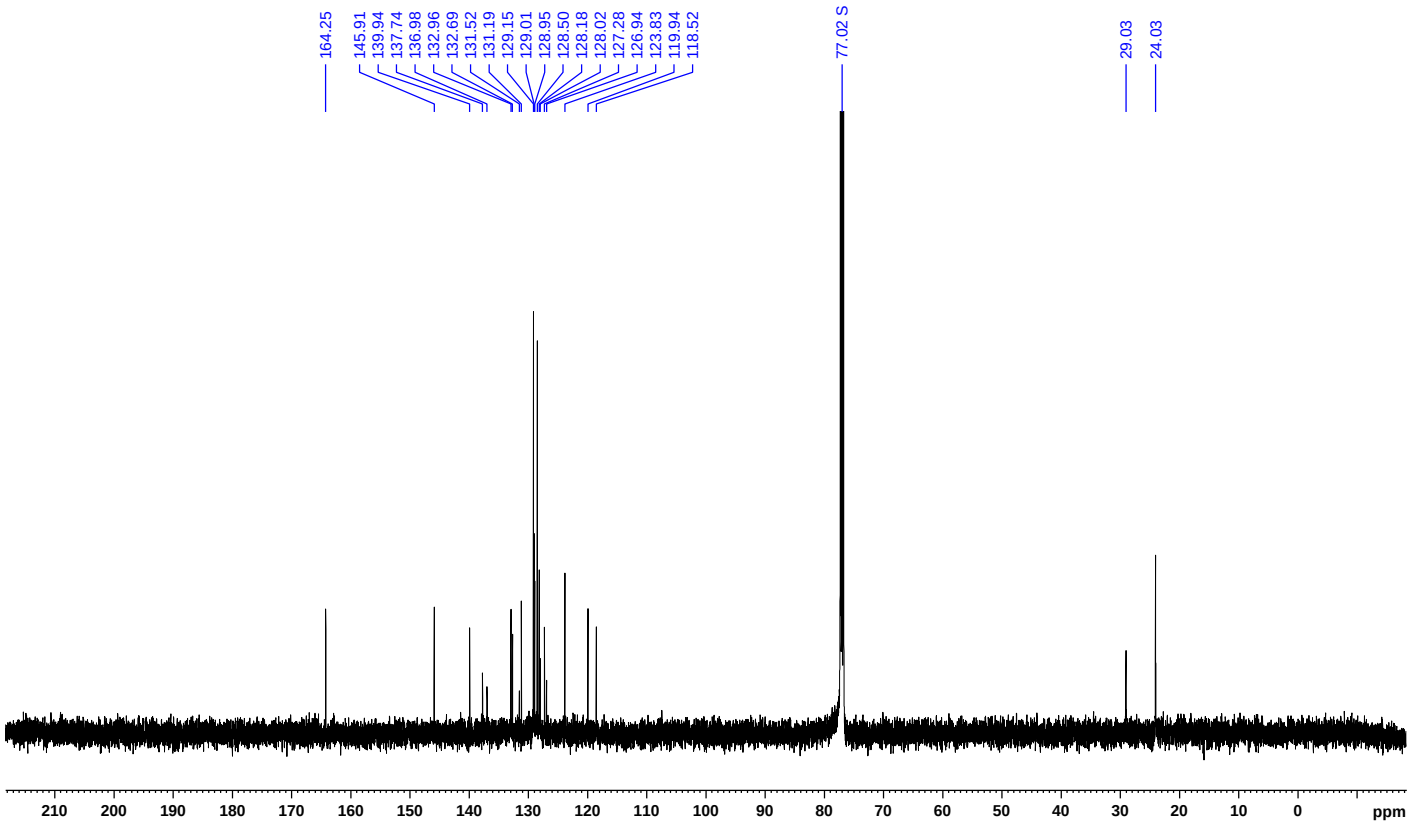

Figure S39. ^{13}C NMR spectrum of **4a** (125 MHz, chloroform-*d*, 300 K).

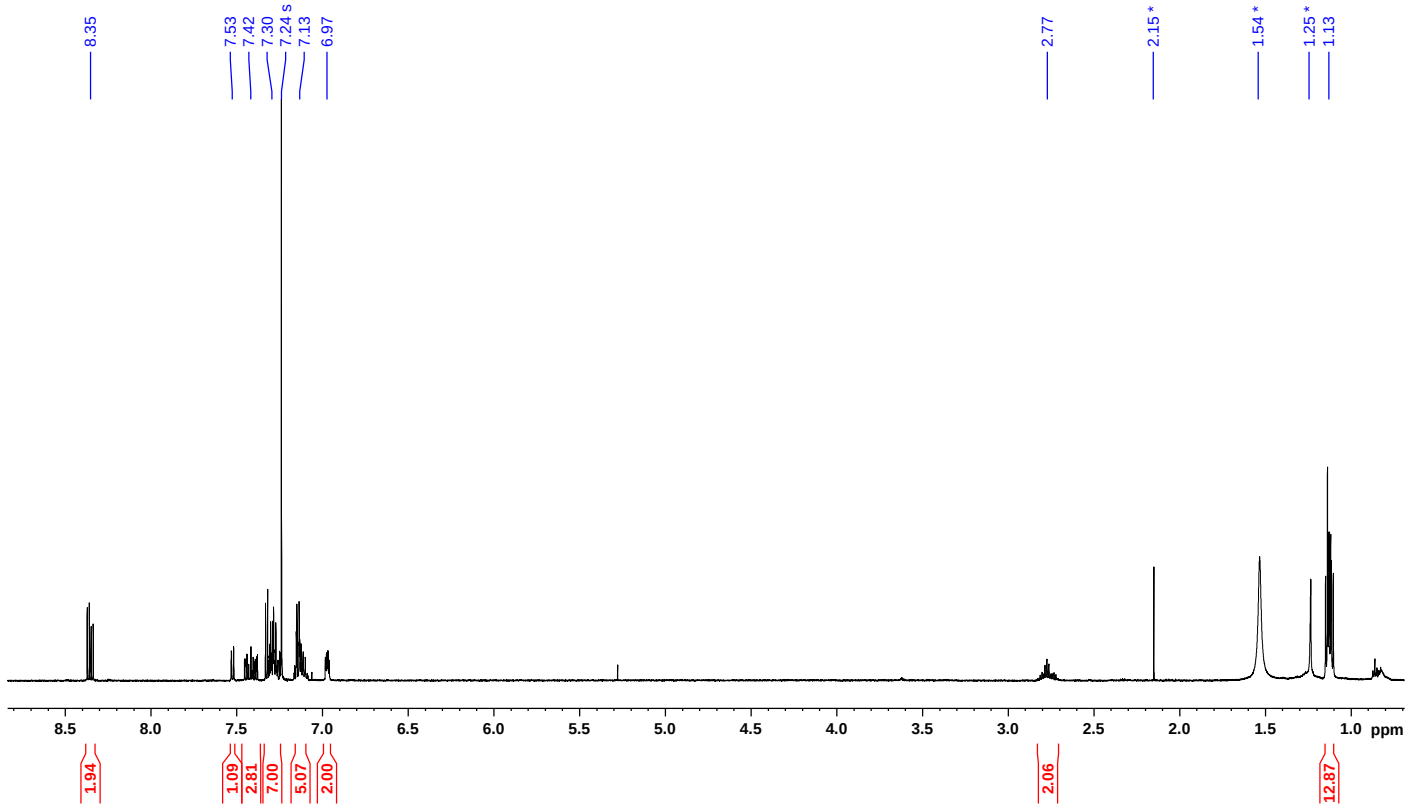

Figure S40. ^{1}H NMR spectrum of **4b** (600 MHz, chloroform-*d*, 300 K).

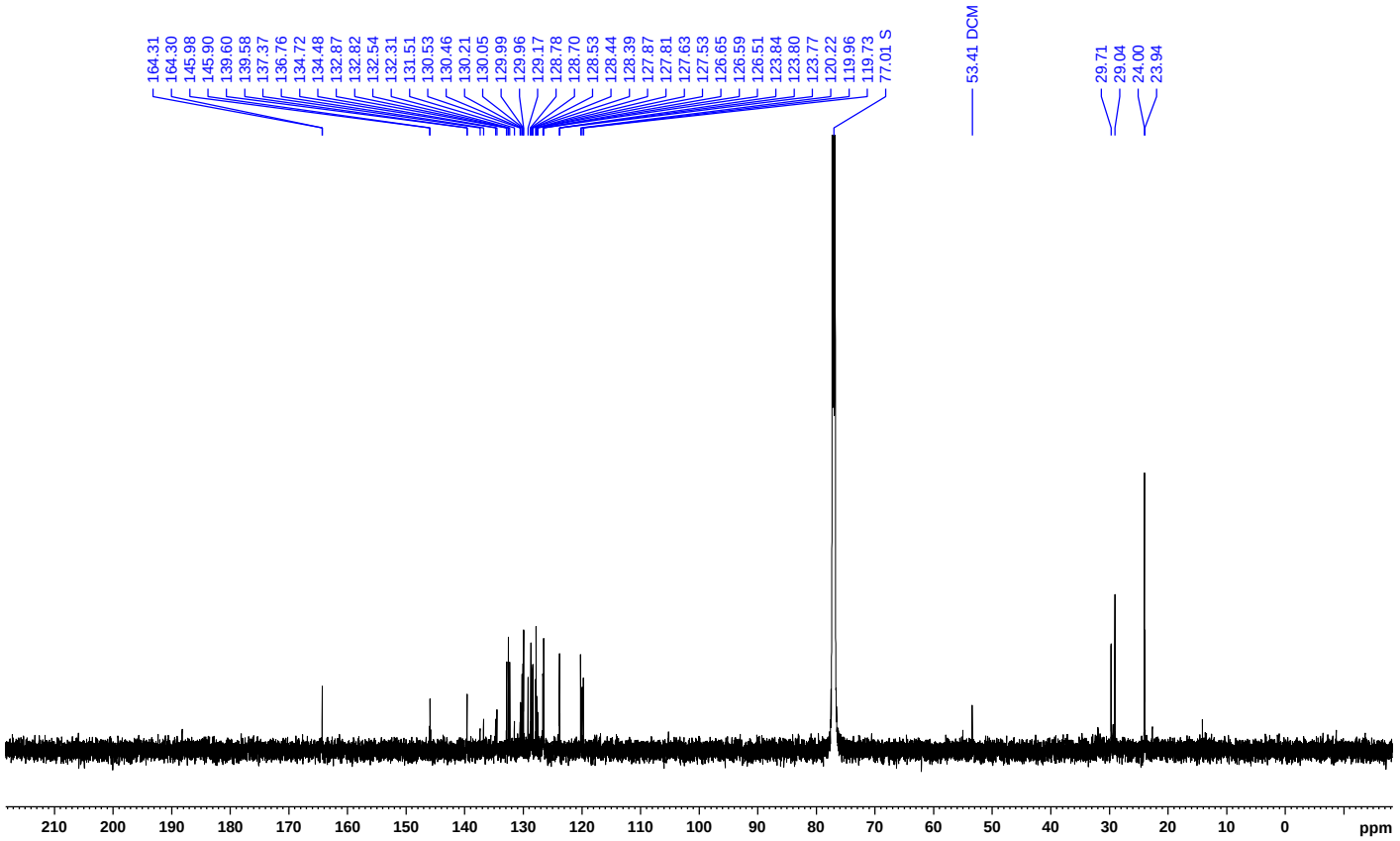

Figure S41. ^{13}C NMR spectrum of **4b** (151 MHz, chloroform-*d*, 300 K).

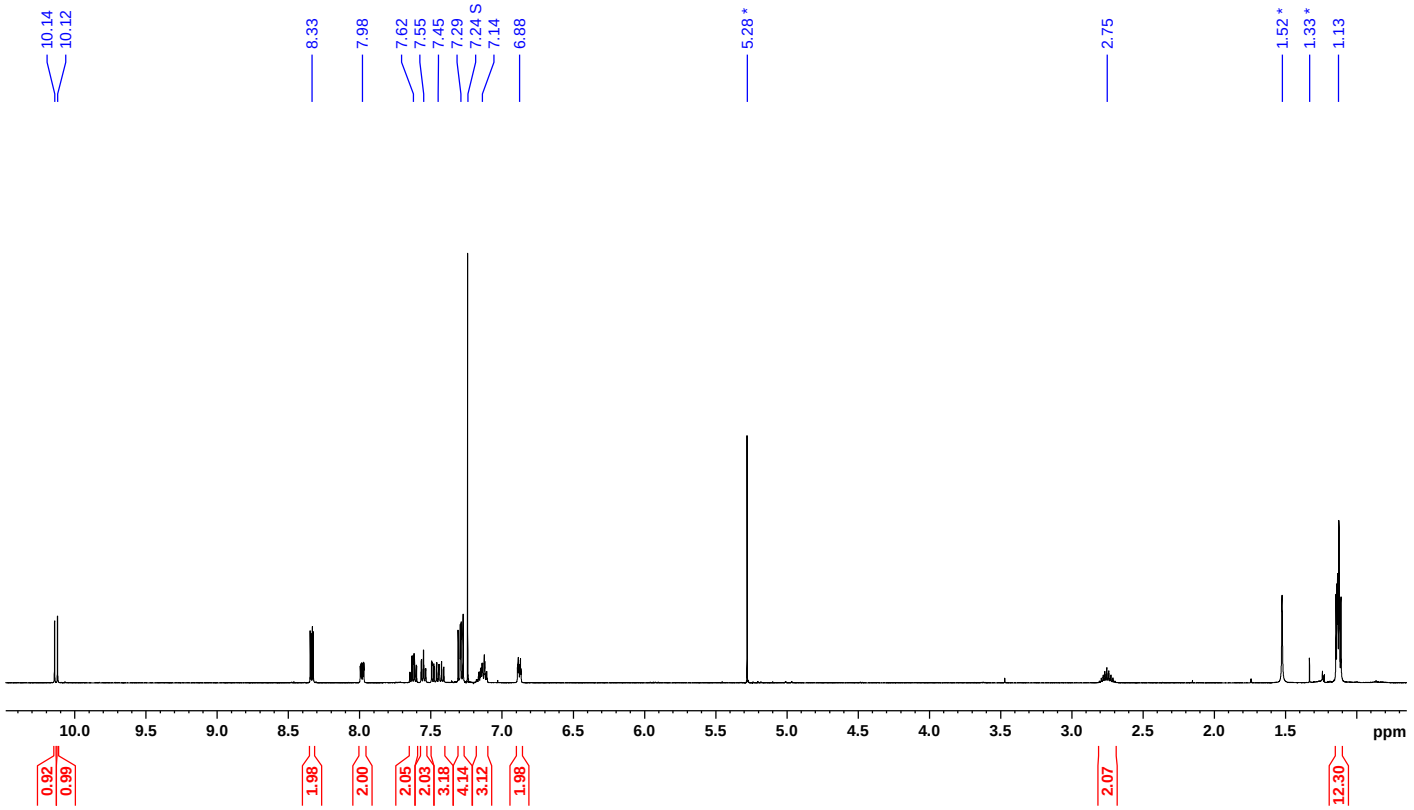

Figure S42. ^{1}H NMR spectrum of **4c** (500 MHz, chloroform-*d*, 300 K).

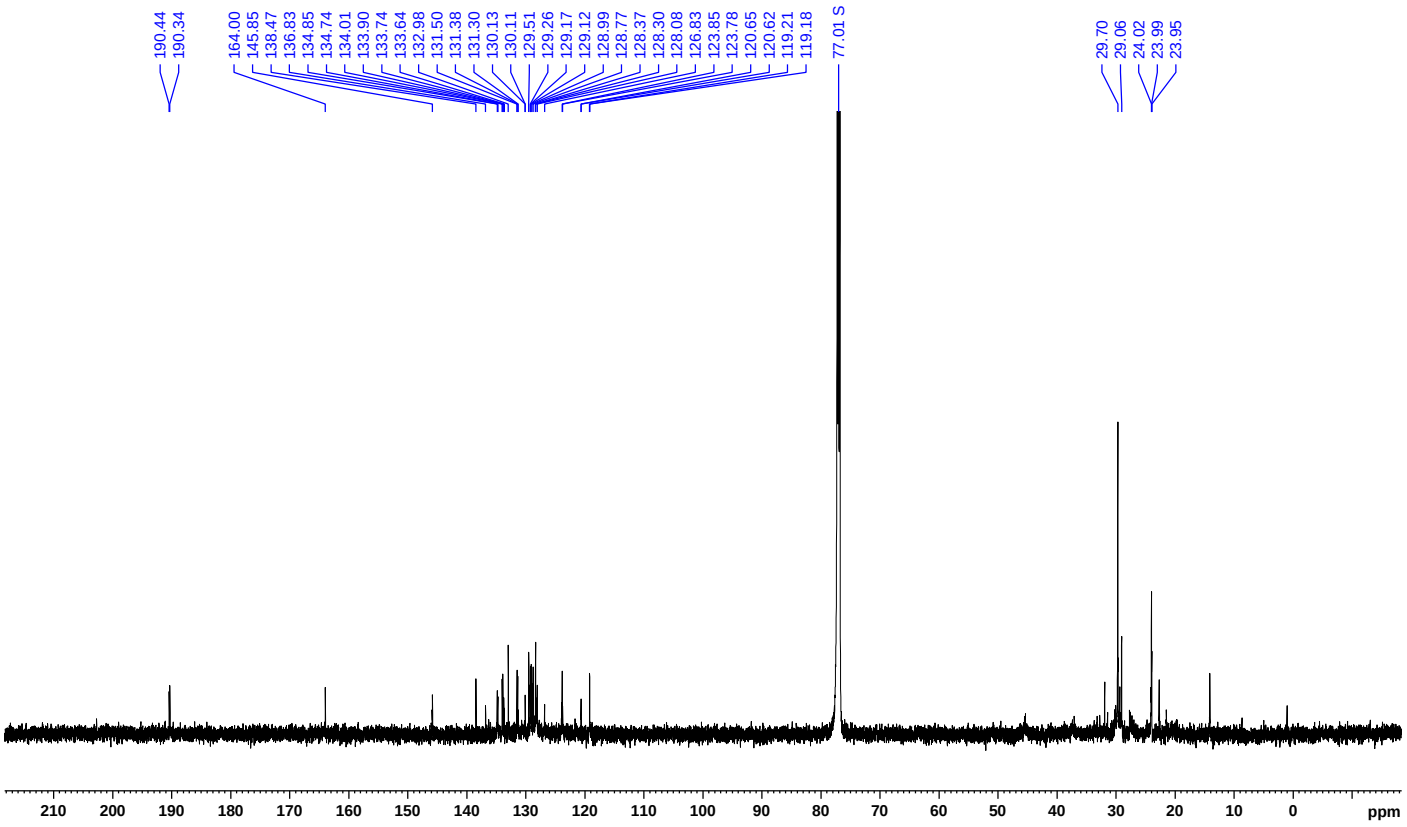

Figure S43. ^{13}C NMR spectrum of **4c** (151 MHz, chloroform-*d*, 300 K).

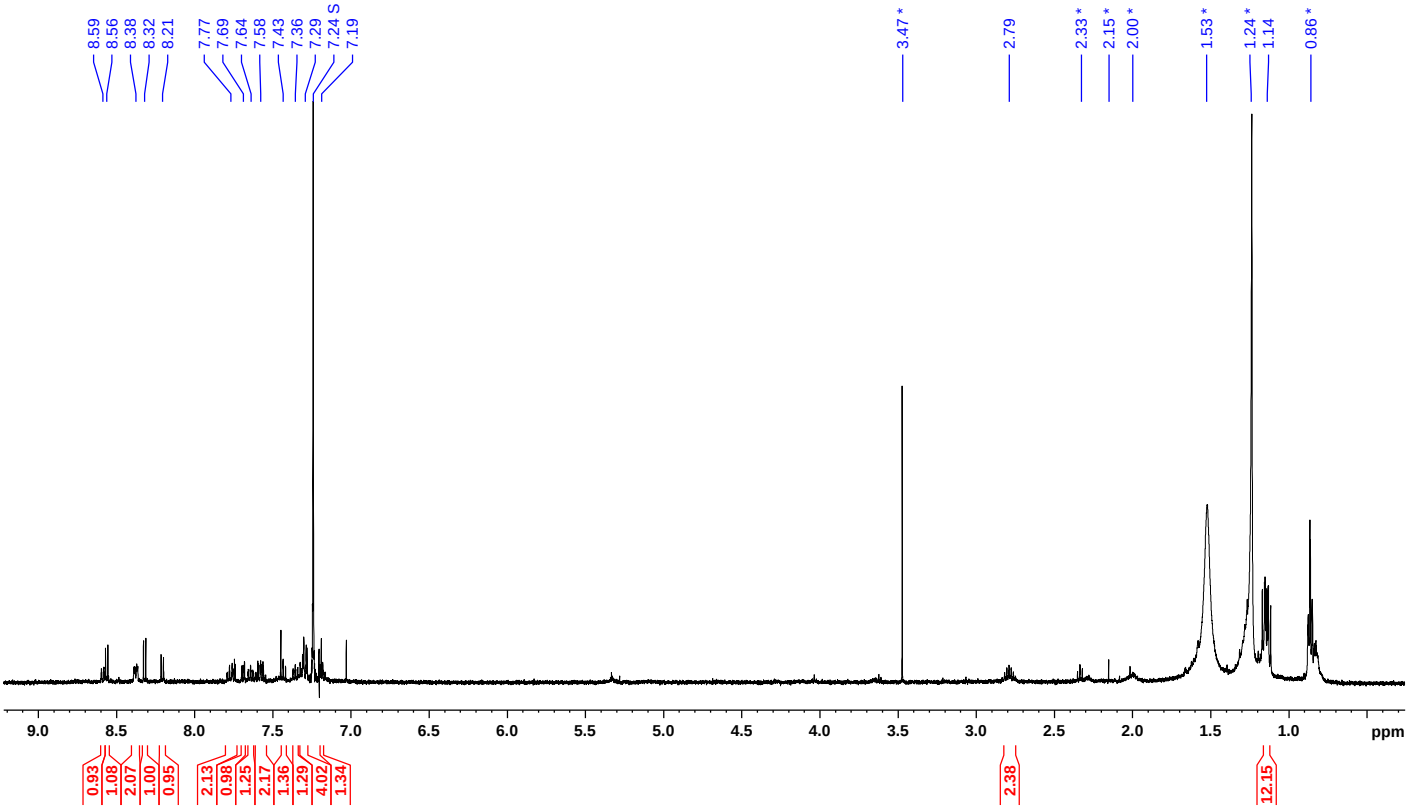

Figure S44. ^{1}H NMR spectrum of **5a** (500 MHz, chloroform-*d*, 300 K).

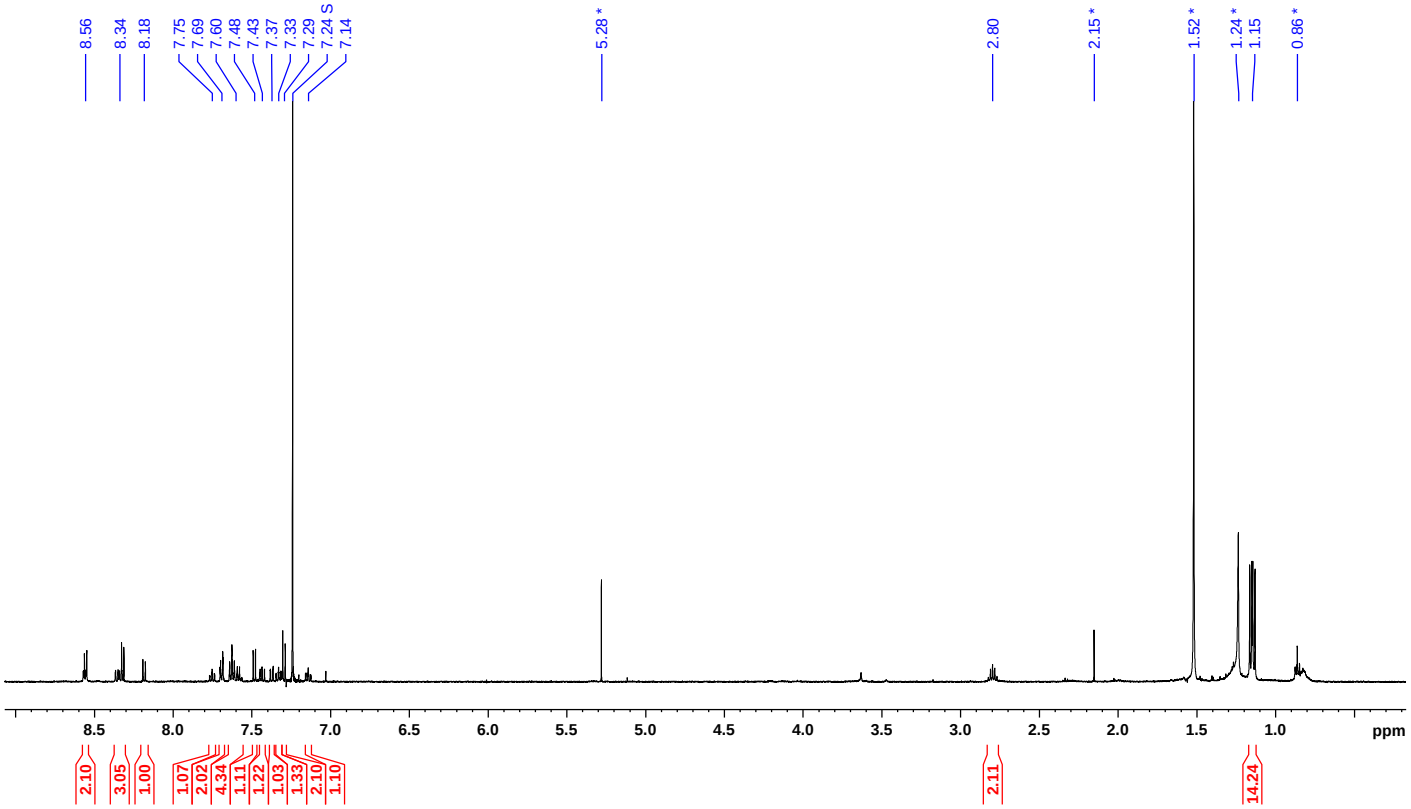

Figure S45. ^{1}H NMR spectrum of **5b** (500 MHz, chloroform-*d*, 300 K).

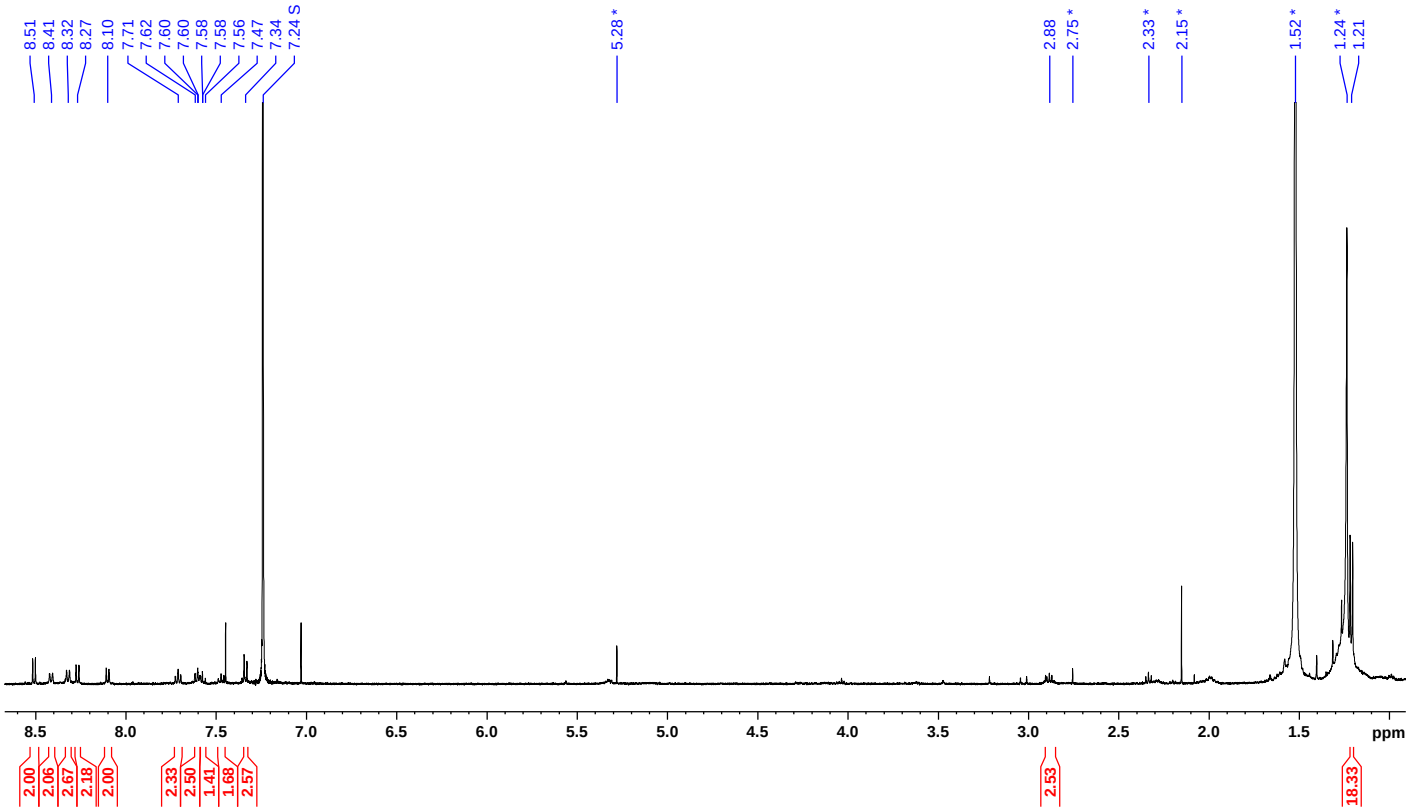

Figure S46. ^{1}H NMR spectrum of **6** (500 MHz, chloroform-*d*, 300 K).

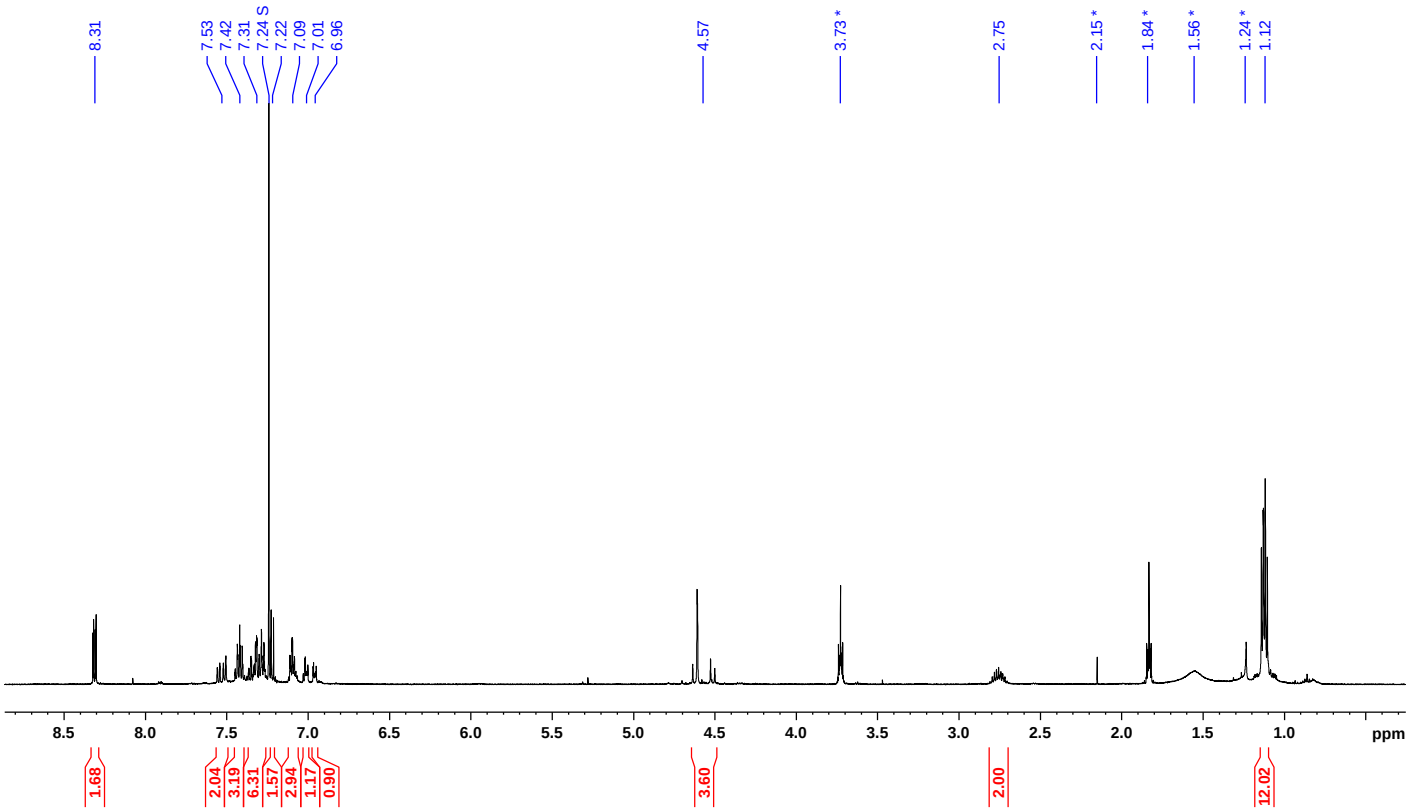

Figure S47. ^{1}H NMR spectrum of **7** (500 MHz, chloroform-*d*, 300 K).

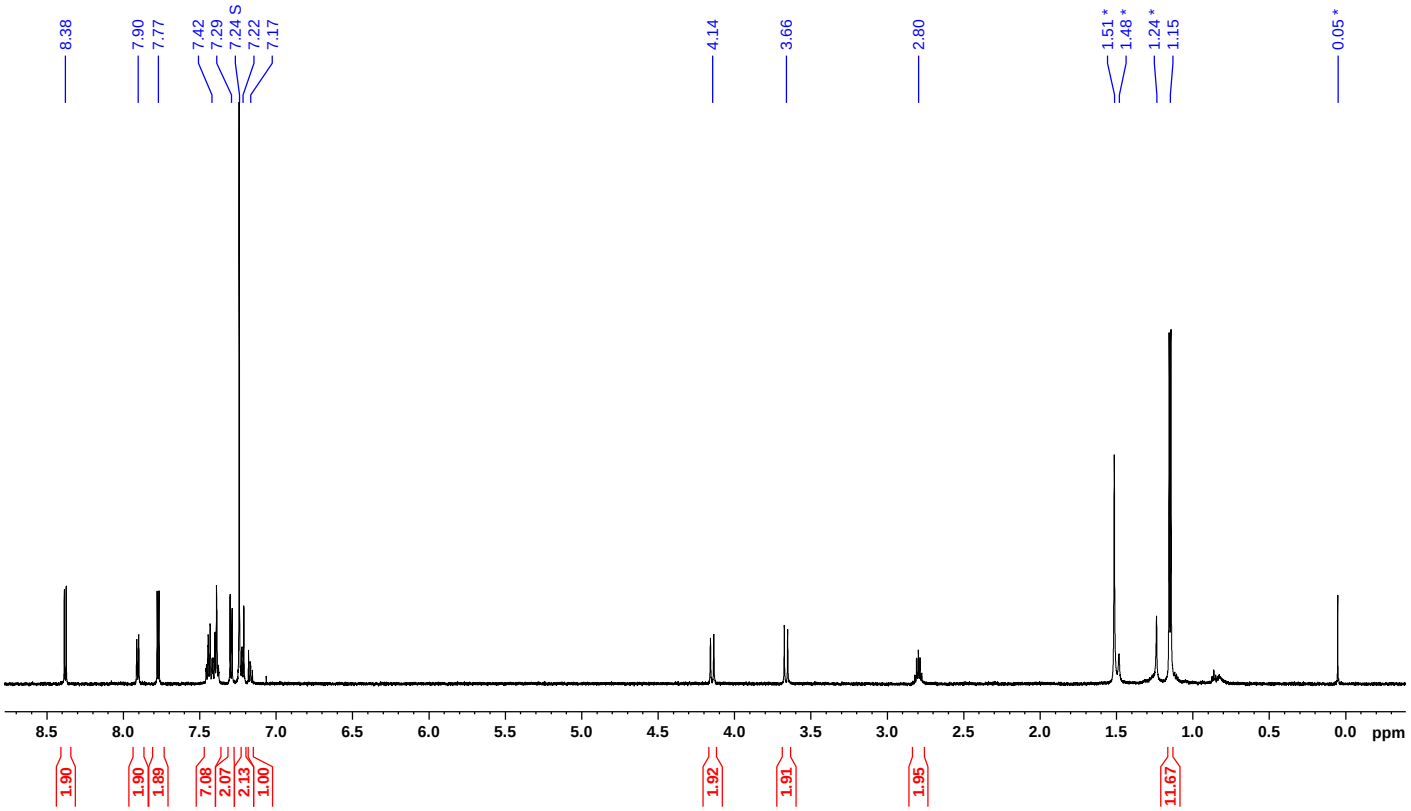

Figure S48. ^{1}H NMR spectrum of **8** (600 MHz, chloroform-*d*, 300 K).

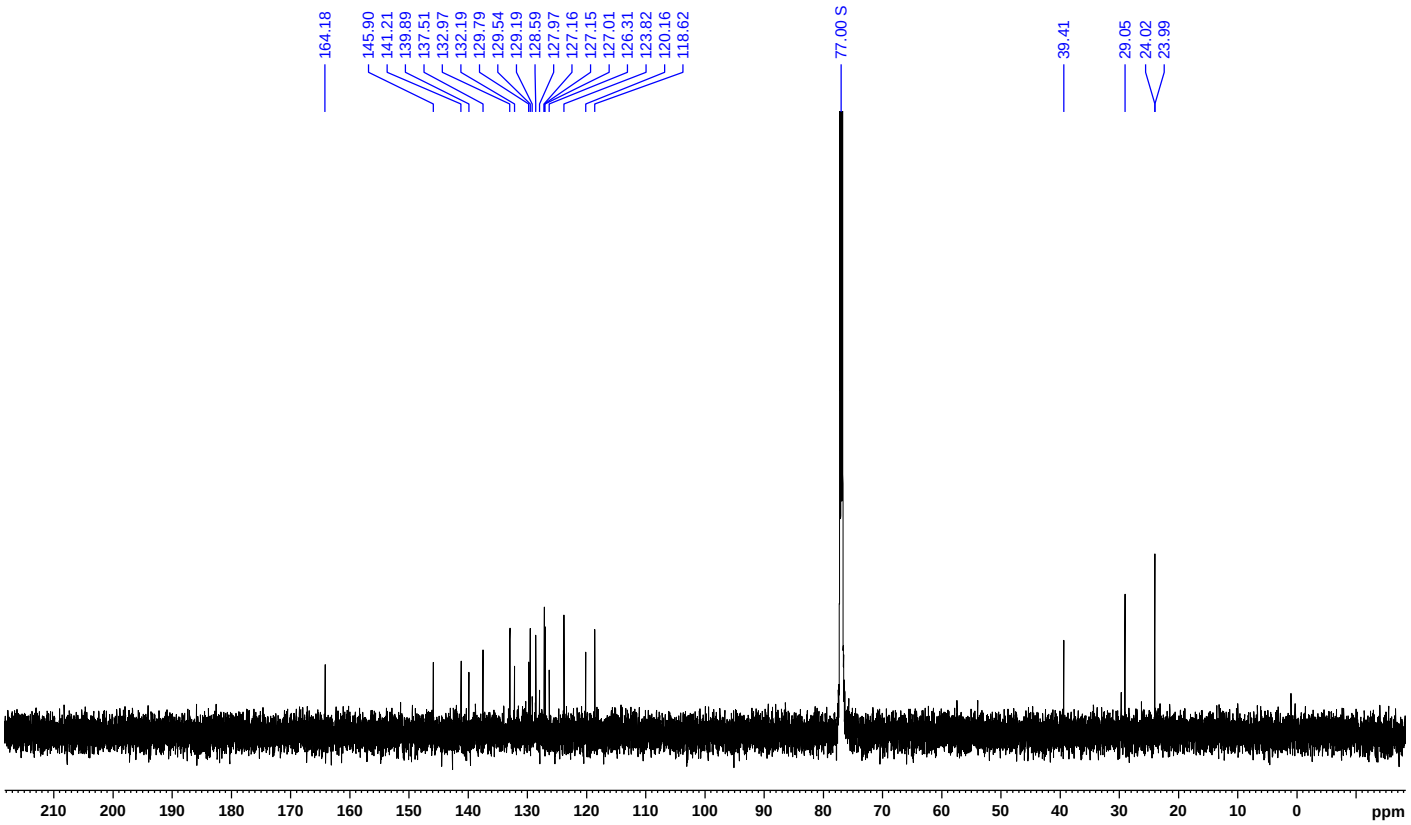

Figure S49. ^{13}C NMR spectrum of **8** (151 MHz, chloroform-*d*, 300 K).

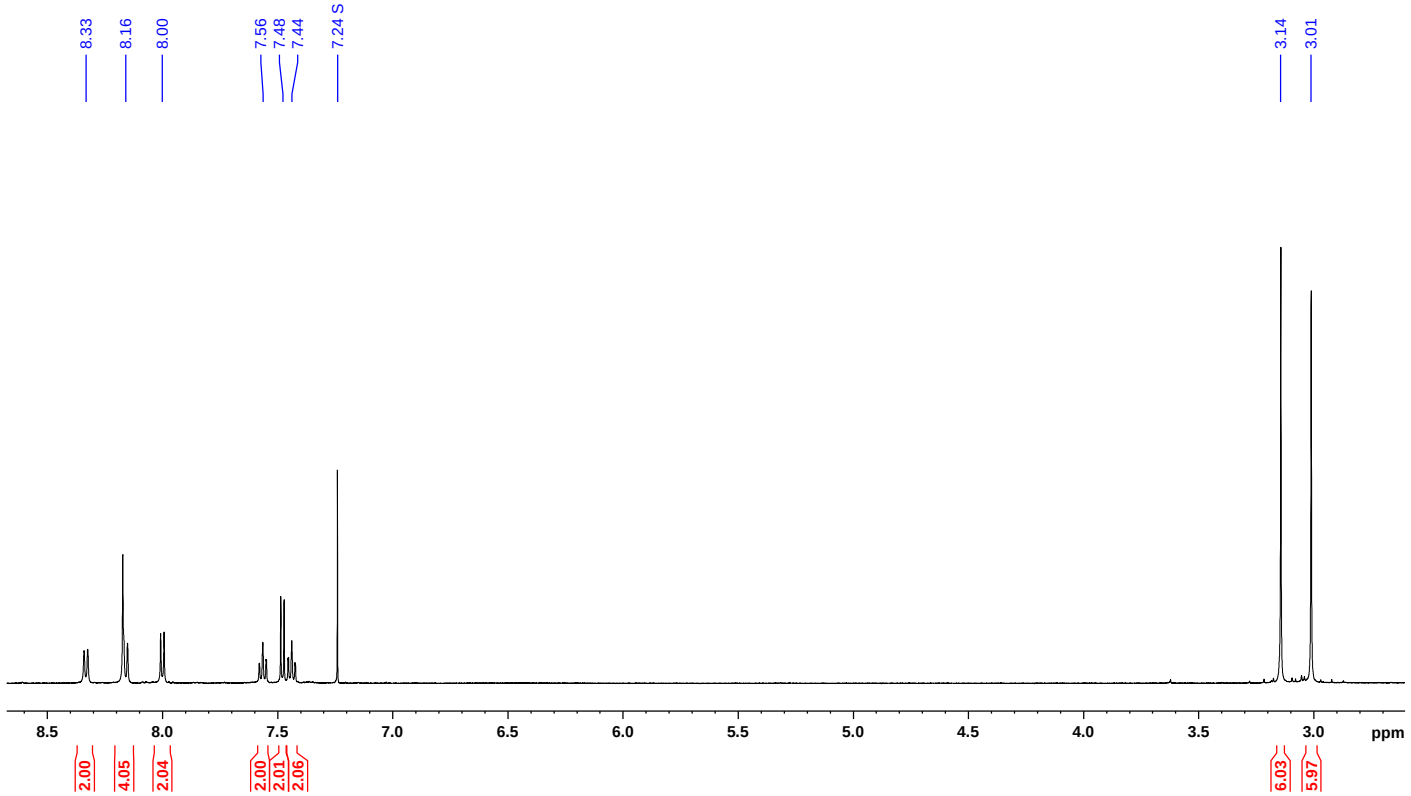

Figure S50. ^{1}H NMR spectrum of **11** (500 MHz, chloroform-*d*, 300 K).

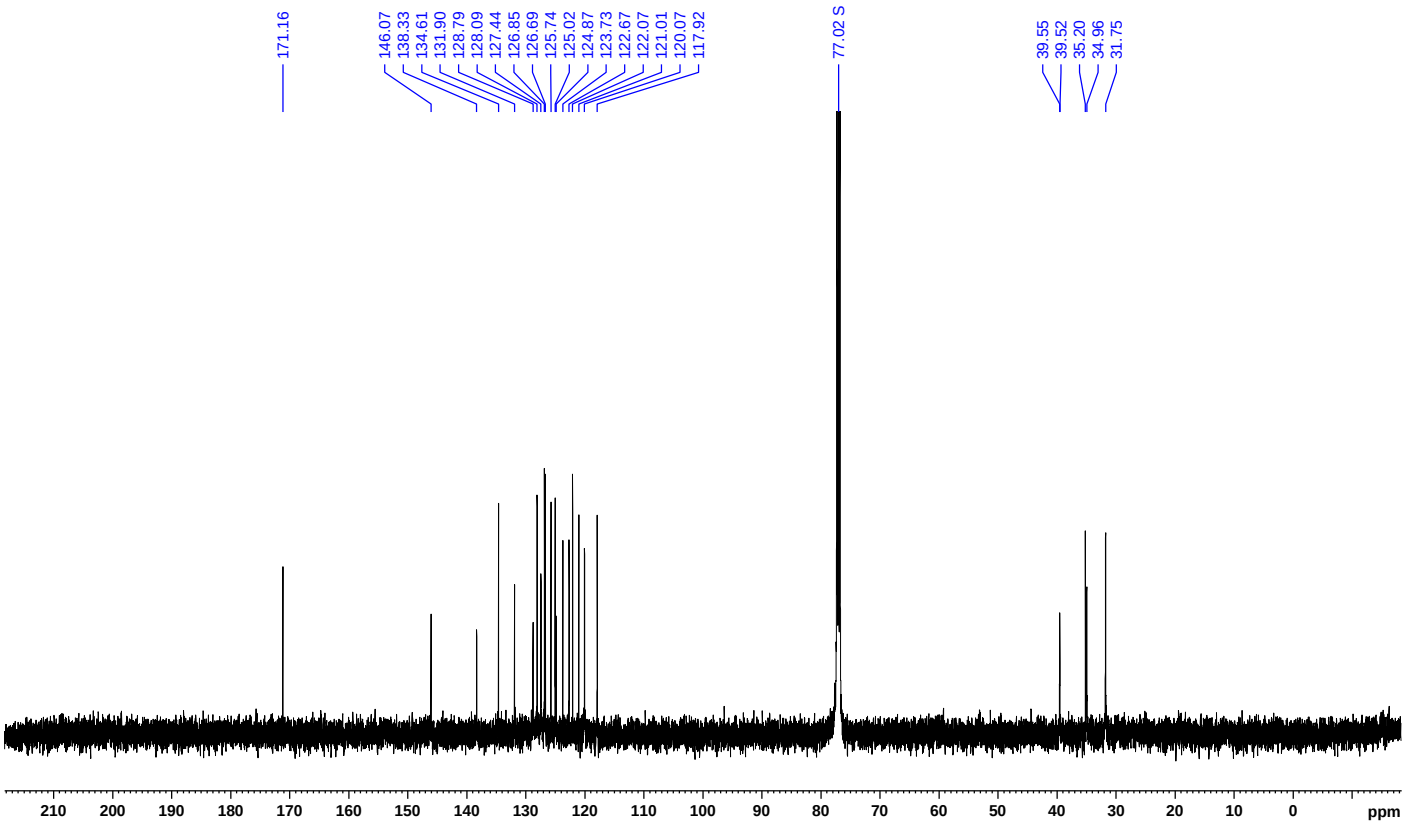

Figure S51. ^{13}C NMR spectrum of **11** (125 MHz, chloroform-*d*, 300 K).

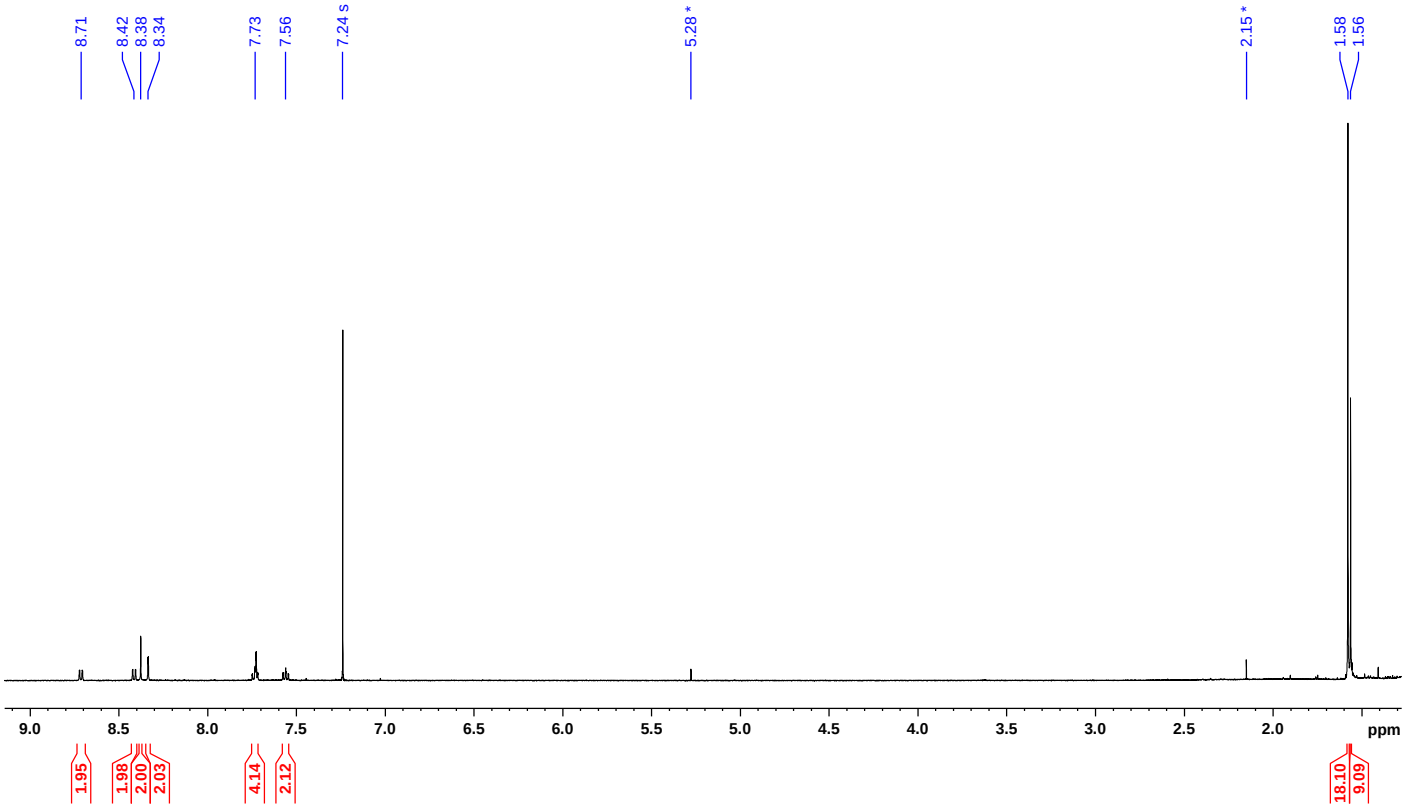

Figure S52. ^{1}H NMR spectrum of **12** (500 MHz, chloroform-*d*, 300 K).

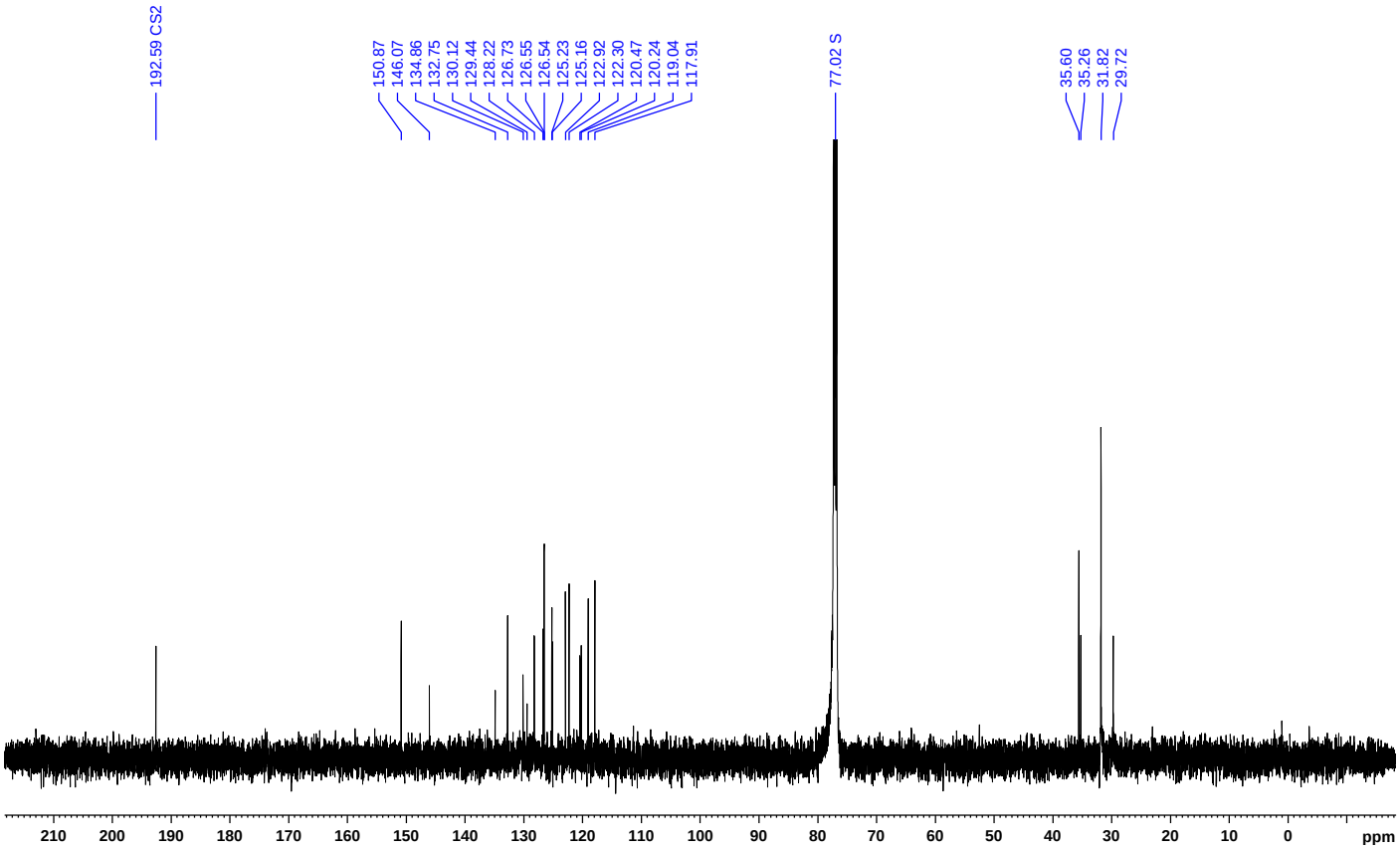

Figure S53. ^{13}C NMR spectrum of **12** (125 MHz, chloroform-*d*, 300 K).

Mass Spectra

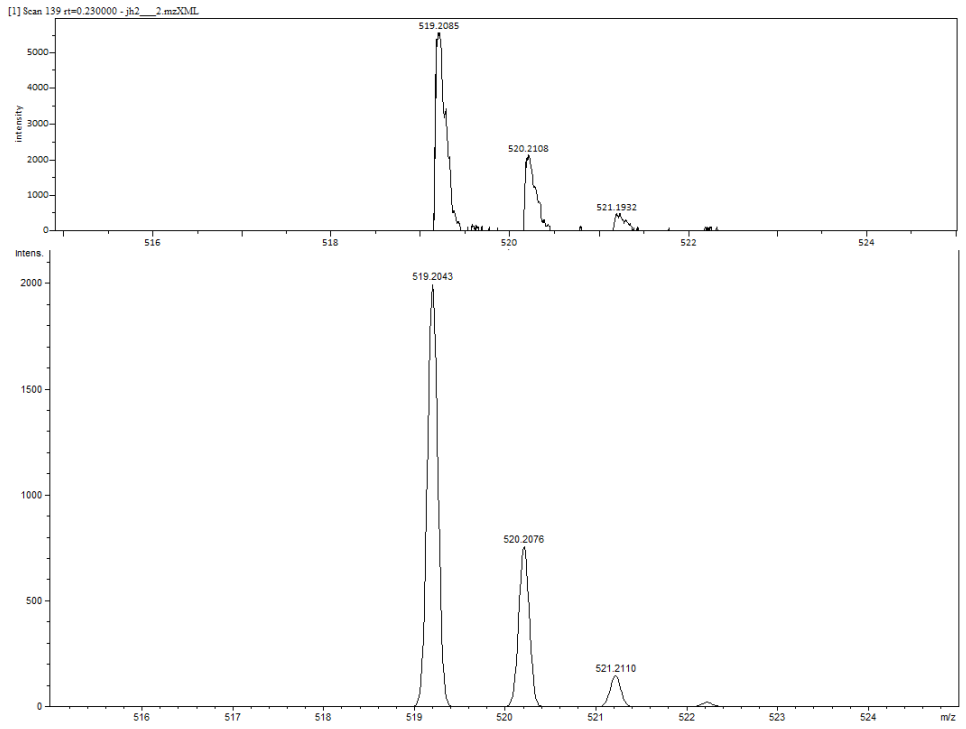

Figure S54. High resolution mass spectrum of **2** (ESI–TOF, top: experimental, bottom: simulated).

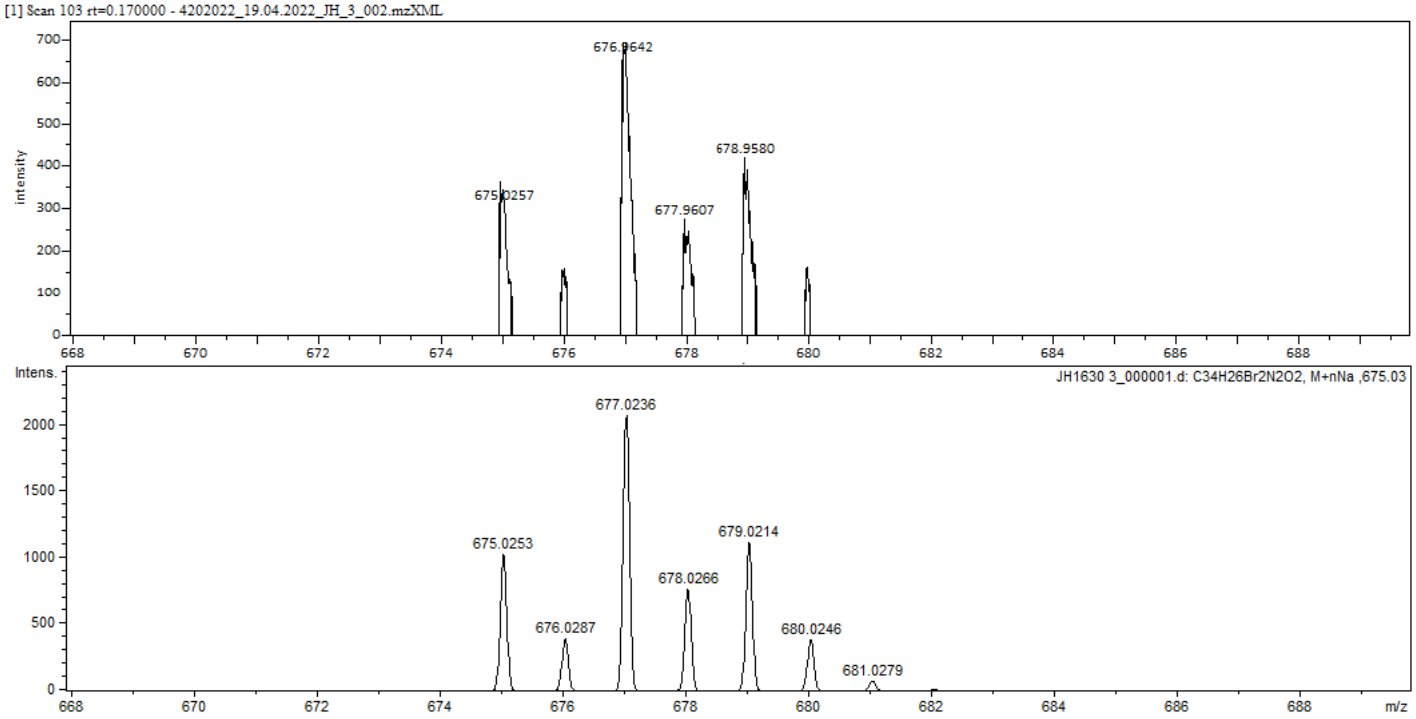

Figure S55. High resolution mass spectrum of **3** (ESI–TOF, top: experimental, bottom: simulated).

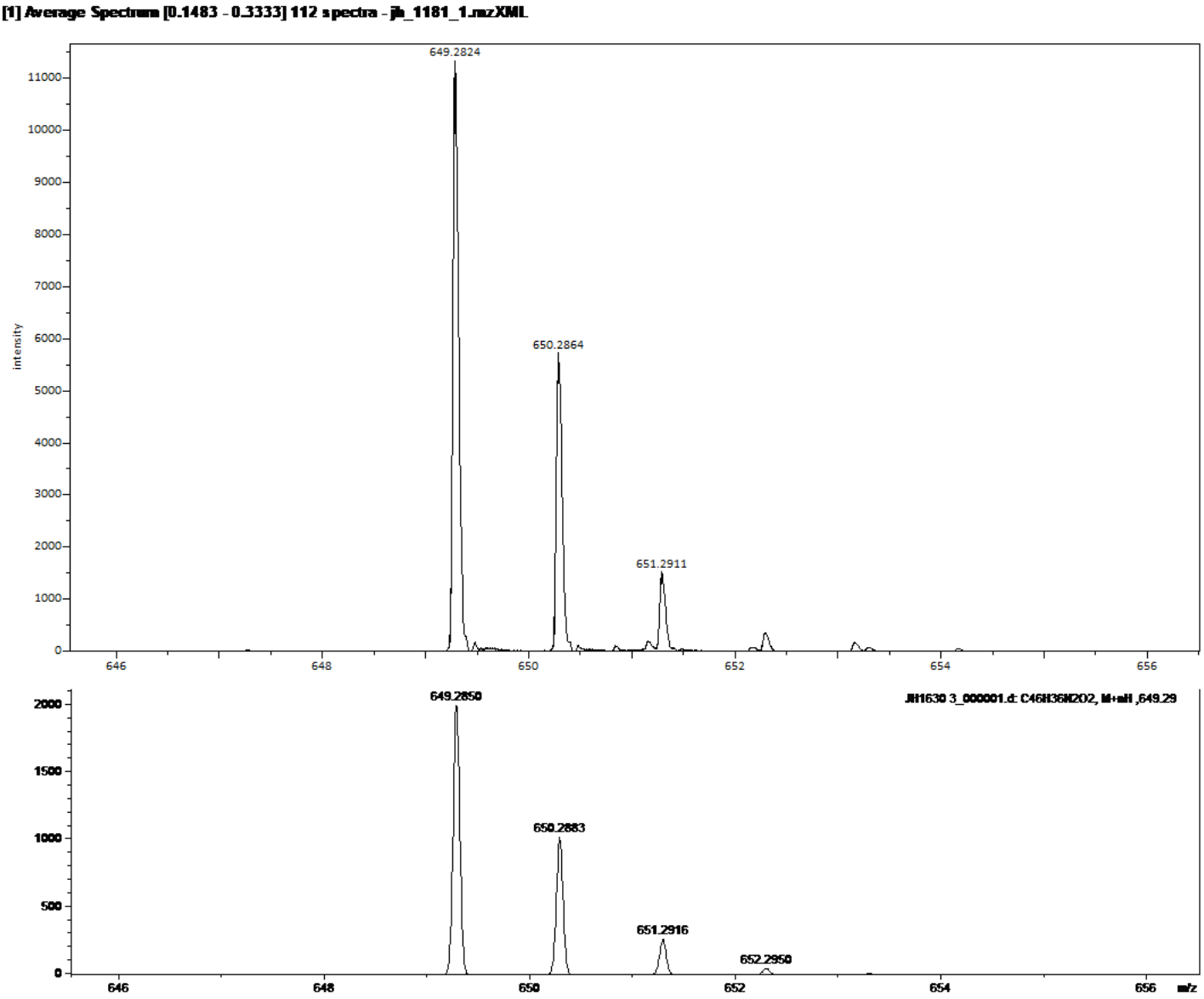

Figure S56. High resolution mass spectrum of **4a** (ESI–TOF, top: experimental, bottom: simulated).

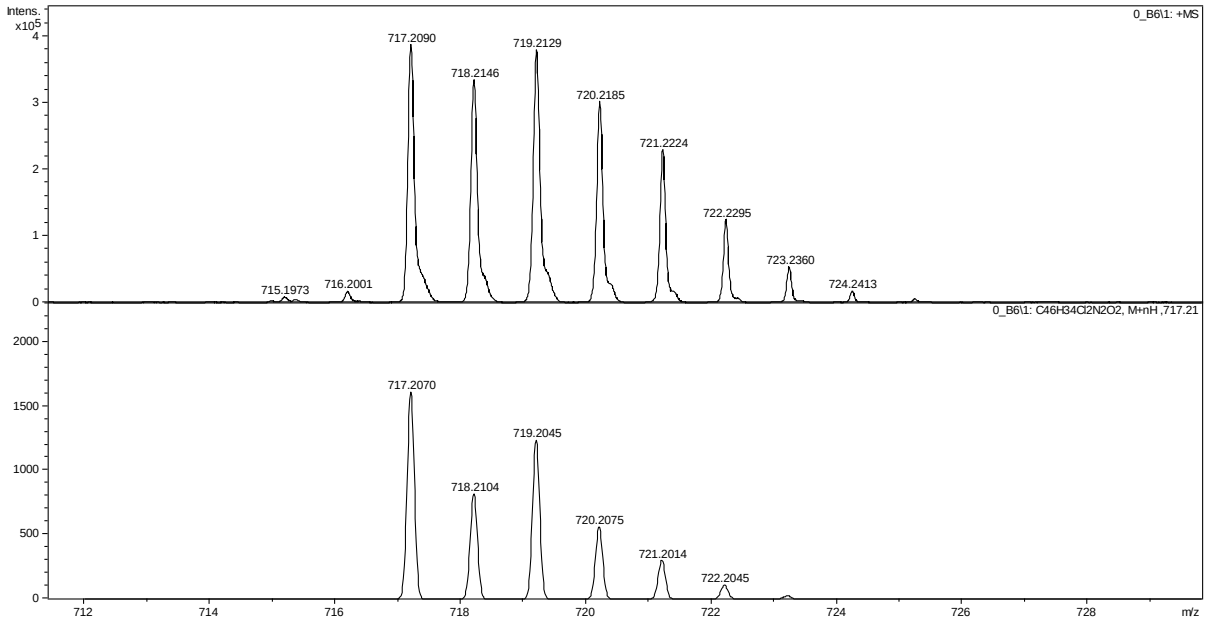

Figure S57. High resolution mass spectrum of **4b** (MALDI–TOF, top: experimental, bottom: simulated).

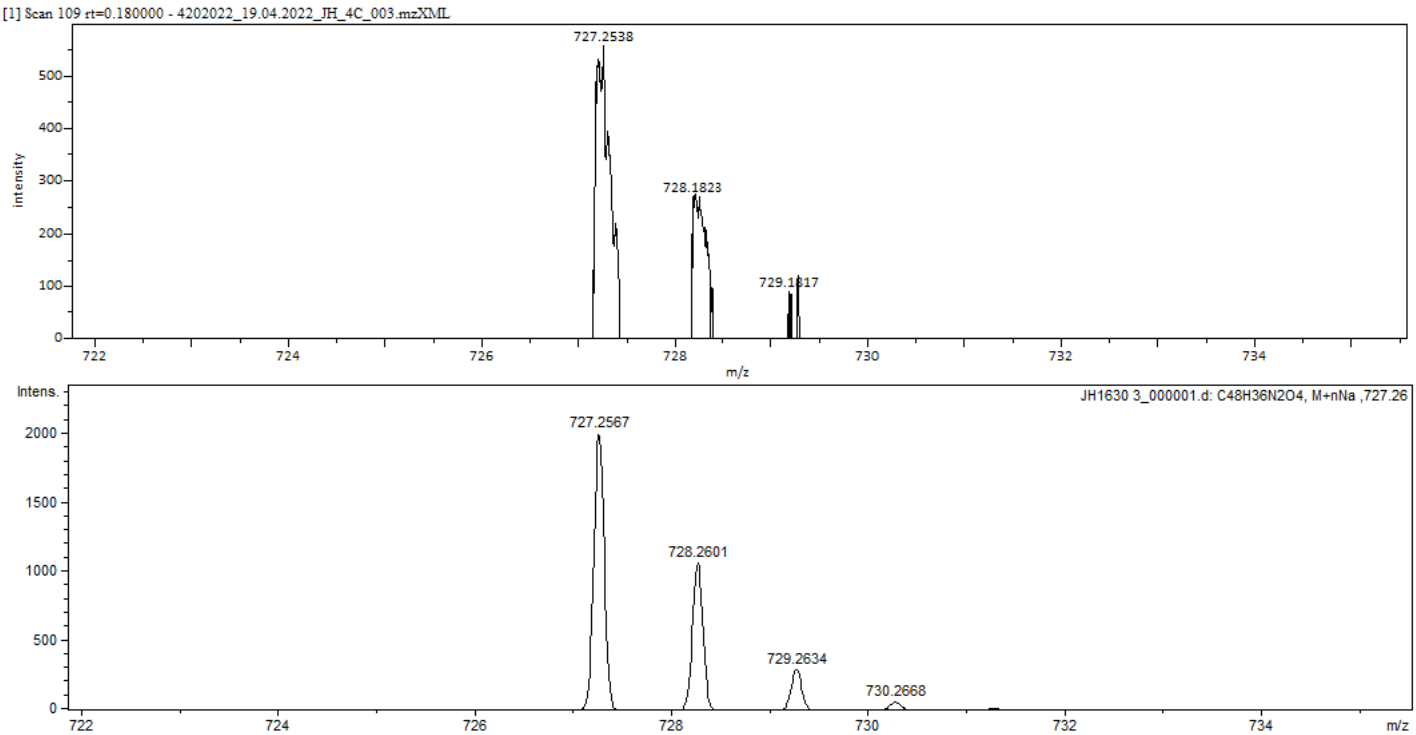

Figure S58. High resolution mass spectrum of **4c** (ESI–TOF, top: experimental, bottom: simulated).

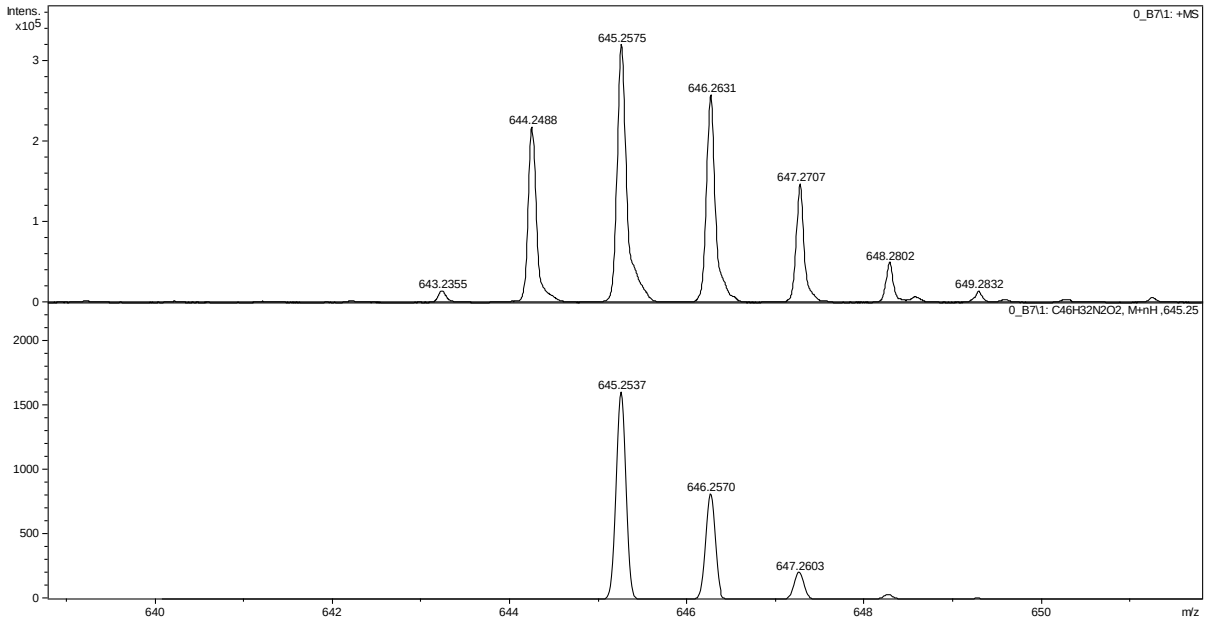

Figure S59. High resolution mass spectrum of **6** (MALDI–TOF, top: experimental, bottom: simulated).

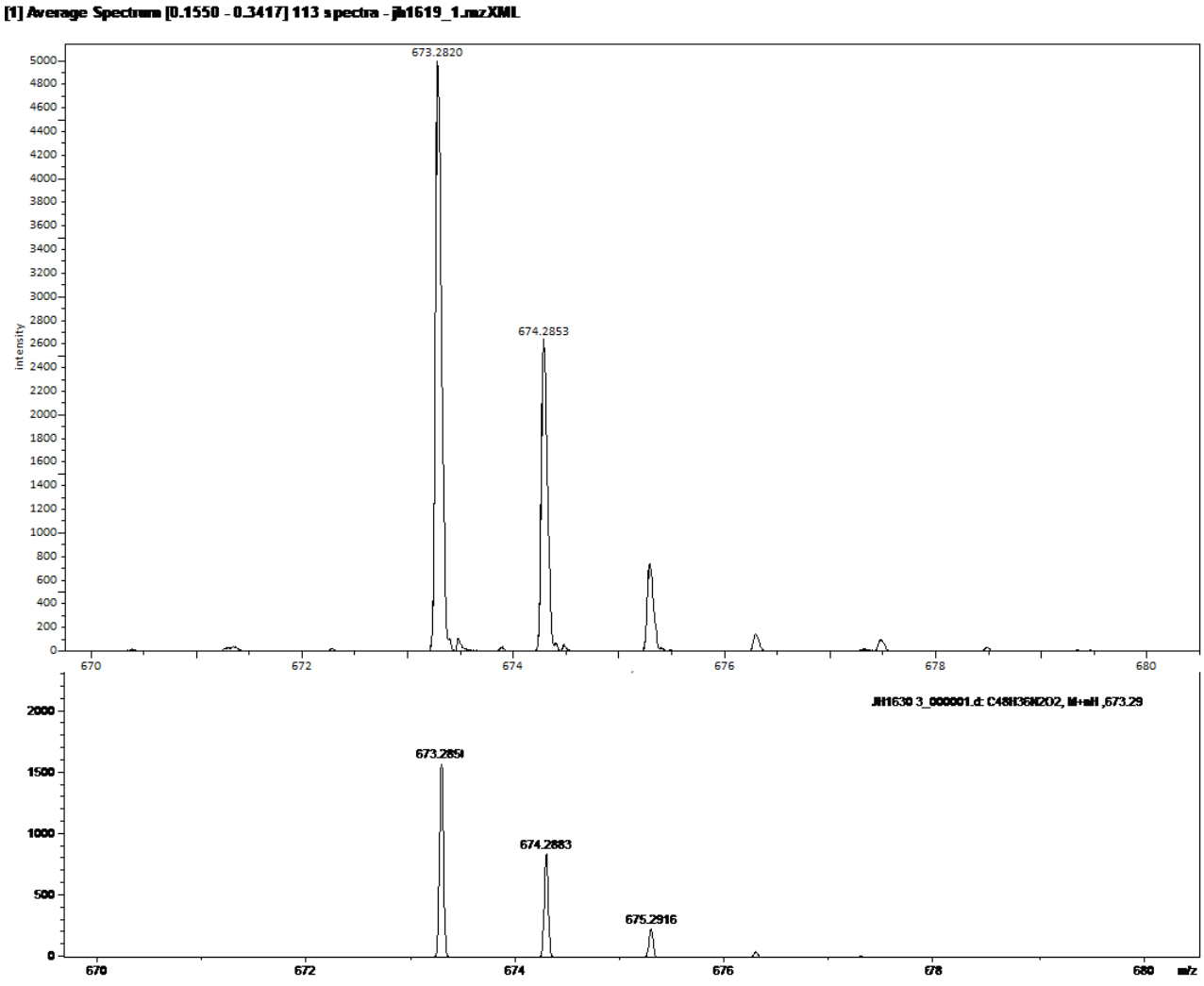

Figure S60. High resolution mass spectrum of **8** (ESI–TOF, top: experimental, bottom: simulated).

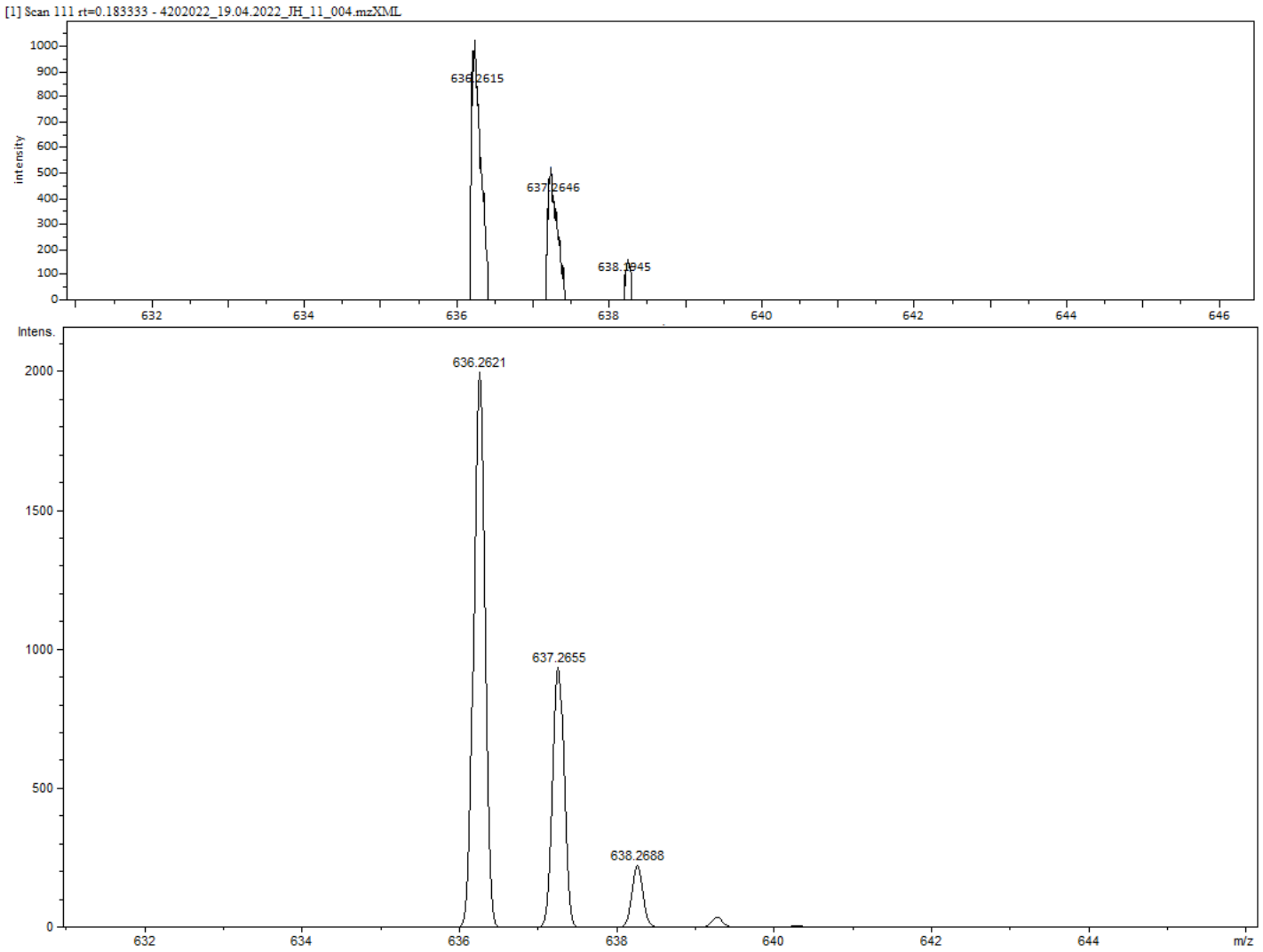

Figure S61. High resolution mass spectrum of **11** (ESI–TOF, top: experimental, bottom: simulated).

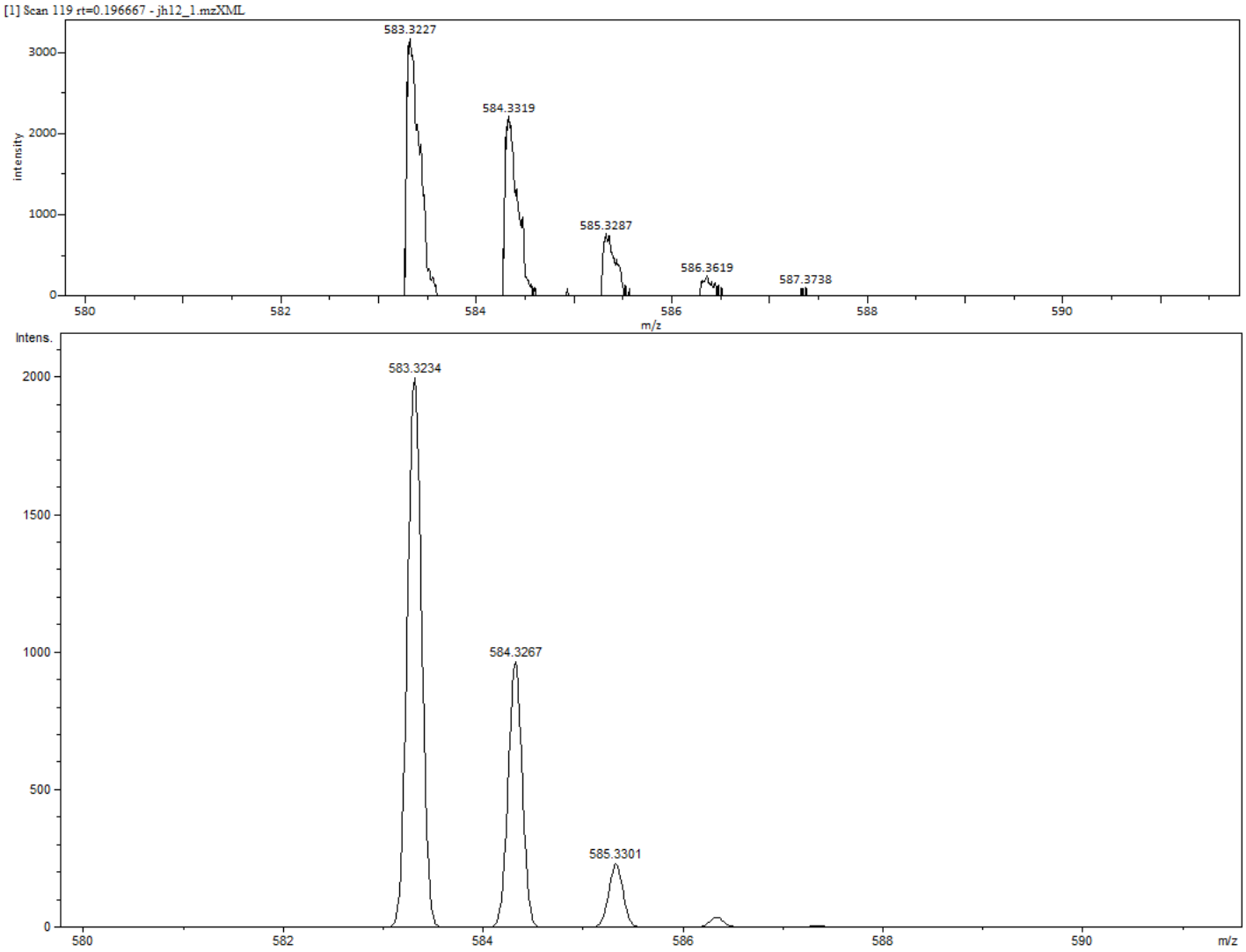

Figure S62. High resolution mass spectrum of **12** (ESI–TOF, top: experimental, bottom: simulated).

References

(1) Zhylitskaya, H.; Cybińska, J.; Chmielewski, P.; Lis, T.; Stępień, M. Bandgap Engineering in π-Extended Pyrroles. a Modular Approach to Electron-Deficient Chromophores with Multi-Redox Activity. *J. Am. Chem. Soc.* **2016**, *138* (35), 11390–11398. https://doi.org/10.1021/jacs.6b07826.

(2) Berger, R.; Giannakopoulos, A.; Ravat, P.; Wagner, M.; Beljonne, D.; Feng, X.; Müllen, K. Synthesis of Nitrogen-Doped ZigZag-Edge Peripheries: Dibenzo-9a-Azaphenalene as Repeating Unit. *Angew. Chem. Int. Ed.* **2014**, *53* (39), 10520–10524. https://doi.org/10.1002/anie.201403302.

(3) Knippen, K.; Matuszczyk, D.; Kraft, M.; Bredenkötter, B.; Eickerling, G.; Lis, T.; Volkmer, D.; Stępień, M. Acenaphtho[1,2-d][1,2,3]Triazole and Its Kuratowski Complex: A π-Extended Tecton for Supramolecular and Coordinative Self-Assembly. *Chemistry – A European Journal n/a* (n/a). https://doi.org/10.1002/chem.202103480.

(4) Frisch, M. J.; Trucks, G. W.; Schlegel, H. B.; Scuseria, G. E.; Robb, M. A.; Cheeseman, J. R.; Scalmani, G.; Barone, V.; Petersson, G. A.; Nakatsuji, H.; Li, X.; Caricato, M.; Izmaylov, A. F.; Zheng, G.; Sonnenberg, J. L.; Hada, M.; Ehara, M.; Toyota, K.; Fukuda, R.; Hasegawa, J.; Ishida, M.; Nakajima, T.; Honda, Y.; Kitao, O.; Nakai, H.; Vreven, T.; Montgomery, Jr., J. A.; Peralta, J. E.; Ogliaro, F.; Bearpark, M.; Heyd, J. J.; Brothers, E.; Kudin, K. N.; Staroverov, V. N.; Kobayashi, R.; Normand, J.; Raghavachari, K.; Rendell, A.; Burant, J. C.; Iyengar, S. S.; Tomasi, J.; Cossi, M.; Millam, J. M.; Klene, M.; Adamo, C.; Gomperts, R.; Stratmann, R. E.; Yazyev, O.; Austin, A. J.; Cammi, R.; Pomelli, C.; Ochterski, J. W.; Martin, R. L.; Morokuma, K.; Zakrzewski, V. G.; Voth, G. A.; Salvador, P.; Dannenberg, J. J.; Dapprich, S.; Daniels, A. D.; Farkas, O.; Foresman, J. B.; Fox, D. J. *Gaussian 16, Revision B.01*; Wallingford CT, 2016.

(5) Becke, A. D. Density-Functional Exchange-Energy Approximation with Correct Asymptotic Behavior. *Phys. Rev., A* **1988**, *38* (6), 3098–3100.

(6) Becke, A. D. Density-functional Thermochemistry. III. The Role of Exact Exchange. *J. Chem. Phys.* **1993**, *98* (7), 5648–5652. https://doi.org/10.1063/1.464913.

(7) Lee, C.; Yang, W.; Parr, R. G. Development of the Colle-Salvetti Correlation-Energy Formula into a Functional of the Electron Density. *Phys. Rev. B* **1988**, *37* (2), 785–789. https://doi.org/10.1103/PhysRevB.37.785.

(8) Chai, J.-D.; Head-Gordon, M. Long-Range Corrected Hybrid Density Functionals with Damped Atom-Atom Dispersion Corrections. *Phys Chem Chem Phys* **2008**, *10* (44), 6615–6620. https://doi.org/10.1039/b810189b.

(9) Sheldrick, G. M. A Short History of SHELX. *Acta Crystallographica Section A Foundations of Crystallography* **2008**, *64* (1), 112–122. https://doi.org/10.1107/S0108767307043930.